# Learning from diversity: comparing nodulation in *Medicago truncatula* to that in the non-legume *Parasponia andersonii*


Helen Wilkinson

A thesis submitted for the degree of Doctor of Philosophy in Life Sciences

University of Warwick
School of Life Sciences

February 2023

Supervisor: Professor Miriam Gifford

# Table of Contents

**List of Figures** VI

**List of Tables** IX

**Acknowledgements** X

**Declarations** XI

**Abbreviations** XII

**Abstract** XIII

**Chapter 1: Introduction** 1

1.1 Current problems feeding the global population 1

1.2 What are legumes and why are they important for food security? 1

1.3 The root is comprised of different cell types with unique roles in nodulation 3

1.4 Stages of nodulation: initial legume-rhizobia interaction 4

1.5 Stages of nodulation: rhizobial entry 6

1.6 Stages of nodulation: nodule organogenesis 7

1.7 The non-legume *Parasponia andersonii* 8

1.8 Nitrogen-fixation in non-rhizobial nodules 10

1.9 Nitrogen fixation in plant-microbe interactions without nodules 10

1.10 More than just nitrogen: defence priming 12

1.11 More than just nitrogen: abiotic stress resistance 15

1.12 Use of cell type analysis to study nodulation & FACS 18

1.13 Thesis aims and objectives 20

**Chapter 2: Materials and Methods** 21

2.1 Materials (plants and microbes) 21

2.2 Plant growth and harvesting methods 21

2.2.1 Germinating *Medicago truncatula* 21

2.2.2 Growth conditions for *Medicago truncatula* 21

2.2.3 Sterilising *Parasponia andersonii* stems and leaves 22

2.2.4 Plant media used 22

2.2.5 Establishing new *Parasponia andersonii* tissue culture 24

2.2.6 Growth conditions for *Parasponia andersonii* 24

2.3 Bacterial growth methods 25

2.4 Experimental rhizobia inoculation 25

2.4.1 Rhizobia inoculation conditions 25

2.4.2 *Medicago truncatula* and *Parasponia andersonii* phenotyping experiment 25

2.4.3 Rhizobia inoculation of *Parasponia andersonii* for root RNA-Seq experiment 26

2.4.4 Rhizobia inoculation of *Parasponia andersonii* for nodule RNA-Seq experiment 26

2.4.5 Generating *Parasponia andersonii* protoplasts 26

2.5 Plant transformation methods 27

2.5.1 Transforming *Agrobacterium tumefaciens* 27

2.5.2 Transforming wild-type *Parasponia andersonii* stems 29

2.5.3 Transforming *Parasponia andersonii* calli from wild-type leaves 29

2.5.4 Generating *Medicago truncatula* transient lines 30

2.5.5 Generating *Medicago truncatula* stable lines 30

2.6 Molecular methods 31

2.6.1 Crude DNA extraction 31

2.6.2 PCR analysis 32

2.6.3 PCR product cleaning and sequencing 32

2.6.4 RNA extraction 32

2.7 Microscopy analysis 33

2.7.1 Confocal Microscopy 33

2.7.2 Electron Microscopy 33

2.8 Data analysis (inc. for RNAseq and for numerical data with stats) 34

2.8.1 RNA-Seq analysis 34

2.8.2 Ortholog analysis 34

2.8.3 Statistical analysis 34

**Chapter 3: Shoot, root and nodule weight and nodule number comparisons between *Medicago truncatula* and *Parasponia andersonii* during nodulation with different rhizobial strains** 35

3.1 Introduction 35

3.2 Results 38

3.2.1 Compatible rhizobia have a significant effect on shoot biomass in *Medicago truncatula* 38

3.2.2 *Bradyrhizobium elkanii* (WUR3) is an effective nodulator of *Parasponia andersonii* 42

3.2.3 Interaction with *Mesorhizobium plurifarium* (BOR2) vs. *Bradyrhizobium elkanii* (WUR3) leads to different *Parasponia andersonii* nodule phenotypes and highlights rhizobial specific responses 44

3.3 Discussion 48

3.3.1 Specificity of nodulation in *Medicago truncatula*, as assessed in response to inoculation with different rhizobial strains 48

3.3.2 Variety of hosting of rhizobia in *Parasponia andersonii* 50

3.4 Conclusion 52

**Chapter 4: Analysing the differences in nodulation of *Parasponia andersonii* with *Mesorhizobium plurifarium* (BOR2) compared to *Bradyrhizobium elkanii* (WUR3)** 53

4.1 Introduction 53

4.1.1 Hormones and nodulation 53

4.1.2 Auxin and nodulation: a positive regulator 53

4.1.3 Ethylene and nodulation: a negative regulator 54

4.1.4 Nodule senescence 55

4.1.5 Aims and objectives 56

4.2 Results 56

4.2.1 Transmission electron microscopy of *Mesorhizobium plurifari*um (BOR2) and *Bradyrhizobium elkanii* (WUR3)-inoculated nodules 56

4.2.2 RNA-Seq identifies no gene expression differences at the whole root level between *Mesorhizobium plurifari*um (BOR2) vs *Bradyrhizobium elkanii* (WUR3) vs control-inoculated *Parasponia andersonii* roots 57

4.2.3 RNA-Seq of *Mesorhizobium plurifari*um (BOR2) vs *Bradyrhizobium elkanii* (WUR3) harbouring nodules found 371 Differentially expressed genes 60

4.2.4 *Mesorhizobium plurifari*um (BOR2) vs *Bradyrhizobium elkanii* (WUR3) harbouring nodules DEGs can be grouped into four clusters 62

4.2.5 Cluster 1 includes highly expressed genes in *Mesorhizobium plurifari*um (BOR2) inoculated nodules that may be related to regulation of nodule senescence 63

4.2.6 *PanWU01x14_152000* is a gene in Cluster 2 involved in abiotic stress response 69

4.2.7 Cluster 3 contained genes potentially involved in nodule senescence 71

4.2.8 Cluster 4 contains a gene involved in senescence 71

4.3 Discussion 73

4.4 Conclusion 75

**Chapter 5: Developing genetic transformation in *Parasponia andersonii* and *Medicago truncatula* to enable cell-type investigation of nodule regulation** 76

5.1 Introduction 76

5.1.1 Cell type location of the nodulation signalling pathway 76

5.1.2 Fluorescence-activated cell sorting can be used to isolate different cell types 81

5.1.3 Aims and objectives 82

5.2 Results 83

5.2.1 Generating *Medicago truncatula* transiently-expressing marker lines 83

5.2.2 Generating *Medicago truncatula* stable lines expressing a marker 85

5.2.3 *Parasponia andersonii* leaves require different conditions compared to *Parasponia andersonii* stems for efficient transformation 89

5.2.4 *Parasponia andersonii* may be resistant to glufosinate 93

5.2.5 Transforming *Parasponia andersonii* with a kanamycin resistance-harbouring vector, following an existing protocol 96

5.2.6 Progress towards a new protocol to transform *Parasponia andersonii* leaves and stems 98

5.2.7 Protoplasts can be generated from *Parasponia andersonii* roots 99

5.3 Discussion 101

5.4 Conclusion 103

**Chapter 6: Discussion** 104

6.1 Importance of research on scope of legume-rhizobia interactions 104

6.2 *Sinorhizobium medicae* WSM419 is an efficient symbiotic partner for *Medicago truncatula* 104

6.3 The promiscuity of *Parasponia andersonii* is not coupled with nodule efficiency 105

6.4 *Parasponia andersonii* has control over the symbiosis even after nodule organogenesis has commenced 107

6.5 Progress towards future tools for analysing symbiosis in legumes and non-legumes 109

6.6 Future directions for this research 110

**References** 112

# List of Figures

**Chapter 1: Introduction**

Figure 1.1 A phylogenetic tree of the plant species mentioned throughout the introduction 2

Figure 1.2 Different tissue types of a *Medicago truncatula* root. 4

Figure 1.3 Some genomic highlights in nodulation research 5

Figure 1.4 *Parasponia andersonii* trees 9

Figure 1.5. Rhizobia confers protection to *Glycine max* from *Halicoverpa zea.* 15

Figure 1.6 Nodule diversity: form and function. 18

Figure 1.7 Fluorescence Activated Cell Sorting (FACS) system 19

**Chapter 2: Methods**

Figure 2.1 Vector map of pEXPA:mCherry-ER used for plant transformation 28

Figure 2.2 Vector map of PEP_pBFWFS7 used for plant transformation 28

**Chapter 3: Shoot, root and nodule weight and nodule number comparisons between *Medicago truncatula* and *Parasponia andersonii* during nodulation with different rhizobial strains**

Figure 3.1. *Medicago truncatula* plants inoculated with *Sinorhizobium meliloti* (WSM1022) or *Sinorhizobium medicae* (WSM419) were larger and visually healthier, in terms of shoot greenness 39

Figure 3.2. Nodule number on *Medicago truncatula* was significantly higher when inoculated with *Sinorhizobium meliloti* (WSM1022) 40

Figure 3.3 Shoot fresh weight of *Medicago truncatula* was significantly larger with Sinorhizobium medicae (WSM419) and *Sinorhizobium meliloti* (WSM1022) rhizobia but no significant difference was found in root fresh weight. 41

Figure 3.4 *Parasponia andersonii* inoculated with *Bradyrhizobium elkanii* (WUR3) were larger and healthier 43

Figure 3.5. Shoot and root fresh weight of *Parasponia andersonii* was significantly larger when inoculated with *Bradyrhizobium elkanii* (WUR3) 44

Figure 3.6 Nodule weight per plant of *Parasponia andersonii* was significantly larger with *Bradyrhizobium elkanii* (WUR3), but *Mesorhizobium plurifarium* (BOR2) had the significantly highest number of nodules 45

Figure 3.7 *Parasponia andersonii* nodule phenotypes when inoculated with different rhizobial species 47

**Chapter 4: Analysing the differences in nodulation of *Parasponia andersonii* with *Mesorhizobium plurifarium* (BOR2) compared to *Bradyrhizobium elkanii* (WUR3)**

Figure 4.1 Electron microscopy images of *Parasponia andersonii* nodules inoculated with either *Bradyrhizobium elkanii* (WUR3) or *Mesorhizobium plurifari*um (BOR2) 57

Figure 4.2 Principal component analysis of RNAseq data from *Mesorhizobium plurifari*um (BOR2) vs *Bradyrhizobium elkanii* (WUR3) vs mock inoculation in a time course of *Parasponia andersonii* roots 59

Figure 4.3 PCA plot and heatmap visualising *Mesorhizobium plurifari*um (BOR2) vs *Bradyrhizobium elkanii* (WUR3) inoculated *Parasponia andersonii* nodules differential gene expression 61

Figure 4.4 An enhanced volcano plot showing the $\log_2$ fold change of gene counts of *Mesorhizobium plurifari*um (BOR2) vs *Bradyrhizobium elkanii* (WUR3 inoculated *Parasponia andersonii* nodules versus the $\log_{10}$ *P*-value 62

Figure 4.5 Clustering of *Mesorhizobium plurifari*um (BOR2) vs *Bradyrhizobium elkanii* (WUR3) inoculated *Parasponia andersonii* DEGs, with a heatmap showing the DEGs within the four clusters 63

Figure 4.6 Box plots of significant DEGs found in enriched GO terms 68

Figure 4.7 Expression of a significant DEG (*PanWU01x14_152000*) found in Cluster 2 enriched GO terms 70

Figure 4.8 An overview of the *Mesorhizobium plurifari*um (BOR2) *Parasponia andersonii* nodule progression 74

**Chapter 5: Developing genetic transformation in *Parasponia andersonii* and *Medicago truncatula* to enable cell-type investigation of nodule regulation**

Figure 5.1 Overview of the nodulation signalling pathway 77

Figure 5.2 Overview of rhizobia colonisation via root hair curling or crack entry to form nodules 80

Figure 5.3 Vector map of pEXPA:mCherry-ER used for plant transformation 83

Figure 5.4 *Medicago truncatula* transiently transformed with a pEXPA:mCherry-ER vector vs wild-type 84

Figure 5.5 pEXPA:mCherry-ER successfully transformed into *Agrobacterium tumefaciens.* 85

Figure 5.6 PCR genotyping of pEXPA:mCherry-ER putative stable *Medicago truncatula* transformants 87

Figure 5.7 Characterisation of fluorescence in *Medicago truncatula* stably transformed with a pEXPA:mCherry-ER vector 88

Figure 5.8 Assessment of media requirements for induction of callus growth on *Parasponia andersonii* shoots on leaves. 91

Figure 5.9 *Parasponia andersonii* leaves must be kept in the dark until a callus has been formed. 92

Figure 5.10 Vector map of PEP_pBFWFS7 used for plant transformation 93

Figure 5.11 Tests for natural resistance to glufosinate in *Parasponia andersonii* stems remain inconclusive. 94

Figure 5.12 *Parasponia andersonii* is more resistance to glufosinate on the abaxial side of the leaf, compared to when the leaves adaxial side. 95

Figure 5.13 *Parasponia andersonii* tissue did not survive the stable transformation selection process 97

Figure 5.14 Green *Parasponia andersonii* tissue on a kanamycin selection 99

Figure 5.15 *Parasponia andersonii* protoplasts generated from root material 100

**Chapter 6: Discussion**

Figure 6.1 An overview of the key findings in this work 111

# List of Tables

**Chapter 2: Methods**

Table 2.1 Modified Fåhraeus medium (MFM) media components 22

Table 2.2 Growth Media for *Medicago truncatula* and *Parasponia andersonii* transformation protocols and for *P. andersonii* tissue culture 23

Table 2.3 Nutrient media used for watering *Medicago truncatula* and *Parasponia andersonii* in pots with perlite and vermiculite 23

Table 2.4 Components of solution A and solution B used for generating protoplasts 27

Table 2.5 Primer sequences used for genotyping stable pEXPA:mCherry-ER transformations 32

Table 2.6 Thermocycler conditions for PCR genotyping 32

**Chapter 4: Analysing the differences in nodulation of *Parasponia andersonii* with *Mesorhizobium plurifarium* (BOR2) compared to *Bradyrhizobium elkanii* (WUR3)**

Table 4.1 Enriched biological function (BP), molecular function (MF) and cellular component (CC) GO terms within the 318 genes in Cluster 1 65

Table 4.2 Enriched biological function (BP), molecular function (MF) and cellular component (CC) GO terms within the two genes in Cluster 2 70

Table 4.3 Enriched biological function (BP), molecular function (MF) and cellular component (CC) GO terms within the two genes in Cluster 3 71

Table 4.4 Enriched biological function (BP) and molecular function (MF)) GO terms within the two genes in Cluster 4 72

## Acknowledgments

I would first like to thank and show huge gratitude towards my supervisor, Professor Miriam Gifford, for all of her guidance and support throughout my PhD. Professor Gifford not only gave me the chance to work on an exciting project but helped me develop myself into a better scientist. I would also like to acknowledge all of the members of the Gifford Lab past and present for creating such a positive experience during these past few years of research. With a special mention of Dr Beatriz Lagunas, Dr Emma Picot, Jamie Burgess, Alice Coppock, Beth Richmond, Monique Rowson, Dr Cantug Bar and Lochlan Chadwick.

For providing the *Parasponia andersonii* plants, without which this project would never have happened, and for answering my *P. andersonii* questions, I would like to thank Dr Rene Guerts and his lab members. I also appreciate Dr Proyash Roy from the Gifford group for introducing me to *P. andersonii*. For keeping my plants thriving in the glasshouse I would like to thank Gary Grant and all the members of the Phytobiology facility team. I am also grateful to Matthew Smoker for his advice on my *Medicago truncatula* stable transformation.

For helping to answer my RNA-Seq questions, I would like to thank Luke Richards, Javier Antúnez-Sánchez and Dr Liam Walker. A special thanks to Dr Laura Baxter for all her help as well and for creating the GO term map file needed for the RNA-Seq of *P. andersonii*

I am grateful to Dr Joe McKenna for not only sharing his work on imaging nodules but for also helping me to get my own nodule images. For creating the electron microscopy nodule images, I would like to recognise the members of the Midlands Regional Cryo-EM Facility, hosted at the Warwick Advanced Bioimaging Research Technology Platform. An extra thanks to Ian Hands-Portman for training me on using the confocal microscope.

I would also like to acknowledge BBSRC MIBTP for funding my PhD.

Thank you to all of my friends and family for their encouragement and support. I am especially grateful for Henry Lamberton for being by my side throughout my academic journey so far from my undergraduate degree, my MRes and now my PhD. I am so lucky to have you, Lilly, and Lyra always be there for me.

## Declaration and Inclusion of Material from a Prior Thesis

This thesis is submitted to the University of Warwick in support of my application for the degree of Doctor of Philosophy. It has been composed by me and has not been submitted in any previous application for any degree.

The work presented (including data generated and data analysis) was carried out by the author except in the cases outlined below:

Dr Laura Baxter created the GO term map that I used to conduct the GO term analysis on the *Parasponia andersonii* RNA-Seq data.

The electron microscopy images were collected by Midlands Regional Cryo-EM Facility, hosted at the Warwick Advanced Bioimaging Research Technology Platform.

Figure 1.3 was created in collaboration with Alice Coppock

## Abstract

Legumes and one of the five species of non-legumes, *Parasponia andersonii*, are capable of having symbiotic relationships with nitrogen fixing rhizobia. This allows them to have a nitrogen source even if the surrounding environment lacks nitrogen. This led to the investigation of how nodulation in *P. andersonii* differs in its phenotypes in nodulation compared to *M. truncatula* and what the difference are at a molecular level. Being able to compare and contrast the nodulation regulatory machinery of *P. andersonii* and *M. truncatula* at the cell type level could help to better elucidate how nodulation might be conserved across plant species.

*P. andersonii* has been found to have a broad range of symbiotic partners, how much of an advantage this relative rhizobial promiscuity gives *P. andersonii* is currently unknown. Therefore, the phenotypic responses and form and regulation of nodulation of *P. andersonii* and *M. truncatula* to different rhizobial strains/species were analysed. *M. truncatula* was found to have a productive symbiotic relationship with *Sinorhizobium medicae* (WSM419) and *Sinorhizobium meliloti* (WSM1022) whilst *P. andersonii* had a productive symbiotic relationship with *Bradyrhizobium elkanii* (WUR3). *P. andersonii* was also found to have nodules form with *Mesorhizobium plurifari*um (BOR2), yet there was no increase in shoot or root fresh weight.

This led to trying to understand the underlying molecular differences between the WUR3 and BOR2 phenotype. Using microscopy and RNA-Seq analysis led to the conclusion that *P. andersonii* is capable of sanctioning rhizobia through rhizobial degradation and nodule senescence.

Due to orthologs of key nodulation regulatory *M. truncatula* genes that have been identified in *P. andersonii* and their role seems to be conserved. Progress towards generating stable cell type fluorescent lines of *M. truncatula* and *P. andersonii* has been made which will allow for further research into nodulation pathway signalling in the different root tissue types.

# Abbreviations

| | |
|---|---|
| ACC | 1-Aminocyclopropane-1-Carboxylic Acid |
| AP2 | Apetala2 |
| ARF | Auxin Response Factor |
| ATG | Autophage-Related Genes |
| BAP | 6-Benzylaminopurine |
| bHLH | Basic Helix-Loop-Helix |
| BP | Biological Processes |
| CAS | Cold-Acclimation-Specific |
| CC | Cellular Components |
| CRE | Cytokinin Response |
| CRISPR | Clustered Regularly Interspaced Short Palindromic Repeats |
| DEG | Differentially Expressed Gene |
| DMI | Does Not Make Infections |
| DNA | Deoxyribonucleic Acid |
| DNF | Defective in Nitrogen Fixation |
| DTT | Dithiothreitol |
| EDTA | Ethylenediaminetetraacetic Acid |
| EIN | Ethylene Insensitive |
| ENOD | Early Nodulin |
| ER | Endoplasmic Reticulum |
| ERF | Ethylene Response Factor |
| ERN | Ethylene Response Factor Required for Nodulation |
| EXPA | Expansin |
| FACS | Fluorescent Activated Cell Sorting |
| GFP | Green Fluorescent Protein |
| GO | Gene Ontology |
| IBA | Indole-3-Butyric Acid |
| IEF | Infection-Related Epidermal Factor |
| IPD | Interacting Protein of DMI3 |
| IPN | Interacting Protein of NSP2 |
| IRLC | Inverted Repeat Lacking Clade |
| IT | Infection Thread |
| LB | Luria Broth |
| LBD | Lob-Domain Protein |
| LYK | LysM Domain Receptor-Like Kinase |
| MAPK | Mitogen-Activated Protein Kinase |
| MES | 2-(N-morpholino)ethanesulfonic acid |
| MF | Molecular Functions |
| MFM | Modified Fåhraeus Medium |
| NAA | 1-Naphthaleneacetic acid |

| | |
|---|---|
| NCR | Nodule Specific Cysteine-Rich |
| NF | Nod Factor |
| NF-YA | Nuclear Transcription Factor Y Subunit A |
| NFP | Nod Factor Perception |
| NIN | Nodulation Inception |
| NPL | Nodulation Pectate Lyase |
| NSP | Nodulation Signalling Pathway |
| OD | Optical Density |
| PCA | Principal Component Analysis |
| PCR | Polymerase Chain Reaction |
| PEP | Endopeptidase |
| RNA | Ribonucleic Acid |
| ROS | Reactive Oxygen Species |
| RPG | Rhizobium-Direction Polar Growth |
| SH | Schenk-Hildebrandt |
| SNARE | N-Ethylmaleimide Sensitive Factor Attachment Protein Receptor |
| STY | Stylish |
| TDZ | Thidiazuron |
| TIR-NBS-LRR | Toll-interleukin receptor/nucleotide-binding site/leucine-rich repeat |
| TY | Tryptone-Yeast |
| VAMP | Vesicle-Associate Membrane Protein |
| WPM | Woody Plant Media |
| XTH | Xyloglucan Endotransglucosylase/Hydrolase |
| YLS | Yellow Leaf Specific |

# Chapter 1: Introduction

## 1.1 Current problems feeding the global population

Following the one billion people that have been added to the population between 2010 and 2022, a population of 9.7 billion is predicted to be reached by 2050 as projected in the most recent United Nations report (United Nations, 2022). Feeding all of these people is one of the major challenges for humanity which adds to the already strained goal to end the current problem of world hunger by 2030 (WHO, 2022). Currently, after decades of steady decline in world hunger, the number of those determined to be suffering from hunger has increased since 2015 (WHO, 2022). In 2021, it was estimated that 923.7 million people had little access to food and over 2.3 billion did not have access to safe, nutritious, and sufficient amounts of food (WHO, 2022). These statistics show that food production needs to be more efficient so food crops can be grown in poorer soils to allow communities that suffer from hunger to have more easily accessible food sources.

## 1.2 What are legumes and why are they important for food security?

An essential family of plants called legumes can be considered some of the most interesting and promising future crop plants that already exist. With more than 22,000 species within 772 genera (le Roux et al., 2022), many have a unique ability to use bacteria located in the soil to enhance their growth. These bacteria are called rhizobia and they are housed in tissues called nodules that are formed on roots of the plants. The rhizobia take in atmospheric nitrogen and turn it into ammonium (through metabolic reactions) which is a useable form of nitrogen for plants to metabolise in essential processes. In return, the plant provides the rhizobia with ions, metabolites, proteins, fixed carbon as reviewed in (Roy et al., 2020a) as well as a protective environment. The host plant also provides its resident bacteria with homocitrate synthase. This synthase is needed as a cofactor of the nitrogenase FeMo complex for nitrogen to be fixed (Hoover et al., 1989). This exchange in nutrients or metabolites creates a mutually benefit symbiosis and many legume crops are able to take advantage of this symbiotic strategy, such as soybeans, groundnuts, and dry beans. Legumes are thus economically and nutritionally significant with an estimated

global agricultural use of over 113 million tonnes in 2020 (FAO, 2022). Farmers can also use legumes to improve soil health and therefore improving crop health of plants that cannot form symbiotic nodules through intercropping. For instance, intercropping *Glycine max* (soybean) with sugarcane (an important crop in sugar production) showed higher biomass in the sugarcane along with significantly higher amounts of carbon and nitrogen found within the soil (Malviya et al., 2021). Legumes alter the pH in the soil which can promote the soil microbiome activity (Epihov et al., 2021) and influence the composition of the soil microbiome as well (Solanki et al., 2020, Yu et al., 2021). However, nodulation is not just limited to the relationship between legumes and rhizobia. As will be discussed later in the introduction (Sections 1.7, 1.8 and 1.9), other nitrogen-fixing symbiotic relationships such as actinorhizal plants and *Frankia*, cycads and cyanobacteria as well as the non-legume *Parasponia andersonii* exist (Figure 1.1).

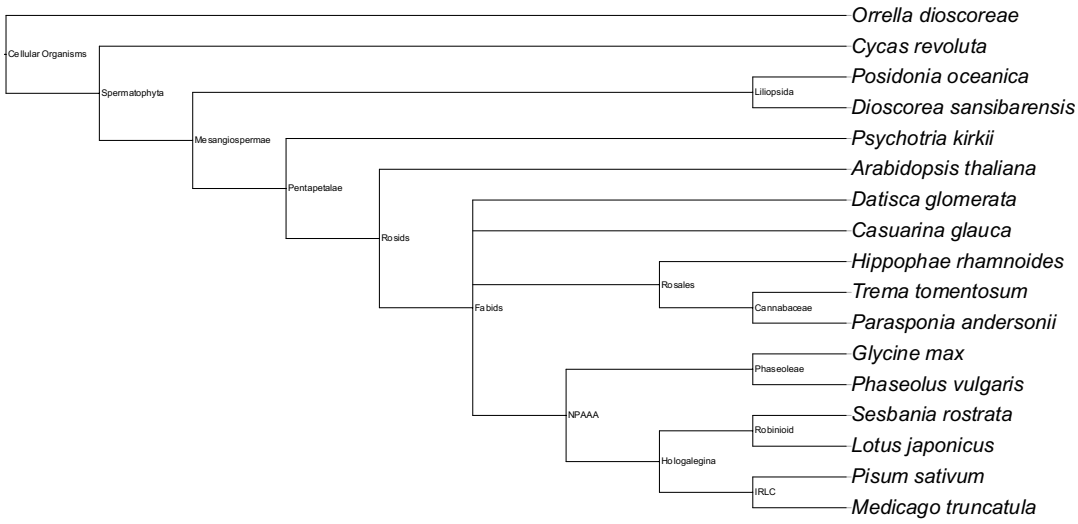


**Figure 1.1 A phylogenetic tree of the plant species mentioned throughout the introduction.**
The evolutionary relationships between the different plant species mentioned throughout this introduction, from legumes such as *Medicago truncatula*, cycads such as *Cycas revoluta* and the non-legume *Parasponia andersonii*.
IRLC = Inverted repeat-lacking clade, NPAAA = non-protein amino acid-accumulating clade. Tree not to scale and made using https://itol.embl.de and the https://www.ncbi.nlm.nih.gov database.

Investigating these nitrogen-fixing symbiotic relationships that could lead to crop application and could result in less synthetic nitrogen fertiliser being used in

agriculture, which is significant because synthetic nitrogen fertiliser is a huge environment strain. In 2018, it was estimated that 6.8 % of global agricultural emissions were caused by the synthetic nitrogen fertiliser supply chain, with 1.13 gigatonnes of $CO_2$ equivalent emissions being produced (Menegat et al., 2022). This applied nitrogen fertilisers can not only be lost as greenhouse gases, but it can also leach into water sources, causing eutrophication (Balasuriya et al., 2022). Bringing the benefits of nodulation into crops that do not already utilise this strategy could therefore help to address issues of hunger and environmental impacts, in the face of a rapidly increasing population problem.

## 1.3 The root is comprised of different cell types with unique roles in nodulation

The root of a plant contains many different tissue types (Figure 1.2). Within the centre of the root is an area called the stele, which houses the vascular bundle consisting of the xylem and phloem used for essential water and nutrient transport. Surrounding the stele is the single layered pericycle, then the single layered endodermis. A large section of the root is comprised by the cortex, which varies in thickness across different species. Whilst the model for plant research, *Arabidopsis thaliana,* has a single cortical layer, the model legume *Medicago truncatula* usually has between four and six layers of cortex (Xiao et al., 2014). In *M. truncatula*, the inner cortex layer is 15 µm thick whilst the other layers are twice as thick at 30 µm thick (Xiao et al., 2014). Finally, a single layer of epidermis forms the outmost layer of the root and so is in contact with the external environment.

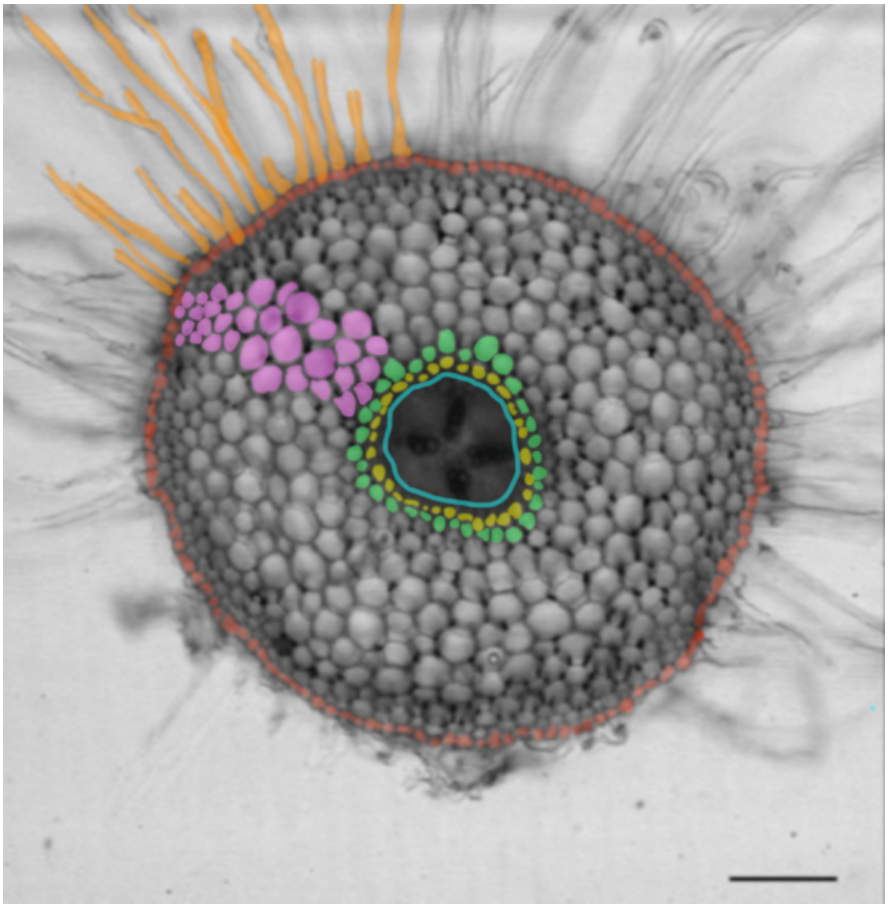

**Figure 1.2 Different tissue types of a *Medicago truncatula* root**.
From the outside in, orange shows the root hairs that have formed from the epidermis outlined in red. The thick pink layer is the cortex, and the internal rings are the endodermis (green) and the pericycle (yellow). The blue circle designates the stele that contains the xylem, phloem, and companion cells. Scale bar = 0.1 mm. Adapted from (Lagunas et al., 2018).

## 1.4 Stages of nodulation: initial legume-rhizobia interaction

The mechanisms that underlie both nodulation and its regulation are complex and the research into these has been ongoing for many years, including the generation of reference genomes (Figure 1.3). Spanning across the entire root and involving many different root tissue types (Xiao et al., 2014), nodulation requires a strict control system. Traditionally, it has been viewed that the first stage of this process within the legumes starts with production of flavonoids via the phenylpropanoid pathway as reviewed in (Dong and Song, 2020). These flavonoids have many roles in plants, this includes a role in the pigmentation in flowers (Wu et al., 2018), modulating auxin distribution (Buer and Muday, 2004) as well as a signal

to rhizobia in the soil. However, it must be noted that there has been recent research suggesting that the importance of flavonoids as a chemoattractant has been inflated and that there may be other attractants that are more important in this process such as amino acids (Compton et al., 2020).

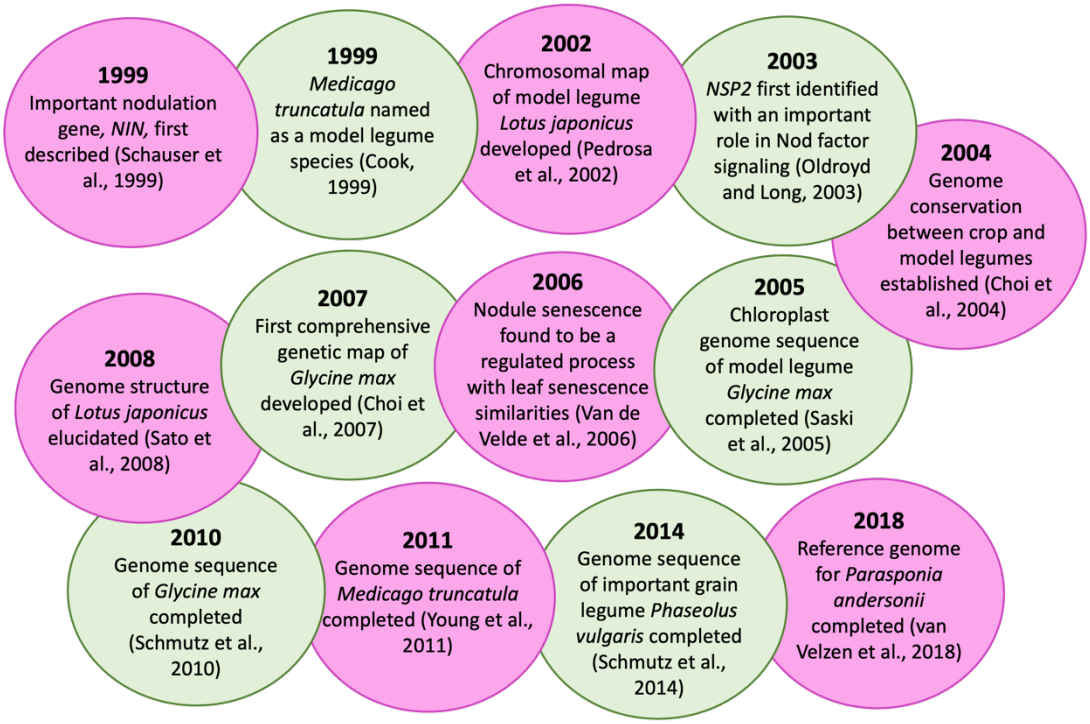


**Figure 1.3 Some genomic highlights in nodulation research**
Uncovering the regulation of nodulation has been ongoing for decades with many important genomes being completed. Adapted from (Sahruzaini et al., 2020).

Akin to a conversation between the two species, rhizobia in the soil respond to the flavonoid signals, or perhaps another chemoattractant, by producing Nod factors (NFs). NFs are lipochitooligosaccharides which are recognised by the plant NF receptor proteins (Cai et al., 2018). However, it must be noted that there are legumes that exist that do not depend on NFs for rhizobia to gain entry (Chaintreuil et al., 2016). In most nodulating plants, NFs receptor genes are then activated, and receptor kinases bind rhizobial NFs at the plasma membrane of the epidermis and the infection thread membrane. These receptor kinases are also involved in host selection, along with the plant immune system, to ensure only certain bacteria gain entry to the plant.

Upon the recognition of NFs, Does Not Make Infections (*DMI1*) is then activated and is involved in regulating the calcium spiking which is essential in early signalling during nodule initiation (Liu et al., 2022a). The calcium oscillations activate the expression of *DMI3* and Interacting Protein of *DMI3* (*IPD3*) complex (Rival et al., 2012, Messinese et al., 2007). The expression of *DMI3* and *IPD3* leads to regulation of gene expression and forms a DELLA linked complex with Nodulation Signalling Pathway 1 (*NSP1*) and *NSP2* (Jin et al., 2016) allowing for the nodulation signalling pathway to continue. Nodule INception (*NIN*) is also first expressed during this stage and is downstream of *NSP1/NSP2* and *DMI3*/*IPD3* (Xiao et al., 2020, Jin et al., 2016), which is an important transcription factor that Is involved throughout the nodulation process. *NIN* is expressed in many tissue types in the root, from the pericycle to the epidermis (Vernié et al., 2015), but its role varies depending on the cell type.

After the initial conversation between the plant host and the rhizobia, the next stage occurs involving rhizobia entry into the plant.

## 1.5 Stages of nodulation: rhizobial entry

After initial perception by the plant, which typically includes alteration of signalling to enable microbial entry, the rhizobia can gain access to the plant. Rhizobia can enter the plant through a “crack entry” method, where they enter through the literal cracks present in the epidermis and it is estimated that around 25 % of legumes allow rhizobia to enter through this method as reviewed in (Sharma et al., 2020).

The other method of entry that is found is via root hair curling and formulation of a microbial infection thread, as seen in *M. truncatula* (Peleg-Grossman et al., 2007). Root hairs curl and trap the rhizobia, then the rhizobia enter what is called the infection chamber. For the rhizobia to reach the forming nodule a structure called an infection thread from the infection chamber that goes down the length of the root hair and into the epidermis (Liu et al., 2019a). Following the initial rhizobial interaction, there is a cellular reactive oxygen species (ROS) burst (Cárdenas et al., 2008), cell wall and membrane remodelling (Fournier et al., 2015) along with cytoskeleton rearrangements (Kitaeva et al., 2015). These changes allow for the

rhizobia to travel through the root via the infection threads towards the nodule primordia (Xiao et al., 2014). This is where more cell wall remodelling is needed to allow for the release of the rhizobia into the nodule primordia. *Glycine max* for example, uses genes involved in the exocytotic pathway, such as vesicle-associated membrane protein 721 d (*VAMP721d)*, to deliver these cell wall modifying enzymes to the location of rhizobial release (Gavrin et al., 2016).

As part of this mechanism to allow rhizobia entry, the NFs the rhizobia produce are degraded. In *M. truncatula*, a hydrolase called *MtNFH1* has been shown to have a role in this degradation and when this gene is mutated, there was delayed infection and formation of infection threads (Cai et al., 2018). Plant symbiotic hosts have also been found to control the amount of nodulation by also degrading another receptor of NFs, *DMI2* (as found in *M. truncatula*) (Pan et al., 2018). The whole process of nodulation is a very controlled one, even at the very beginning, the host is not allowing for overnodulation.

## 1.6 Stages of nodulation: nodule organogenesis

There are two types of nodules that legumes can possess, indeterminate and determinate. Determinate nodules, formed by plants such as *Lotus japonicus* (Kohlen et al., 2018), lose their meristem at an early stage of development (Xiao et al., 2014). Indeterminate nodules, formed by plants such as *M. truncatula*, retain their meristem and continue producing different nodule tissue cells throughout the lifetime of the nodule (Xiao et al., 2014). There is also a difference between indeterminate and determinate nodules in where the nodule primordium develops and where cell divisions occur, and the way that the nodule undergoes maturation (Roy et al., 2020b, Kohlen et al., 2018). One other major different between them is that the rhizobia inside indeterminate nodules will terminally differentiate and if the nodule is determinate are still similar to free-living bacteria (Mergaert et al., 2006).

However, the fundamentals of nodule organogenesis are similar. During nodulation, the pericycle cells are the first to become mitotically active in *M. truncatula*, followed by the inner cortex (Timmers et al., 1999). This leads to cell division that starts at the pericycle but includes the endodermis and cortical layers

and leads to formation of a nodule primordium (Xiao et al., 2014). Important contributors to nodulation appear throughout the root cell types, some are more restricted to the cell types (for example Cytokinin Response 1 (*CRE1*)) is restricted to the cortex (Liu et al., 2019b), whilst others are found in many of the different root tissue types. One that is found throughout the root tissue types from the epidermis to the pericycle is *NIN. NIN* plays a role co-ordinating the responses of the epidermis and cortex nodulation (Vernié et al., 2015) and is also required for regulation of development of the infection thread from the root hair to the outer cortex (Liu et al., 2019a). A more in depth look at the nodulation signalling pathway for nodule organogenesis can be found in Section 5.1.1.

Even after nodule organogenesis, the host plant can control the symbiotic relationship through nodule senescence (degradation of the nodule) (Van de Velde et al., 2006). Further details on this process can be found in Section 4.1.4, but nodule senescence again shows another control process the plant has over nodulation.

## 1.7 The non-legume *Parasponia andersonii*

The *Parasponia* genus contains the only five non-legume species that can have nitrogen-fixing nodules in partnership with rhizobia (van Velzen et al., 2018, Van Zeijl et al., 2018). One of these species is *Parasponia andersonii* (Figure 1.4), found in tropical areas such as Papua New Guinea. This relatively fast-growing tree lives on the side of volcanic hills (Wardhani et al., 2019).

Despite not being a legume, *P. andersonii* has 290 putative orthologs of *M. truncatula* genes showing enhanced nodule expression between *P. andersonii* and *M. truncatula* that have been found (Wardhani et al., 2019). Whilst there has been much discussion on whether nodulation evolved more than once or whether it came from a single origin (Cannon et al., 2015), these shared orthologs between *M. truncatula* and *P. andersonii* show that there is evidence that there was a single origin for nodulation. This has also been explained by analysing the non-nodulator *Trema tomentosa* that is closely related to *P. andersonii*, which showed that non-nodulators simply lost the ability to nodulate (van Velzen et al., 2018).

**Figure 1.4 *Parasponia andersonii* trees**
3+ month old *Parasponia andersonii* plants (red arrow) and more mature *P. andersonii* trees at around 1+ year old (blue arrow).

*P. andersonii* is relatively promiscuous compared to legumes where there is a high degree of rhizobial partner specificity (Op den Camp et al., 2012). There have been mixed findings on whether host promiscuity is advantageous, and such a plant can be described as a "Jack of all trades and master of none", potentially outcompeted by hosts which have a more specialised and fine-tuned rhizobial partner which can potentially provide more nitrogen (Keet et al., 2017, Klock et al., 2016, Ehinger et al., 2014). However, promiscuity can also be viewed as an advantage as it can mean there is a higher chance of finding at least one symbiotic partner, enabling wide niche colonisation that the gain of nitrogen or other benefits enable (Harrison et al., 2018, Klock et al., 2022). Perhaps being a "Jack of all trades" is important for promiscuous plants to establish themselves as the rhizobia within nodules give the host nitrogen for growth as well as other benefits such as defence priming as will be discussed further.

## 1.8 Nitrogen-fixation in non-rhizobial nodules

Beyond the rhizobial symbiotic relationships described so far, there are other examples of plants that can form nitrogen-fixing nodules with bacteria other than rhizobia. Actinorhizal plants consist of 8 families and 25 genera including *Hippophae rhamnoides*, *Datisca glomerata* and *Casuarina glauca.* Actinorhizal plants are able to form nitrogen fixing nodules with *Frankia* bacteria rather than rhizobia (Diagne et al., 2013). Remarkably, this relationship is estimated to account for as much as 15 - 25 % of global nitrogen fixation as reviewed in (Dawson, 2007). The research on nitrogen fixation in actinorhizal plants is limited compared to legumes but major progress is being made. Both *C. glauca* and *H. rhamnoides* have been suggested as model species for acintorhizal symbiosis, and the generation of a reference genome for *H. rhamnoides* is enabling some progress to be made on elucidating the molecular mechanism of actinorhizal interactions (Wu et al., 2022, Zhong et al., 2013).

*Frankia* bacteria are gram-positive, branching, filamentous soil bacteria (Echbab et al., 2007), many of which have the ability to form a symbiosis with plants (Nguyen et al., 2019), *Frankia* share many similarities with rhizobia in terms of nitrogen fixation as they both produce nitrogenase (Nouioui et al., 2019) and invade via infection threads (Gasser et al., 2022). However, they differ from rhizobia in that they can also fix nitrogen in aerobic conditions outside of the roots of plants. They can do this due to the presence of vesicle structures at the ends of their hyphae that protects the nitrogenase from oxygen (Meesters et al., 1987, Parsons et al., 1987). For both *Frankia* and rhizobia, the number of nodules is controlled by the plant, suggesting there are also host regulatory similarities (Wall et al., 2003).

## 1.9 Nitrogen fixation in plant-microbe interactions without nodules

Whilst actinorhizal plants can have a symbiotic relationship with *Frankia* in nodules, cycads have a symbiotic relationship with cyanobacteria and host them within their roots instead of having nodules. Cycads are the oldest extant seed plant and offer an ancient and non-legume example of another nitrogen fixing relationship. Cycads once dominated forests across the globe after they evolved around 300 million years ago but were ousted from that dominating top spot by angiosperms as

reviewed in (Iwanycki Ahlstrand and Stevenson, 2021). A species of cycad called *Cycas revoluta*, also known as sago palm, is a woody plant found today in Japan that originated in Southeast Asia (Kanesaki et al., 2018). Currently, all known species of cycads, such as *C. revoluta*, have been found to form endophytic relationships with photosynthetic cyanobacteria which are housed in coralloid roots as reviewed in (Chang et al., 2019). The cyanobacteria live in a cortical cell layer termed the cyanobacterial zone, which can be seen as a green ring when the coralloid root is cut open (Gutiérrez-García et al., 2019). *C. revoluta* tends to be found in nutrient poor soils such as coastal cliffs, and so the advantage of a symbiotic partner supplying nitrogen can be hypothesised to have enabled them to colonise a challenging environment (Hashidoko et al., 2019).

Cyanobacteria are multicellular bacteria that can photosynthesise as well as fix nitrogen. Whilst this seems contradictory, as nitrogenase is inactivated by oxygen, cyanobacteria separate these two systems spatially, through cellular differentiation (by creating a heterocyst for nitrogen fixation to occur) (Burnat et al., 2014) or temporally, via a biological clock (Compaoré and Stal, 2010). Cycads use cyanobacteria chemoattractions, which are referred to as hormogonium-inducing factors, and include molecules such as diacylglycerol 1-palmitoyl-2-linoleoyl-sn-glycerol (Hashidoko et al., 2019). Once cyanobacteria are inside the plant, the plant produces hormogonium-repressing factors which allows for the heterocyst to form (Hashidoko et al., 2019).

A recent discovery highlights another potentially ancient symbiosis between nitrogen fixing bacteria and *Posidonia oceanica,* a highly-productive mediterranean seagrass (Mohr et al., 2021). The roots of nitrogen fixing *P. oceanica* plants were found to harbour an abundant population of a novel *Celerinatantimonas sp.* of bacteria, '*Candidatus Celerinatantimonas neptuna'* with direct evidence of the transfer of up 98 % of fixed nitrogen being transferred to the plant (Mohr et al., 2021). These bacteria were identified throughout the root cortex – housed both intercellularly and within the root cells (Mohr et al., 2021). This example, demonstrates the evolution of a nitrogen-fixing symbiosis in a non-legume within an aquatic environment and highlights the novelty of symbioses that might be found in unexpected places.

Another structure that shows the variety in plant-bacteria symbiosis is found in aerial roots which some orchids possess and are thought to be play a role in nutrient uptake and even photosynthesis (Zotz and Winkler, 2013, Sma-Air and Ritchie, 2020). There are some species of orchids that interact with cyanobacteria housed within the cracks of their aerial roots which could provide fixed nitrogen for the host, although this needs to be further studied (Tsavkelova et al., 2022). There is also been evidence that maize brace roots, a type of aerial root, can accommodate nitrogen fixing bacteria within mucilage exuded by the aerial roots that can provide as much as 82 % of the plant-required nitrogen (Van Deynze et al., 2018). These examples show that non-legumes have the potential to interact with nitrogen fixing microbes, albeit in more unconventional structures.

The occurrence of different types of nitrogen fixing activity in plants show us that nodulation is not the only mode of plant-nitrogen-microbe interaction. Reciprocally, we also know that symbiotic bacteria can provide more than just nitrogen, as will be discussed below.

## 1.10 More than just nitrogen: defence priming

Plants that house symbiotic bacteria have to regulate the defence systems they possess to allow symiotic bacteria to form a relationship with them whilst keeping pathogens from invading. However, the interaction is even more complicated since it has been found that symbiotic bacteria can provide priming of defences for its host plant. Defence priming can include different aspects, including accumulation of salicylic acid (a phytohormone key to the defence response (Bhar et al., 2018)) and enabling plant defence genes to be activated more quickly in the face of subsequent pathogen interaction. For instance, it was found by (Díaz-Valle et al. 2019) *Rhizobium etli* protected *Phaseolus vulgaris* (common bean) from the pathogen *Pseudomonas syringae.* In this example, the bacterial population of *P. syringae* within the leaf tissue was halved in plants pre-inoculated with *R. etli* in comparison to the uninoculated control as well as lesions caused by the pathogen in the leaf being 75 % smaller in pre-inoculated plants. Not only did *R. etli* protect *P. vulgaris* when directly inoculated, this defence priming was also passed down to the

next generation. Unlike the parent plants, the next generation were not exposed to *R. etli,* yet the plants still exhibited about a 3-fold decrease in the abundance of *P. syringae* in the leaf tissue and approximately an 80 % reduction in the size of lesion tissue formed in comparison to the control (Díaz-Valle et al. 2019). *M. truncatula* and *Pisum sativum* have also been found to benefit from symbiotic bacteria defence priming. When inoculated with *Sinorhizobium meliloti* and *Rhizobium leguminosarum*, the amount of free salicylic acid in the plant shoots increased in comparison to uninoculated plants by approximately 10 % in *M. truncatula* and 30 % in *P. sativum* when exposed to *Erysiphe pisi* (mildew fungus), increasing resistance to the fungus (Smigielski et al., 2019).

Alongside root nodules, a structure that has also been linked to potentially increasing defence responses are leaf nodules. These have been reported in less than 500 species and their size and shape differs from species to species. One example of a plant capable of forming leaf nodules is the dicot *Psychotria kirkii*, which houses its endosymbiont *Burkholderia sp.* within leaf nodules (Carlier et al., 2013). Whilst these endosymbionts are not associated with nitrogen fixation, they have been suggested to provide the host secondary metabolites to aid in defence (Lemaire et al., 2011, Carlier et al., 2016). The symbionts are transmitted through the seeds, however some bacteria do enter though leaf stomata openings as reviewed in (Pinto-Carbó et al., 2018). This is a very specialised form of symbiosis which is so tightly integrated that the plant and bacteria cannot survive without each other; to cultivate the leaf bacteria outside *of P. kirkii* has thus far proven unsuccessful (Carlier et al., 2013). However, recent work has also established an alternate leaf nodule symbiosis model between the monocot *Dioscorea sansibarensis* and *Orella dioscoreae* where it has been possible to culture the host and symbiont independently of one another. The bacterial symbiont *O. diocoreae* also produces secondary metabolites but the exact role of them is as of yet undertermined. However, these secondary metabolites could have a similar role in aiding the plant's defence system like the *Burkholderia* sp. symbiosis with *P. kirkii* (De Meyer et al., 2019). The development of these leaf nodule systems could enable further investigation into how these different forms of nodulation may be able to aid the plant defence response, perhaps acting as a

valuable comparison to the defence priming related to root nodulation as described earlier.

Not only can rhizobia prime their hosts against microbial pathogens in a number of cases, they have also been found to potentially offer anti-herbivory features. In (Dean et al., 2014), differing levels of *Bradyrhizobium japonicum* inoculation of *Glycine max* (soybean) were carried out, with plants also grown on different levels of soil nitrogen; high soil nitrogen and high rhizobial inoculation led to similar amounts of plant % total nitrogen. After five weeks of growth, plants were then infected with *Halicoverpa zea* (soybean podworm). It was found that the larvae preferred the plants with lower rhizobial colonisation, despite all plants having similar total nirogen levels and regardless of the origin of the nitrogen (taken up from soil or fixed via rhizobia) (Figure 1.5). This was also surprising as *H. zea* larvae had higher growth rates on plants with high levels of rhizobial inoculation (0.881 ± 0.059 g/g/day) compared to high soil nitrogen (0.677 ± 0.051 g/g/day). This could potentially be due the rhizobial-related fixed nitrogen but also other rhizobial plant growth promotion activities leading to increasing the nutritional quality such as carbohydrates and phosphates in the plant. Such improvement in plant nutrition has been found in *Rhizobium radiobacter* inocultion of lettuce (Verma et al., 2020).

The observation that *H. zea* preferred high soil nitrogen compared to conditions with high rhizobial inoculum was found to be linked to the defence-related hormone jasmonic acid being found to be produced to a higher level in plants inoculated with larger amounts of rhizobia (Dean et al., 2014). It would be interesting to discover if promiscuous plants are able to better defend themselves against herbivores as they are able interact with a larger number of rhizobial species, as a possible evolutionary advantage of entering in widespread interactions.

Increasing plant defence against pathogens via the use of rhizobial inoculants in plants could also help replace the use of harmful pesticides if we can better understand their protectant function and range as reviewed in (Rani et al., 2021). This could not only offer a benefit for crops that already interact with nitrogen fixing microbes, but for crop varieties that may be developed as the research to transfer nodulation ability to new crops develops, informed by research on species such as

the non-legume *P. andersonii* as well as understanding of leaf nodules and aerial roots housing nitrogen fixing bacteria.

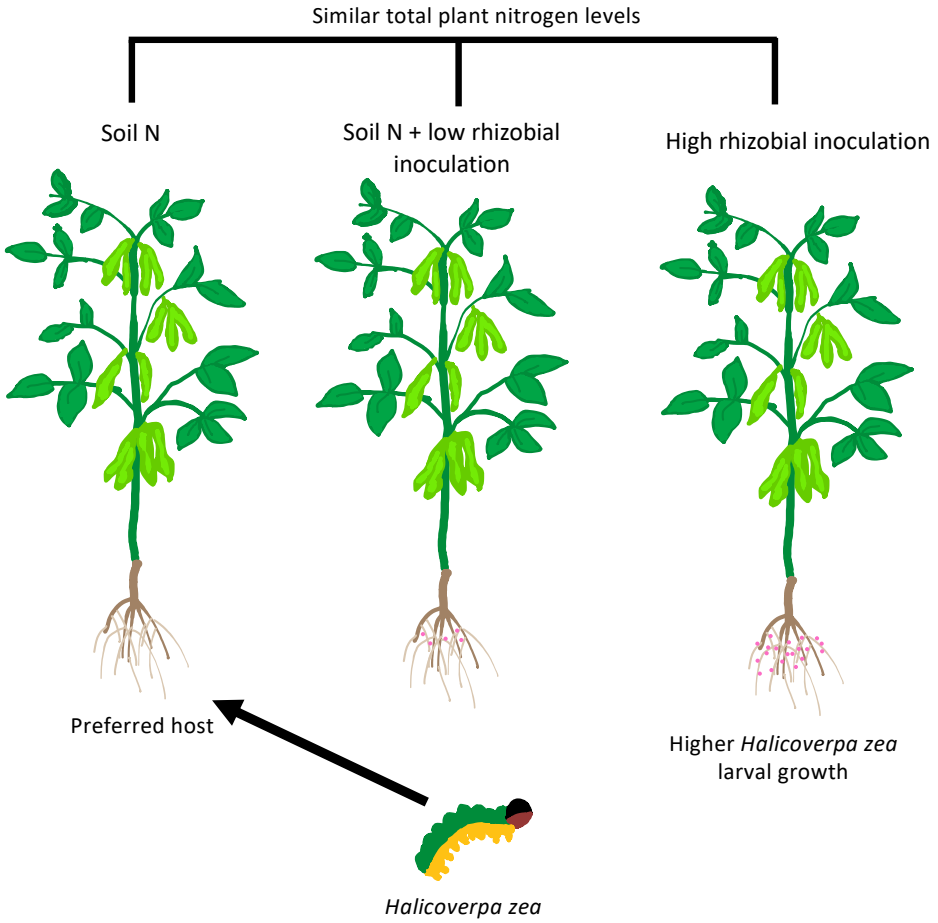


**Figure 1.5. Rhizobia confers protection to *Glycine max* from *Halicoverpa zea*.** Despite *Halicoverpa zea* larvae growing larger on plants with a high amount of rhizobia present, when offered a choice, *H. zea* chooses plants with the lowest rhizobial load.

## 1.11 More than just nitrogen: abiotic stress resistance

Not only do plants face a threat from biotic stress including pathogens and herbivores, but there are also many abiotic and environmental stresses such as drought, high temperature, flooding, and high salt levels. Drought has been shown to reduce cereal production by 10 % on average across the globe (Lesk et al., 2016) and droughts will become more common due to climate change. Under drought, salt excess can become a major issue as it builds up in the soil and can change the osmotic balance, with resultant salt stress being shown to reduce yields in crops such as rice (Hussain et al., 2017); flooding also causes major crop losses and reduced yields

(Shirzaei et al., 2021). Exploring how rhizobia can help plants mitigate the effects of abiotic stress is therefore highly relevant in developing sustainable crop production in the face of a warming planet. It has been found that nitrogen fixing bacteria can indirectly provide drought stress tolerance to their hosts. By providing extra nitrogen, symbiotic bacteria such as *Mesorhizobium huakuii* can allow for plants such as *Astragalus sinicus* L. to produce more arginine which is linked to drought stress tolerance (Liu et al., 2022b). However, it goes further than just providing extra nitrogen; nodulating *M. truncatula* has been shown to recover from drought faster compared to when it is not being nodulated. The rhizobia within the nodules may aid the plant through the period of drought by delaying senescence of the leaves by allowing the accumulation of the osmolyte proline by the plant (Staudinger et al., 2016). It has also been shown that nodulation with different rhizobial strains can result in different performance of *Glycine max* under drought stress. Rhizobial strains showing higher osmotic stress resistance outside of symbiosis were found to have the highest antioxidative parameters and more osmotic stress tolerance in the host (Marinković et al., 2019).

Salt-tolerant rhizobia has been shown to provide better drought resistance in *Phaseolus vulgaris* (common bean); shoot dry weight was almost 30 % higher in plants inoculated with a more salt-tolerant rhizobia compared to plants inoculated with lower salt tolerant rhizobia after seven days of drought (Mnasri et al., 2007). This indicates that rhizobial salt tolerance properties can influence how well the plant host can survive higher salt levels. This has also been shown to be the case with *Vicia faba* (faba bean) where rhizobia strains with different levels of salt tolerance could lead to increased salinity tolerance for the host. Rhizobia with higher salt tolerance themselves had on average higher nitrogen fixing capacity (32.28 ± 1.47 µmol $h^{-1}Plant^{-1}$) compared to rhizobia with a lower salt tolerance (13.83 ± 1.65 µmol $h^{-1}Plant^{-1}$) and testing these under salt conditions may help *V. faba* survive these conditions (Marinković et al., 2019). Salt-tolerant rhizobia have also been shown to directly improve the salt tolerance of plants by changing amino acid composition towards accumulation of amino acids with protective functions in the nodules, such as proline that is involved in osmoregulation (Bertrand et al., 2015, Bertrand et al., 2016). Sulphur is an important macronutrient and a major component of thiols which

act as antioxidant protectants, protecting plants from ROS damage caused by stress such as high levels of salt as reviewed in (Mangal et al., 2022). It has been found that nodules could be important in sulphur assimilation and thiol biosynthesis and that the bacteria within the nodules are important in this process as genes for sulphur uptake and metabolism are upregulated in rhizobia within nodules. For example, when *L. japonicus* was inoculated with *Mesorhizobium loti* it was found that the nodules were rich in these protective thiols (Kalloniati et al., 2015).

By employing rhizobial nodulation under particular environmental conditions *Sesbania rostrata*, a tropical, semi-aquatic legume is able to withstand high levels of salinity as well as flooding. Under aerobic conditions root nodules can be infected via root hair infection threads (Goormachtig et al., 2004). It has been found that the presence of rhizobia stimulates the activity of enzymes that protect against Reactive Oxygen Species (ROS) damage caused by high levels of salt (Liu et al., 2022c). Under flooding, *S. rostrata* can form nitrogen fixing nodules on the roots or on the stem at dormant root primordia, which are structures that can develop into roots when submerged, with the rhizobia entering via a "crack-entry" system under flooded conditions (Capoen et al., 2007). Both stem and root nodules have similar nitrogenase activity which shows that *S. rostrata* gains an advantage of fixed nitrogen in both non-flooded and flooded conditions (Parsons et al., 1992). Perhaps learning more about stem nodules can help the host to overcome environmental issues such as flooding would therefore help in understanding how to mitigate climate-related abiotic impacts including flooding (Edmonds et al., 2020), drought (Pokhrel et al., 2021) and salt (Corwin, 2021). This demonstrates that looking at unusual examples of nodulation that exist (Figure 1.6) is an important aspect in research to help combat global issues. *P. andersonii* being a non-legume that can nodulate can broaden the knowledge base on nodulation and perhaps find new ways to help feed the expanding population.

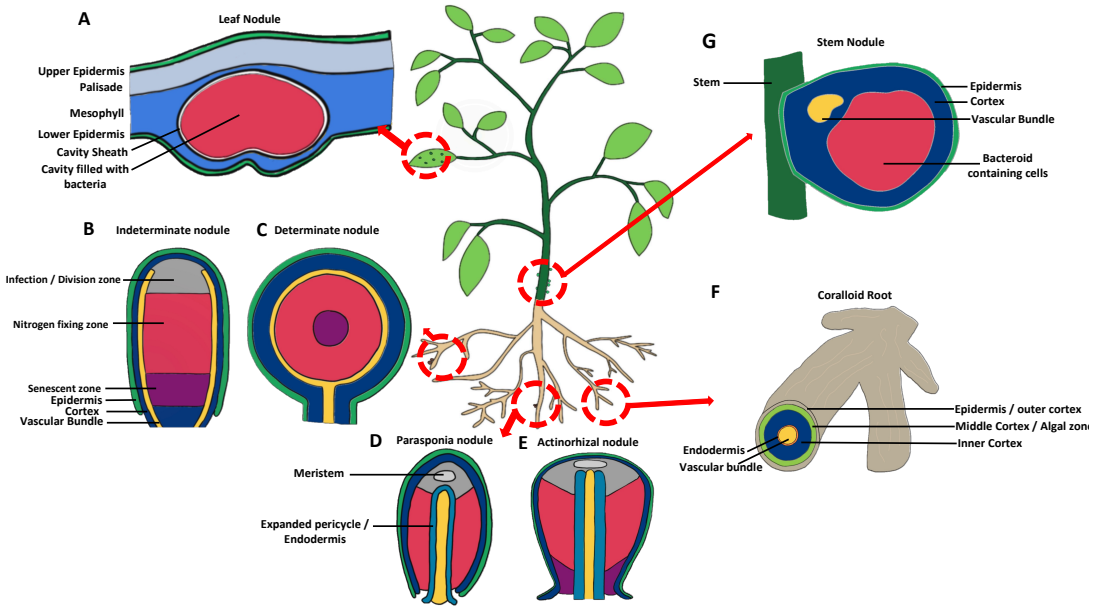


**Figure 1.6 Nodule diversity: form and function.**
An overview of the different types of nodules mentioned throughout this introduction:
(A) Leaf nodules such as those found on *Psychotria kirkii* may not provide fixed N but can bring defence-priming benefits.
(B) Indeterminate nodules are found on legumes such as *Medicago truncatula*.
(C) Determinate nodules are found on legumes such as *Lotus japonicas*.
(D) One of five non-legumes which forms nodules with rhizobia, *Parasponia andersonii*.
(E) Actinorhizal nodules found on actinorhizal plants that house $N_2$-fixing *Frankia* bacteria.
(F) Coralloid roots as found on the cycads, which have a green ring (algal zone) where the cyanobacteria are found.
(G) Stem nodules such as the ones found on *Sesbania rostrata* and *Aeschynomene* spp.
Figure created by Alice Coppock and Helen Wilkinson from figures and original microscope images from (Pinto-Carbó et al., 2018), (Kazmierczak et al., 2020), (Behm et al., 2014), (Pawlowski and Demchenko, 2012), (Chang et al., 2019) and (Fleischman and Kramer, 1998).

## 1.12 Use of cell type analysis to study nodulation and fluorescence activated cell sorting

Fluorescence Activated Cell Sorting (FACS) is an important system for separating fluorescent cells from the rest of a sample to precisely study a specific group. FACS has long been established as an excellent technique in plants science as well by allowing the sort of fluorescent plant protoplasts and provide enough material for 'omics methods such as RNA-seq to be conducted on the sorted cells (Bargmann and Birnbaum, 2010) (Figure 1.7). This establishes FACS as a tool that can

be used for further studying individual tissue types throughout nodule initiation and organogenesis.

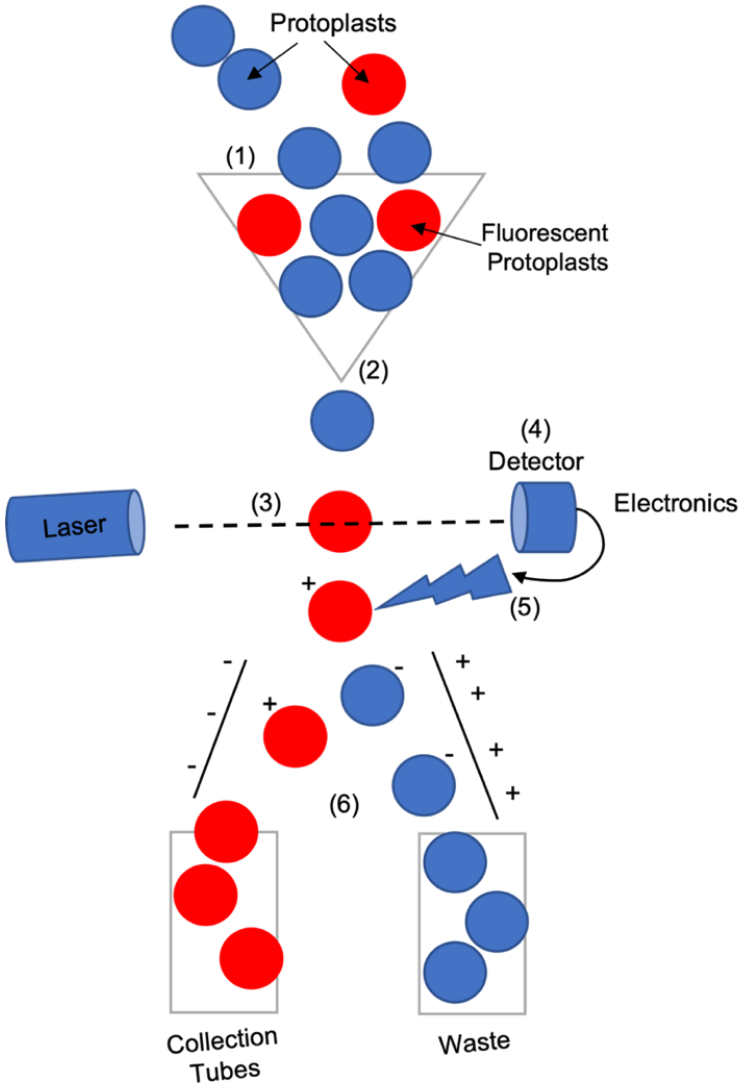


**Figure 1.7 Fluorescence Activated Cell Sorting (FACS) system**
As reviewed in (Carter et al., 2013) plant protoplasts (plant cells with the cell wall removed) with different properties, such as a subset (e.g. cell type) that express a fluorescent marker can be sorted using FACS.
(1) A stream of cells is drawn into the FACS machine, and the stream is enveloped within a sheath fluid via fluidics.
The stream is vibrated at high frequency, leading to the stream breaking into droplets, with the user tuning this process to ideally lead to the presence of one cell per droplet.
(2) The droplet stream passes perpendicularly through a laser stream.
(3) The deflected light is recorded via a series of filters and detectors (optics) that can enable fluorescence and properties of the cells within droplets to be compared via electronic transformation of the data.
(4) The user can then define a 'gate' of properties that describe cells of interest are and can set the machine to apply an electrical charge to matching droplets.
(5) When the cells pass between electrically charged plates the charged droplets are deflected into collection tubes/plates to be taken for further analysis such as RNA-Seq or proteomics.

## 1.13 Thesis aims and objectives

The aims of this thesis are to investigate how nodulation in *P. andersonii* differs in its phenotypes in nodulation compared to *M. truncatula* and what are the difference at a molecular level. Firstly, as *P. andersonii* is already known to be promiscuous and forms a symbiosis with a much broader range of rhizobial strains, including strains of variable nitrogen-fixing efficiencies (Op den Camp et al., 2012). How much of an advantage this relative rhizobial promiscuity this gives *P. andersonii* is currently unknown. Therefore, the first aims of this thesis are to assess shoot, root and nodule weight and nodule number of *P. andersonii* and *M. truncatula* to different rhizobial strains/species (Chapter 3: Shoot, root and nodule weight and nodule number comparisons between *Medicago truncatula* and *Parasponia andersonii* during nodulation with different rhizobial strains).

Secondly, once these phenotypes are known, understanding the underlying molecular differences between any found phenotypes is important. This led to using microscopy and RNA-Seq analysis to further understand the phenotypes found in Chapter 3 (Chapter 4: Analysing the difference in nodulation of *Parasponia andersonii* with *Mesorhizobium plurifarium* (BOR2) compared to *Bradyrhizobium elkanii* (WUR3)).

Finally, orthologs of key nodulation regulatory *M. truncatula* genes have been identified in *P. andersonii* and their role seems to be conserved. For instance, orthologs of *NIN* and Nuclear Transcription Factor Y Subunit A-1 (*NF-YA1*) have been found that are involved in nodule organogenesis and early symbiotic expression in both species (Bu et al., 2020). *P. andersonii* also has a LysM Domain Receptor-Like Kinase 3 (*LYK3*) *M. truncatula* ortholog that recognises rhizobia NFs (Rutten, 2020). Being able to compare and contrast the nodulation regulatory machinery of *P. andersonii* and *M. truncatula* at the cell type level could help to better elucidate how nodulation might be conserved. Generating stable cell type fluorescent lines of *M. truncatula* and *P. andersonii* will allow for further research into nodulation pathway signalling in the different root tissue types (Chapter 5: Developing genetic transformation in *Parasponia andersonii* and *Medicago truncatula* to enable cell-type investigation of nodule regulation).

# Chapter 2: Materials and Methods

## 2.1 Materials (plants and microbes)

The rhizobia used were *Sinorhizobium medicae* (WSM419), *Sinorhizobium meliloti* 1022 (WSM1022), *Mesorhizobium plurifari*um (BOR2) and *Bradyrhizobium elkanii* (WUR3). For the transient transformations, *Agrobacterium rhizogenes* was used whilst for the stable transformations *Agrobacterium tumefaciens* strain AGL1 was used. BOR2, WUR3 and AGL1 were kindly provided by the Guerts lab. The plants used in this study were *Parasponia andersonii* (original plants were kindly provided by the Guerts lab) and *Medicago truncatula* A17.

## 2.2 Plant growth and harvesting methods

### 2.2.1 Germinating *Medicago truncatula*

*M. truncatula* seeds were placed into sulphuric acid for between 10 - 30 minutes until brown spots appeared on most seeds. Seeds were washed seven times in sterile water. *M. truncatula* seeds were then sterilised with 7 % bleach for five minutes before being washed in sterile water seven times. Seeds were placed onto 1.5 % water Phytoagar™ plates and watered three times until the seeds have swollen. Plates were sealed and put in the dark at 4 °C for five days before being moved into 25 °C growth cabinets in the dark for three days. Plantlets were either used for experiments or seed propagation in the climate-controlled growth chamber.

### 2.2.2 Growth conditions for *Medicago truncatula*

*M. truncatula* A17 seedlings were grown at 25 °C with 16 hours of light and 8 hours of dark in growth cabinets. *M. truncatula* plants were also grown in a climate-controlled growth chamber at 24 °C in 16 hours of light and at 20 °C in 8 hours of dark; plantlets used for seed propagation were placed into Levington F2 soil (Sphagnum moss peat plus sand containing 144 mg/l nitrogen, 73 mg/l phosphorus and 239 mg/l potassium).

### 2.2.3 Sterilising *Parasponia andersonii* stems and leaves

To sterilise *Parasponia andersonii* tissue, (Knyazev et al., 2018) and (Wardhani et al., 2019) protocols were combined. Young, healthy, and non-infected stems and leaves were cut from adult *P. andersonii* trees. Stems needed to have around 1 $cm^2$ of leaf tissue left at the end of petioles. First, the tissue was rinsed with sterile water and then surface sterilised with 70 % ethanol for two minutes. For leaves, 0.5 % sodium hypochlorite with a few drops of sterile TWEEN® 20 (polysorbate-20) was added for 15 minutes, with continuous agitation. For stems, 3.5 % sodium hypochlorite with a few drops of sterile TWEEN® 20 was used for 15 minutes with consistent agitation. After bleaching, the tissue was washed seven times in sterile water and dried on sterile filter paper.

### 2.2.4 Plant media used

*M. truncatula* would be germinated on 1.5 % Phytoagar™ plates (Section 2.2.1), however, if they needed to be grown for longer than three days for experiments, a nutrient Modified Fåhraeus Medium (MFM) media was used (Table 2.1). Numerous different media were also used throughout this research for plant material grown and maintained in tissue culture (Table 2.2). A nutrient media that did not contain nitrogen was used to water plants in experiments using pots with perlite and vermiculite (Table 2.3).

| **MFM Media** | |
|---|---|
| **Chemical** | **Concentration** |
| $MgSO_4$ | 0.5 mM |
| $KH_2PO_4$ | 0.7 mM |
| $Na_2HPO_4$ | 0.8 mM |
| $NH_4NO_3$ | 5 mM |
| $C_6H_5FeO_7$ | 20 µM |
| $MnSO_4$ | 8 µM |
| $CuSO_4$ | 4 µM |
| $ZnSO_4$ | 7.34 µM |
| $H_3BO_3$ | 16 µM |
| $Na_2MoO_4$ | 4.13 µM |
| $CaCl_2$ | 1 mM |
| Phytoagar™ | 1.5 % |

**Table 2.1 Modified Fåhraeus medium (MFM) media components**

| | Infiltration | SH-10 | Propagation | Rooting | Medicago Rooting | Calli | TDZ Propagation | Regeneration |
|---|---|---|---|---|---|---|---|---|
| SH Vitamins | 3.2 g/l | 3.2 g/l | 3.2 g/l | 3.2 g/l | 3.2 g/l | 3.2 g/l | 3.2 g/l | 3.2 g/l |
| SH Salts | 1.01 g/l | 1.01 g/l | 1.01 g/l | 1.01 g/l | 1.01 g/l | 1.01 g/l | 1.01 g/l | 1.01 g/l |
| Sucrose | 10 g/l | 10 g/l | 20 g/l | 10 g/l | 10 g/l | 20 g/l | 20 g/l | 20 g/l |
| BAP | - | - | 1 mg/l | - | - | - | - | - |
| IBA | - | - | 0.1 mg/l | 1 mg/l | 1 mg/l | - | 0.05 mg/l | 3 mg/l |
| NAA | - | - | - | 0.1 mg/l | 0.1 mg/l | 0.05 mg/l | - | 0.1 mg/l |
| TDZ | - | - | - | - | - | 0.1 mg/l | 0.2 mg/l | - |
| MES | 0.6 mg/l | 0.6 mg/l | 0.6 mg/l | 0.6 mg/l | 0.6 mg/l | 0.6 mg/l | 0.6 mg/l | 0.6 mg/l |
| pH | 5.8 | 5.8 | 5.8 | 5.8 | 5.8 | 5.8 | 5.8 | 5.8 |
| Daishin Agar | - | - | 8 g/l | 8 g/l | - | 8 g/l | 8 g/l | 8 g/l |
| Phytagel | - | - | - | - | 0.25 % | - | - | - |

**Table 2.2 Growth Media for *Medicago truncatula* and *Parasponia andersonii* transformation protocols and for *P. andersonii* tissue culture**

| Chemical | Concentration |
|---|---|
| $CaCl_2*2H_2O$ | 1 mM |
| $KH_2PO_4$ | 1 mM |
| FeNAEDTA | 75 µM |
| $MgSO_4*7H_2O$ | 1 mM |
| $K_2SO_4$ | 0.25 mM |
| $MnSO_4*H_2O$ | 6 µM |
| $H_3BO_3$ | 20 µM |
| $ZnSO_4*7H_2O$ | 1 µM |
| $CuSO_4*5H_2O$ | 0.5 µM |
| $CoSO_4*7H_2O$ | 0.05 µM |
| $Na_2MoO_4*2H_2O$ | 0.1 µM |

**Table 2.3 Nutrient media used for watering *Medicago truncatula* and *Parasponia andersonii* in pots with perlite and vermiculite**

### 2.2.5 Establishing new *Parasponia andersonii* tissue culture

For stems, sterilised *P. andersonii* stems were placed onto propagation media (Table 2.2) at 28 °C, with 16 hours of light and 8 hours of dark until shoots form from the original stem. It can take several months for shoots to form, and the propagation media was refreshed monthly. Dead and contaminated tissue was removed during the plate refresh.

For leaves, sterilised *P. andersonii* leaves are placed onto calli media (Table 2.2) with the abaxial side of the leaf touching the agar. The calli media was refreshed every two weeks for four to six weeks and left in the dark at 28 °C until yellow/white calli appear. Once the calli appeared, healthy calli and the surrounding leaf tissue were moved onto thidiazuron (TDZ) propagation at 28 °C, with 16 hours of light and 8 hours of dark with the non-calli side touching the agar. The TDZ propagation media (Table 2.2) was refreshed every two weeks. Once the calli turned green or had shoots the tissue was moved onto propagation media at 28 °C, with 16 hours of light and 8 hours of dark.

### 2.2.6 Growth conditions for *Parasponia andersonii*

*P. andersonii* tissue cultures were kept in growth cabinets on propagation media (Table 2.2) at 28 °C, with 16 hours of light and 8 hours of dark and refreshed monthly, unless otherwise specified. Shoots that were rooted were placed onto rooting media (Table 2.2) and placed in the dark for five days at 28 °C. These were then placed into 16 hours of light and 8 hours of dark cycle at 28 °C for another 16 days. These rooted shoots from tissue culture were then either used for experiments of used to grow adult trees. Shoots that had been rooted and were to be turned into adult trees were grown in a climate-controlled growth chamber at 28 °C with 16 hours of light and 8 hours of dark. The young, rooted *P. andersonii* shoots were grown in *Arabidopsis* soil mix (Levington F2 soil mixed with silver sand at a 2:1 ratio). Adult *P. andersonii* trees were kept in a climate-controlled growth chamber at 24 °C with 16 hours of light and 8 hours of darkness. The adult trees were grown in large pots in Levington M2 compost (sphagnum moss peat containing 180 mg/l nitrogen, 90 mg/l phosphorus and 299 mg/l potassium) with osmocote fertiliser added as needed.

## 2.3 Bacterial growth methods

Rhizobial strains were grown on Tryptone-Yeast (TY) media (5 g/l bacto-tryptone, 3 g/l yeast extract, HEPES 4.766 g/l and 6 mM $CaCl_2$). BOR2 and WUR3 were grown without antibiotics; WSM1022 and WSM419 were grown with 50 µg/ml chloramphenicol added. *A. tumefaciens* and *A. rhizogenes* were grown on Luria Broth (LB) media with 25 µg/ml kanamycin.

## 2.4 Experimental rhizobia inoculation

### 2.4.1 Rhizobia inoculation conditions

For all the experiments involving a rhizobial inoculation, an overnight rhizobial culture was grown for each required rhizobial strain with appropriate added antibiotics. The overnight culture was spun down at 1900 rcf and diluted to $OD_{600}$ = 0.5 with sterile water. 300 µl of the required rhizobial culture was then spot inoculated around each plant except for in Section 2.4.4 and Section 2.7.2 where an additional 5 ml of fresh overnight rhizobial culture was added after four weeks due to lack of nodulation of *P. andersonii*.

### 2.4.2 *Medicago truncatula* and *Parasponia andersonii* phenotyping experiment

Germinated *M. truncatula* and rooted *P. andersonii* were planted into sterile perlite and vermiculite pots in a climate-controlled growth chamber with *M. truncatula* grown at 24 °C and *P. andersonii* grown at 28 °C. Plants were watered with nutrient media (Table 2.3) and left to acclimatise overnight. The plants were inoculated with WSM1022, WSM419, BOR2, WUR3 rhizobia (Section 2.4.1) or water as a control. *M. truncatula* was left for four weeks before harvesting and *P. andersonii* was left for 12 weeks before harvesting. There were three biological repeats with 16 technical repeats for each condition for the *M. truncatula*/rhizobia experiment and five biological repeats with between 10 to 16 technical repeats for each condition for the *P. andersonii*/rhizobia experiment.

### 2.4.3 Rhizobia inoculation of *Parasponia andersonii* for root RNA-Seq experiment

Rooted *P. andersonii* were planted into sterile perlite and vermiculite pots in a climate-controlled growth chamber at 28 °C. Plants were watered with nutrient media (Table 2.3) and left to acclimatise for two weeks. The plants were inoculated with 300 µl of $OD_{600}$ = 0.05 BOR2 or WUR3 rhizobia (see Section 2.4.1) or 300 µl of water as a control. *P. andersonii* roots were then harvested and flash frozen in liquid nitrogen at 0 hours, 24 hours, and 7 days. There were three biological repeats with three plants worth of *P. andersonii* roots.

### 2.4.4 Rhizobia inoculation of *Parasponia andersonii* for nodule RNA-Seq experiment

Rooted *P. andersonii* were planted into sterile perlite and vermiculite pots in a climate-controlled growth chamber at 28 °C. Plants were watered with nutrient media (Table 2.3) and left to acclimatise overnight. These plants were initially inoculated with 300 µl of $OD_{600}$ = 0.05 of BOR2 or WUR3, however, after four weeks, nodules had not emerged. These four-week-old plants were then inoculated with 5 ml of $OD_{600}$ = 0.05 of BOR2 or WUR3 rhizobia (Section 2.4.1). *P. andersonii* nodules were then harvested and flash frozen in liquid nitrogen after eight weeks from the second inoculation. There were two biological repeats with four plants worth of the *P. andersonii* nodules in each.

### 2.4.5 Generating *Parasponia andersonii* protoplasts

An adapted protocol of protoplast generation for Fluorescent Activated Cell Sorting (FACS) from *Arabidopsis thaliana* (Birnbaum et al., 2005; Gifford et al, 2008) was used. *P. andersonii* shoots from tissue culture were rooted for three weeks (Section 2.2.6) and five roots were cut into very small pieces with a scalpel. The roots were placed inside a 70 µm cell strainer inside a 35 mm petri dish and 7 ml of solution B was added (Table 2.4). The petri dish was incubated at room temperature on an orbital shaker at 120 rpm for 60 minutes and the roots were agitated via pipetting every 20 minutes. The cell strainer with the roots inside were removed and the now turbid solution in the petri dish was then removed and gently transferred into a 50

ml Falcon tube. The solution was then centrifuged at 260 x g for 10 minutes at 4 °C and the supernatant was removed. 500 μl of Solution A was gently added to the protoplasts before filtering them through a 40 μm cell strainer.

| Solution A | Solution B |
|---|---|
| 0.5 M Mannitol | 0.5 M Mannitol |
| 4 mM MES, pH 5.7 | 4 mM MES, pH 5.7 |
| 20 mM KCl | 20 mM KCl |
| 2 mM $MgCl_2$ | 2 mM $MgCl_2$ |
| 10 mM $CaCl_2$ | 10 mM $CaCl_2$ |
| 0.1 % BSA | 0.1 % BSA |
| | 1.2 % (w/v) Cellulase RS |
| | 1.5% (w/v) Macerozyme R10 |
| | 0.24 % Pectinase |
| pH 5.7 with filter sterilised 1M HEPES (pH 7.6) | pH 5.7 with filter sterilised 1M HEPES (pH 7.6) |

**Table 2.4 Components of solution A and solution B used for generating protoplasts**

## 2.5 Plant transformation methods

### 2.5.1 Transforming *Agrobacterium tumefaciens*

Electrocompetent *A. tumefaciens* were incubated on ice with 600 ng of a vector that had an endoplasmic reticulum (ER)-localised fluorescent protein under the control of the Expansin (EXPA) epidermal promoter (Gaudioso-Pedraza et al., 2018) (Figure 2.1) for five minutes. The cells were transferred to an electroshock cuvette and pulsed at 50 μF, 1.8 kv and 150 Ω. 1 ml of cold low salt LB was immediately added to the cells and incubated at 28 °C for 2.5 hours at 220 rpm. 200 μl was plated onto LB plates with 25 μg/ml kanamycin, grown at 28 °C for two days. Colonies that grow on the antibiotic selection plates were used for glycerol stocks and transformation of plants.

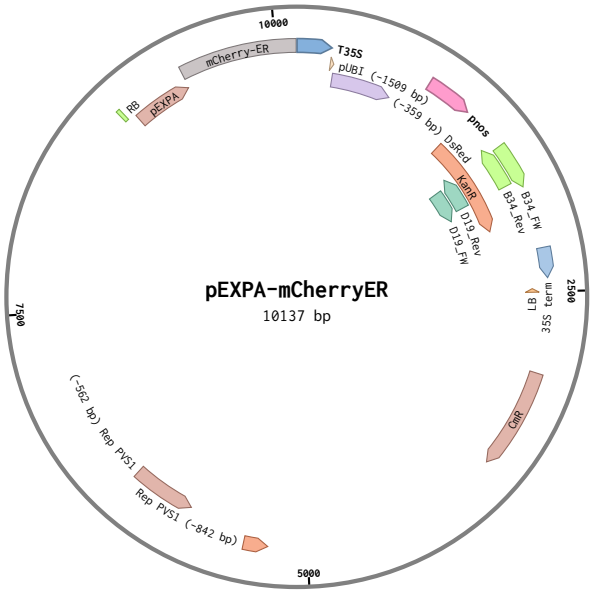


**Figure 2.1 Vector map of pEXPA:mCherry-ER used for plant transformation**
A pEXPA:mCherry-Endoplasmic reticulum (ER)-localised fluorescent protein under the control of the Expansin (EXPA) epidermal promoter (Gaudioso-Pedraza et al., 2018). Primers for the kanamycin gene for genotyping B34 (lime green) and D19 (teal) lines.

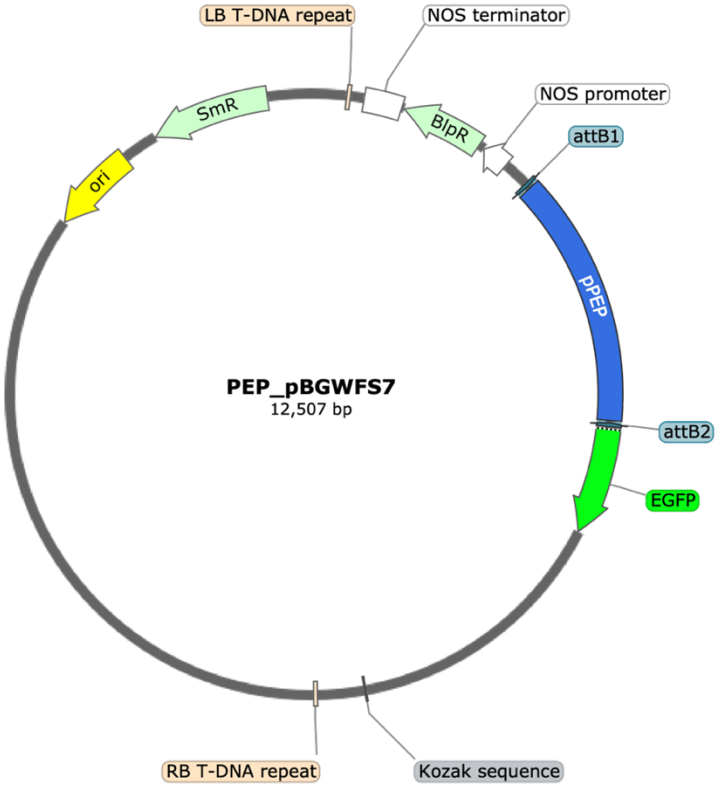


**Figure 2.2 Vector map of PEP_pBFWFS7 used for plant transformation**
A pBFWFS7 vector with a GFP gene that would be expressed specifically in the cortex via the PEP promotor. This particular vector has a glufosinate resistance gene (BlpR) that would be needed for selected successful *Parasponia andersonii* transformants.

### 2.5.2 Transforming wild-type *Parasponia andersonii* stems

*A. tumefaciens* with the desired vector was grown in a LB liquid culture overnight. 10 ml of overnight culture was diluted with 25 ml of infiltration media with 20 mg/ml acetosyringone and a few drops of TWEEN® 20 added. After sterilisation, stems were added to the diluted *A. tumefaciens* infiltration media and cut with a scalpel. Cut stems were left covered in the liquid for half an hour then stems were dried on sterile filter paper, ensuring they were completely dry. Transformed stems were placed onto rooting media with 20 mg/ml acetosyringone added and left for two days in the dark at 21 °C. The infected stems were washed four times in SH-0 liquid media with 500 mg/l Timentin™ (Ticarcillin/Potassium Clavulanate Mixture 15:1 Ratio) and a few drops of TWEEN® 20 added. These were slowly rotated in the liquid for a few hours each wash at 28 °C. Once thoroughly cleaned from *A. tumefaciens*, the stems were dried on sterile filter paper. Stems were placed on rooting media with 500 mg/l Timentin™ and 50 µg/ml kanamycin was used. Any tissue segments with *A. tumefaciens* overgrowth or contamination were discarded. After one week, stem pieces were moved onto propagation media with 500 mg/l Timentin™ and the appropriate antibiotics. The plates were refreshed every week.

### 2.5.3 Transforming *Parasponia andersonii* calli from wild-type leaves

To transform *P. andersonii*, two methods were used. First, the protocol for wild type stems was used, infecting sterilised leaves (Section 2.2.3) with *A. tumefaciens* hosting the pEXPA:mCherry-ER vector (Figure 2.1). The leaf segments were moved onto 'calli-induction' media (Table 2.2) with added 20 mg/l acetosyringone for two days in the dark at 21 °C before washing and drying (as described in Section 2.6.2). The cleaned tissue was then placed onto 'calli-induction' media with 500 mg/l Timentin™ and 50 µg/ml kanamycin in the dark at 28 °C for four weeks and then moved onto 'TDZ propagation' media (Table 2.2) with 500 mg/l Timentin™ and 50 µg/ml kanamycin with a 16-hour light/8-hour dark cycle at 28 °C.

The second protocol involves sterilising the leaves then placing them onto calli-induction media in the dark at 28 °C for four weeks to form calli. The calli were then infected as described above and placed onto 'calli-induction' media with 20

mg/l acetosyringone for two days in the dark at 21 °C before washing and drying as previously described (Section 2.6.2) The cleaned transformed leaves were moved onto calli-induction media with 500 mg/l Timentin™ and 50 µg/ml kanamycin in the dark 28 °C for one week. The leaf sections were then moved onto TDZ propagation media (Table 2.2) with 500 mg/l Timentin™ with 50 µg/ml kanamycin with a 16-hour light/ 8-hour dark cycle at 28 °C.

### 2.5.4 Generating *Medicago truncatula* transient lines

*M. truncatula* was sterilised and germinated (Section 2.2.1), the tips of the roots were cut off and the cut ends were dragged across a plate with a lawn of *A. rhizogenes* with the hosting the pEXPA:mCherry-ER vector (Figure 2.1). Plants were left to grow for two weeks at 25 °C in growth pouches, soaked in liquid MFM media on an MFM plate (Table 2.1).

### 2.5.5 Generating *Medicago truncatula* stable lines

*M. truncatula* was sterilised and germinated (Section 2.2.1) then transformed according to an adapted protocol of (Zhou et al., 2004). Using a sterile scalpel, four-day old *M. truncatula* plants were split 1 - 2 mm below the cotyledons to remove the radicle and most of the hypocotyl. The remaining tissue was then bisected so that each explant had one cotyledon and half of the embryonic axis. The tissue was infected with *A. tumefaciens* (AGL1) hosting the pEXPA:mCherry-ER vector (Figure 2.1). Explants were immersed in the *A. tumefaciens* solution ($OD_{600}$ = 0.8) in inoculation medium without agar and shaken gently for 30 minutes. These were dried on sterile filter paper and placed adaxial side face-up on inoculation media with 20 mg/l acetosyringone and 1 mM Dithiothreitol (DTT). These explants were kept for five days in the growing cabinet at 25 °C. Explants were washed four times in sterile distilled water with added 500 mg/l Timentin™ for at least 30 minutes each wash then dried on sterile filter paper and placed onto regeneration medium with 500 mg/l Timentin™ and incubated for 15 days at 25 °C.

Explants were then transferred to regeneration media with 50 µg/ml kanamycin and 500 mg/l Timentin™. They were transferred to fresh media every two

weeks; any explants not regenerating shoots were discarded. Well-developed kanamycin-resistant shoots were separated from the explants with a surgical blade, ensuring some meristematic tissues were included, and transferred to rooting medium in jars. The rooting jars were maintained at 25 °C with the lid slightly loose. Shoots were moved to fresh media every three weeks, removing the dead tissue, and cutting the ends of the shoots off if not roots had yet developed. Any shoots that produced well developed roots were moved into sterilised jiffy pellets (Elixir Gardens®) with added rooting media in sterile magenta boxes at 25 °C. After three to four weeks, the magenta boxes were opened the jiffy pellet was planted into Levington F2 compost (Sphagnum moss peat plus sand containing 144 mg/l nitrogen, 73 mg/l phosphorus and 239 mg/l potassium). Plants were grown in an environmentally controlled growth cabinet at 25 °C with a 16-hour/8-hour light/dark cycle until seeds were produced. These were classed as T0s, the seeds of which (T1s) were germinated for the PCR genotyping and sequencing to check for the presence of the vector. T2s were then used for the confocal microscopy analysis.

## 2.6 Molecular methods

### 2.6.1 Crude DNA extraction

Leaves were cut from *M. truncatula* plants and put in 2 ml Eppendorf tubes containing two glass beads. They were lysed in a tissue lyser for one minute at 30 $s^{-1}$. 400 µl of extraction buffer (200 mM Tris-HCl pH 7.5 - 8.0, 250 mM NaCl, 25 mM EDTA and 0.5 % SDS) was added. This was vortexed for five seconds and left at 35 °C for 15 minutes. The tubes were spun for two minutes in a microfuge at maximum speed to pellet the debris. 250 µl of the supernatant was added to 250 µl of isopropanol and mixed by inverting. This was left at room temperature for 15 minutes and then spun at full speed for five minutes to pellet the DNA. All of the supernatant was removed, and the pellet was left to dry at room temperature for 10 minutes. 70 µl of sterile water was added to dissolve the pellet.

### 2.6.2 PCR analysis

For the genotyping, MyTaq™ Red DNA Polymerase (Bioline) was used with the chosen primers (Table 2.5). Thermocycling conditions can be found in (Table 2.6). PCR products were then run on a 1 % agarose gel with 1 x GelRed®. The gel was run at 110 V for at least 30 minutes and then imaged.

| Primer Name | Sequence |
|---|---|
| mCherry_Forward | ACCTACAAGGCCAAGAAGCC |
| mCherry_Reverse | TTGTACAGCTCCTCCATGCC |
| Kanamycin_Forward | TGCTCGACGTTGTCACTGAA |
| Kanamycin_Reverse | TGATATTCGGCAAGCAGGCA |

**Table 2.5 Primer sequences used for genotyping stable pEXPA:mCherry-ER transformations**

| Temperature (°C) | Time | Number of Cycles |
|---|---|---|
| 95 | 5 minutes | 1 |
| 95 | 30 seconds | 35 |
| 52 | 30 seconds | |
| 72 | 90 seconds | |
| 72 | 7 minutes | 1 |

**Table 2.6 Thermocycler conditions for PCR genotyping**

### 2.6.3 PCR product cleaning and sequencing

The QIAquick PCR purification kit (Qiagen) was used to purify the PCR products generated following protocol provided. Purified products were then sent for Sanger sequencing using the Eurofins Genomics GATC LightRun service. Each required primer was sent, and the Eurofins Genomics sample preparation protocol was followed.

### 2.6.4 RNA extraction

Tissue from *P. andersonii* roots or nodules were ground in liquid nitrogen using a pestle and mortar. RNA was extracted from the ground tissue using a

Monarch Total RNA Miniprep Kit (NEB) using the protocol provided. The extracted RNA was analysed for quality and quantity with a Bioanalyzer 2100 RNA 6000 Pico Total RNA Kit (Agilent Technologies). Good quality RNA was sent for sequencing at (Novogene) with reactions for paired end, unstranded, 150 bp read length sequences using an Illumina NovoSeq 6000. The depth of sequencing was determined to be at least 20 million reads per sample.

## 2.7 Microscopy analysis

### 2.7.1 Confocal Microscopy

*M. truncatula* plants were germinated (Section 2.2.1) and were two weeks old from germination for stable lines or from transformation for transient lines. Sections of root were cut and embedded in a 5 % bacto-agar plate. Agar blocks were cut out and superglued to blocks and sectioned using a Vibrotome at around 200 µm thickness. A Zeiss LSM 880 confocal microscope was used with a 578 – 696 nm wavelength and a 561 nm laser for the mCherry fluorescence. Fiji (Schindelin et al., 2012) was used to process the images and remove confocal noise.

### 2.7.2 Electron Microscopy

Rooted *P. andersonii* were planted into sterile perlite and vermiculite pots in a climate-controlled growth chamber at 28 °C. Plants were watered with nutrient media (Table 2.3) and left to acclimatise overnight. These plants were initially inoculated with 300 µl of $OD_{600}$ = 0.05 BOR2 or WUR3, however, after four weeks, nodules had not emerged. These four-week-old plants were then inoculated with 5 ml of $OD_{600}$ = 0.05 of BOR2 or WUR3 rhizobia (Section 2.4.1). Seven weeks after the second inoculation, nodules were harvested and were prepared for electron microscopy by osmium fixation following the (Lodwig et al., 2005) protocol. Images were collected by Midlands Regional Cryo-EM Facility, hosted at the Warwick Advanced Bioimaging Research Technology Platform using a Jeol 2100Plus, a 200kV LaB6 electron microscopy.

## 2.8 Data analysis (inc. for RNAseq and for numerical data with stats)

### 2.8.1 RNA-Seq analysis

Initial quality control of raw reads was performed using FastQC. The raw reads were trimmed using fastp (Chen et al., 2018) with the following parameters: cut window size = 4, cut mean quality = 20, minimum length required = 40 using default quality filtering and overrepresentation analysis enabled. FastQC was used to quality check throughout. Alignment of trimmed reads was performed using STAR (Dobin et al., 2013) using only paired reads. The index files for STAR were generated with the *P. andersonii* genome and genome annotation (found on parasponia.org) with the sjdbOverhang parameter set to 149 (read length -1).

Differential expression analysis was carried out using DESeq2 (Love et al., 2014). Genes were considered differentially expressed (DE) if they had a log2 fold change ≥ 1.5 and or ≤ -1.5 and had a Bonferroni-corrected *P*-value < 0.05. Lists of DE genes generated from DESeq2 were queried for enriched gene ontology (GO) terms using the topGO (Alexa and Rahnenfuhrer, 2022). The GO term annotations were mapped to the genome from a combination of UniProt and InterProScan provided by Dr Laura Baxter. GO terms were considered enriched if they had a *P*-value < 0.05 using a weighted fisher test.

### 2.8.2 Ortholog analysis

Protein sequences of genes of interest were found using the NCBI GenBank database (Sayers et al., 2022). BLASTp (Johnson et al., 2008) was used to find orthologs compared to the *P. andersonii*, *M. truncatula* or *A. thaliana* databases. An orthologs was determined if there was a high query cover (at least 90 %) and an E value < 0.05.

### 2.8.3 Statistical analysis

A one-way Analysis of Variance (ANOVA) test with a post-hoc Tukey analysis was conducted on data sets as these had more than two groups in the phenotyping experiments. Where a *P*-value generated by a test was < 0.05, datapoints were concluded to be statistically significantly different. GraphPad Prism 7.04 software was used to carry out all the statistical analysis for the phenotyping experiments.

# Chapter 3: Shoot, root and nodule weight and nodule number comparisons between *Medicago truncatula* and *Parasponia andersonii* during nodulation with different rhizobial strains

## 3.1 Introduction

The process of nodulation can be considered to begin with a 'molecular conversation' between the host plant and the rhizobia in the soil. Flavonoids are produced via the phenylpropanoid pathway by the plant during times of low nitrogen within the surrounding environment as reviewed in (Dong and Song, 2020). The flavonoids are traditionally thought of as a chemoattractant for the rhizobia, however, this may not be the case and could be another chemoattractant responsible (Compton et al., 2020). The rhizobia do, however, signal back to the plant with Nod Factors (NFs). These NFs are lipochitooligosaccharides which are recognised by the host via NF receptor proteins and after this mutual recognition the nodulation signalling pathway is switched on (Cai et al., 2018) and nodule organogenesis is triggered. Signalling between the symbiotic partners occurs so that the plant can regulate its defence mechanisms and allow the bacterial symbiont to colonise the host through what is mostly a host-controlled process in a way that involves reduction or avoidance of immune response activation.

However, not every rhizobial host will interact with every rhizobial species or form nitrogen-fixing capable nodules to the same extent even if there is an interaction. Nodulation is an investment for the plant and so the capacity of rhizobia to act mutualistically rather than as pathogens is monitored (Oono et al., 2020). This is because nodulation not only requires energy to generate the nodule tissue via cell division, but the plant also needs to expend carbon in provision to rhizobia. As reviewed in (Sulieman et al., 2022), it has been estimated that soybean nodules consume between 7 - 12 g of carbon per gram of nitrogen fixed.

As reviewed in (Walker et el., 2020), there are several opportunities for the host plant to assess the viability of the symbiotic interactions. The first stage is though recognition of compatibility at the initial stages of the interaction. An

incompatible interaction involving either the plant failing to recognise the NFs expressed by the bacteria (Radutoiu et al., 2007), or the activation of plant defence responses that would usually have been dampened, acts as the first level of regulation. These early interaction-repressive responses can include strengthening the cell walls to help resist invasion at the plant-microbe interface (Tsyganova et al., 2019), accumulation of reactive oxygen species, activation of the defence response genes such as WRKY (Cui et al., 2019), and regulatory activity of plant resistance proteins such as Toll-interleukin receptor/nucleotide-binding site/leucine-rich repeat (TIR-NBS-LRR) class of plant resistance proteins (Yang et al., 2010).

Legumes have also been shown to exert control over their symbionts as they can degrade nodules, and the bacteria inside, that are either non-functional, are functional but not productive enough (measured via reception of the amount of fixed nitrogen provided to the plant) or due to an environmental stress. A number of genes and mechanisms have been found to be involved in nodule sanctioning. These include genes encoding for cysteine proteases, for instance overexpression of Cysteine Protease 2 (*MtCP2*) in *Medicago truncatula* caused early nodule senescence (Karmarkar, 2014) and enzymes involved in ethylene biosynthesis (Serova et al., 2017) In fact, ethylene has been shown to have a role in nodule senescence as genes related to ethylene were found to be upregulated once nodule senescence was triggered (da Silva et al., 2019).

Whilst it could be easy to simplify the role of a nodule to provision of nitrogen alone, there is evidence to suggest that rhizobia can provide more than just this nitrogen fixation activity. Rhizobial interaction with the plant can lead to enhanced abiotic and biotic plant defence systems both directly and indirectly. For instance, nodulating *M. truncatula* has been shown to recover from drought faster compared to when it is not being nodulated and the rhizobia within the nodules may help through delaying senescence of the leaves by allowing the accumulation of the osmolyte proline by the plant (Staudinger et al., 2016). *M. truncatula* and *Pisum sativum* have also been found to benefit from symbiotic bacteria defence priming. When inoculated with *Sinorhizobium meliloti* or *Rhizobium leguminosarum*, the amount of free salicylic acid (involved in increasing defence responses (Bhar et. al., 2018)) in the plant shoots was

found to be increased in comparison to uninoculated plants by approximately 10 % in *M. truncatula* (Smigielski et al., 2019). For *P. sativum* salicylic acid was found to be increased by 30 % when exposed to *Erysiphe pisi* (mildew fungus), thus leading to increased resistance to the fungus as there was a reduced number of spores on *P. sativum* leaves (Smigielski et al., 2019).

Whilst the symbiotic relationship between legumes and rhizobia can be seen as very selective, sometimes this relationship can be seen as more promiscuous. For instance, *Lotus burtii* was found to form nodules with far more species of rhizobia compared to *Lotus japonicus* (Zarrabian et al., 2022). *Parasponia andersonii* is also known to undergo symbiosis with a much broader range of rhizobial strains, including strains of variable nitrogen-fixing efficiencies (Op den Camp et al., 2012).

How much of an advantage this relative rhizobial promiscuity this gives *P. andersonii* and the underlying mechanism that enables is a topic currently being investigated. For instance, whilst *L. burtii* formed more nodules with a wider variety of rhizobia compared to *L. japonicus*, not all of these symbiotic partnerships had an effect on the shoot length (Zarrabian et al., 2022). By comparing rhizobial strains that are known to be efficient nodulators of *P. andersonii* or *M. truncatula* in symbiosis with each legume, we can investigate the impact that plant-rhizobial host range has for legume productivity. *Sinorhizobium medicae* WSM419 and *Sinorhizobium meliloti* WSM1022 have already been established as efficient rhizobial strains in *M. truncatula* (Terpolilli et al., 2008) and *Bradyrhizobium elkanii* WUR3 and *Mesorhizobium plurifari*um BOR2 are known to nodulate *P. andersonii* (Op den Camp et al., 2012, van Velzen et al., 2018, Dupin et al., 2020). Characterising nodulation of *P. andersonii* with *M. truncatula* can be very informative, but the aims of this chapter are to assess the shoot, root and nodule weight and nodule number of *P. andersonii* and *M. truncatula* to different rhizobial strains/species. This will establish which symbiotic partners are efficient nodulators of *P. andersonii* and *M. truncatula*.

## 3.2 Results

### 3.2.1 Compatible rhizobia have a significant effect on shoot biomass in *Medicago truncatula*

An experiment was conducted that involved inoculating four-day old *Medicago truncatula* with 300 µl of one of four rhizobial strains at $OD_{600}$ = 0.05: *Mesorhizobium plurifarium* (BOR2), *Bradyrhizobium elkanii* (WUR3), *Sinorhizobium meliloti* 1022 (WSM1022) and *Sinorhizobium medicae* 419 (WSM419), as well as a mock-inoculation of water alone. All plants were treated with a nutrient solution that had no nitrogen (See Section 2.2.4 for nutrient solution components). WUR3 was provided by the Guerts lab and was previously isolated from the nodules of *Chamaecrista fasciculata* (Partridge pea) and has already been shown to form nodules on *Parasponia andersonii* (Op den Camp et al., 2012). BOR2 was also provided by the Guerts lab and has also already been found to form nodules on *P. andersonii* and was previously isolated from the rhizosphere of a close non-nodulating relative to *P. andersonii* called *Trema orientalis* (van Velzen et al., 2018). WSM1022 and WSM419 have already been shown to be efficient nodulators for *M. truncatula* (Beatriz Lagunas. Personal Communication). WSM1022 was previously isolated from *Medicago orbicularis* and WSM419 was previously isolated from soil in Sardinia, Italy (Terpolilli et al., 2008).

Four weeks after inoculation the shoot biomass, root biomass (with nodules removed) and nodule number were measured. Data was then analysed in order to compare the impact of each rhizobial strain on the host plant. *M. truncatula* inoculated with WSM1022 and WSM419 had visually greener leaves, which was indicative of them being healthier (Figure 3.1).


**Figure 3.1. *Medicago truncatula* plants inoculated with *Sinorhizobium meliloti* (WSM1022) or *Sinorhizobium medicae* (WSM419) were larger and visually healthier, in terms of shoot greenness**

*Medicago truncatula* plants after four weeks of inoculation with 4 different rhizobial inoculations and a water control. (A) *Sinorhizobium medicae* (WSM419) and (B) *Sinorhizobium meliloti* (WSM1022) were the largest and visually healthiest. (C) BOR2 *Mesorhizobium plurifarium* (BOR2), (D) *Bradyrhizobium elkanii* (WUR3), (E) Control. Red arrows indicate examples of nodules.

After inoculation with both WSM1022 there were significantly more nodules on average per *M. truncatula* plant compared to the BOR2, WUR3 and control treatments, with 12 nodules for WSM1022. In comparison, BOR2, WUR3 and the control had on average 0 nodules per plant. Whilst WSM419 was not found to be

significantly different from any of the other treatments, there were on average 6 nodules per plant (showing WSM419 can nodulate *M. truncatula*), half of what was found on WSM1022 (Figure 3.2).

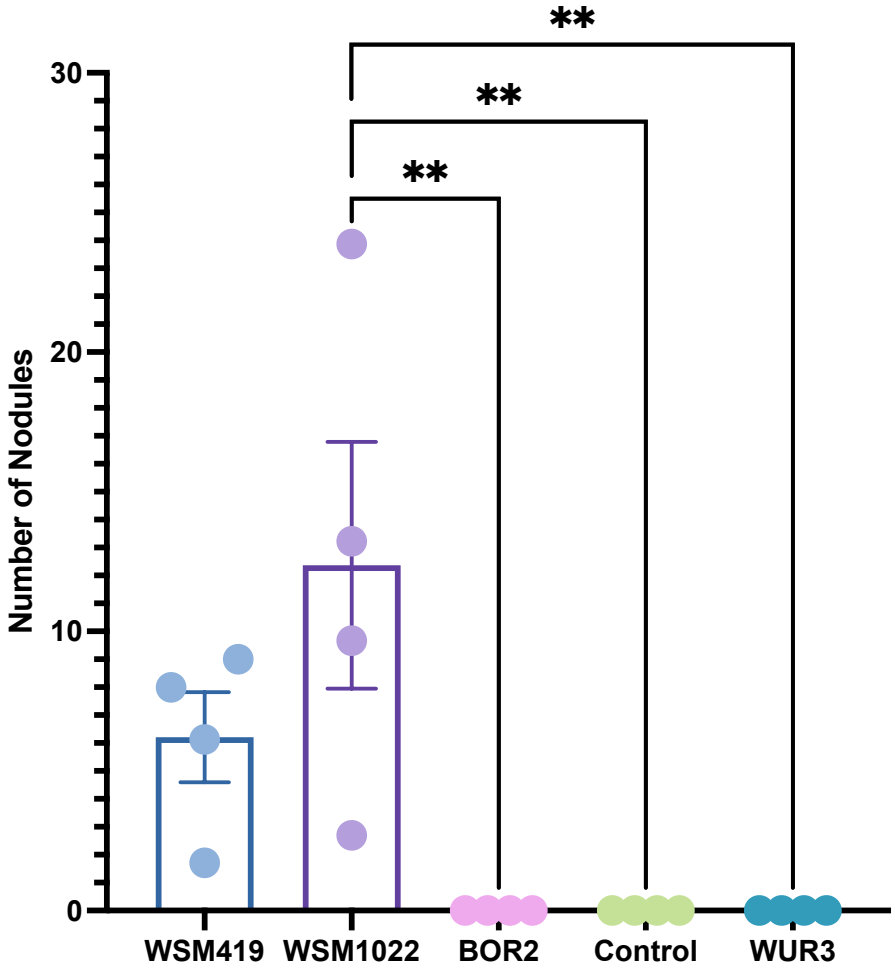


**Figure 3.2. Nodule number on *Medicago truncatula* was significantly higher when inoculated with *Sinorhizobium meliloti* (WSM1022)**
A significant difference was found between *Sinorhizobium meliloti* (WSM1022) compared to the *Mesorhizobium plurifarium* (BOR2), *Bradyrhizobium elkanii* (WUR3) rhizobial strains and the control. No significant different was found for *Sinorhizobium medicae* (WSM419). Significant differences found using a one-way ANOVA and a post-hoc Tukey test are indicated by ** = *P*-value ≤ 0.01. There were four biological repeats (represented by the dots) of the experiment with between 6 - 16 plants in each biological repeat. Error bars show ±SEM.

There was a significant increase in fresh shoot biomass for *M. truncatula* inoculated with WSM419 (on avg. 0.119 g per plant) and WSM1022 (on avg. 0.128 g per plant) compared to the control (on avg. 0.034 g per plant) (Figure 3.3A). There was no difference in fresh root biomass between WSM1022/WSM419 and the control

(Figure 3.3B). *M. truncatula* inoculated with BOR2 and WUR3 were not significantly different to the control in terms of shoot or root phenotypes (Figure 3.3).

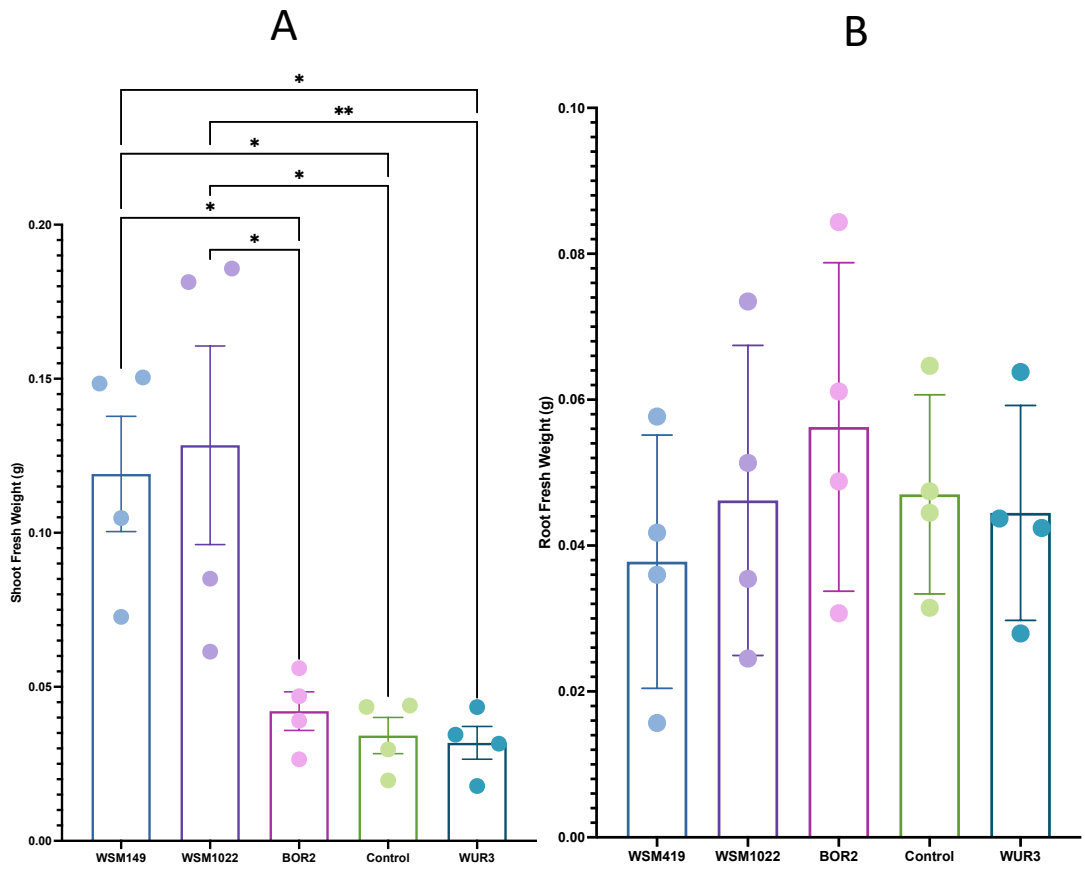


**Figure 3.3 Shoot fresh weight of *Medicago truncatula* was significantly larger with *Sinorhizobium medicae* (WSM419) and *Sinorhizobium meliloti* (WSM1022) rhizobia but no significant difference was found in root fresh weight**
(A) Shoot fresh weight of *Medicago truncatula* inoculated with *Sinorhizobium medicae* (WSM419), *Sinorhizobium meliloti* (WSM1022), *Mesorhizobium plurifarium* (BOR2), *Bradyrhizobium elkanii* (WUR3) or a water control. Both WSM419 and WSM1022 were significantly different to the other treatments. Significant differences found with a one-way ANOVA and a post-hoc Tukey test are indicated by * = *P*-value ≤ 0.05, ** = *P*-value ≤ 0.01. (B) Root fresh weight of *M. truncatula* inoculated with WSM419, WSM1022, BOR2, WUR3 or a water control. No significant difference was found between the different treatments. There were four biological repeats (represented by the dots) with between 6 - 16 plants in each biological repeat. Error bars show ±SEM.

Together the phenotypic data suggests that there are differences effect of rhizobial strains on *M. truncatula* nodulation outcome and shoot fresh weight. It was found that the impact of rhizobial-linked yield differences most marked on the shoot, despite the variation in nodule number in roots (roots had no difference). This shows the impact on the root-shoot nutrient transport (and likely communication).

### 3.2.2 *Bradyrhizobium elkanii* (WUR3) is an effective nodulator of *Parasponia andersonii*

In previous research (Op den Camp et al., 2012) found that *P. andersonii* has a broad range of rhizobial partners. To investigate the impact of different symbiotic partnerships with *P. andersonii*, the phenotypic impact of nodulation with BOR2, WUR3, WSM1022 and WSM419 on the shoot and root fresh biomass was examined. Rooted *P. andersonii* plants from tissue culture were inoculated with 300 µl of one of four rhizobial strains at $OD_{600}$ = 0.05 or 300 µl of a water control. The plants were harvested 12 weeks after inoculation and the shoot biomass and root biomass (with nodules removed) was measured. All plants were watered with a nutrient solution that had no nitrogen (See Section 2.2.4 for nutrient solution components).

*P. andersonii* plants inoculated with WUR3 had visually larger shoots compared to the rest of the inoculations (Figure 3.4) and shoot fresh weight was found to be significantly larger on average when plants were inoculated with WUR3 (on avg. 0.592 g per plant) compared to the other rhizobial strains (on avg. between 0.21 g per plant to 0.332 g per plant) and the mock-inoculated control (on avg. 0.22 g per plant) (Figure 3.5A).

Unlike for nodulated *M. truncatula* (Figure 3.3B), there was a significant difference in fresh root weight between WUR3-inoculated plants (on avg. 0.62 g per plant) compared to BOR2 (on avg. 0.353 g per plant) and the mock-inoculated control (on avg. 0.363 g per plant) (Figure 3.5B). There was, however, no significant difference found for WSM419 (on avg. 0.421 g per plant) and WSM1022 (on avg. 0.51 g per plant) and the other treatments. This demonstrates that an effective nodulator of *P. andersonii* impacts the plant at more than just the shoot level, and we can speculate that nitrogen being provided by the nodules to *P. andersonii* is allowing for growth investment in the roots, either directly or indirectly. This in turn may lead to a greater surface area of the roots, enabling the plant to obtain more nutrients from its surroundings. Perhaps this could be tested in future by using a technique such as Inductively Couple Mass Spectrometry that analyses the elements within a sample.


**Figure 3.4 *Parasponia andersonii* inoculated with *Bradyrhizobium elkanii* (WUR3) were larger and healthier**

Phenotypes of 12 week old *Parasponia andersonii* plants inoculated with (A) *Sinorhizobium medicae* (WSM419), (B) *Sinorhizobium meliloti* (WSM1022), (C) control, (D) *Mesorhizobium plurifarium* (BOR2), or (E) *Bradyrhizobium elkanii* (WUR3).
Scale bar = 2 cm for (A), (B), (C), (D), and (E).
A zoomed in view of (F) BOR2 and (G) WUR3. Scale bar = 1 cm for (F) and (G).

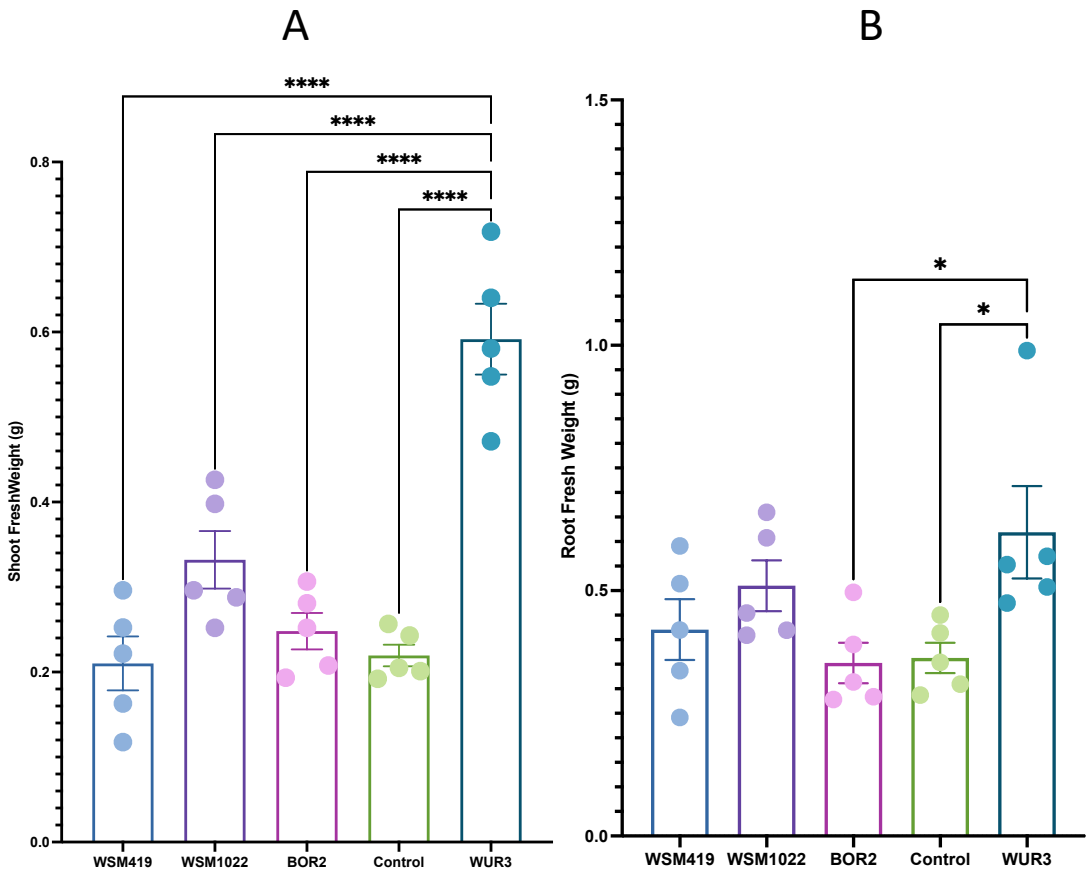


**Figure 3.5. Shoot and root fresh weight of *Parasponia andersonii* was significantly larger when inoculated with *Bradyrhizobium elkanii* (WUR3)**
(A) Shoot fresh weight of *Parasponia andersonii* with *Sinorhizobium medicae* (WSM419), *Sinorhizobium meliloti* (WSM1022), *Mesorhizobium plurifarium* (BOR2), *Bradyrhizobium elkanii* (WUR3) or a water control. A significant difference was found between WUR3 and the other four inoculations. (B) Root fresh weight of *P. andersonii* with WSM419, WSM1022, BOR2, WUR3 and a water control. A significant difference was found between WUR3 and the control and between WUR3 and BOR2. Significant differences found using a one-way ANOVA and a post-hoc Tukey test are indicated by * = *P*-value ≤ 0.05 and **** = *P*-value ≤ 0.0001. There were five biological repeats (represented by the dots) with between 3 - 15 plants in each repeat. Error bars show ±SEM.

### 3.2.3 Interaction with *Mesorhizobium plurifarium* BOR2 vs. *Bradyrhizobium elkanii* WUR3 leads to different *Parasponia andersonii* nodule phenotypes and highlights rhizobial specific responses

To ask whether the significant difference in shoot and root fresh weight found in *P. andersonii* when inoculated with WUR3 (Figure 3.5) was linked to a difference in nodulation between WUR3, BOR2, WSM419, WSM1022 and the control, weight

(on average per plant) of nodules (Figure 3.6 A) and the number of nodules were measured (Figure 3.6 B).

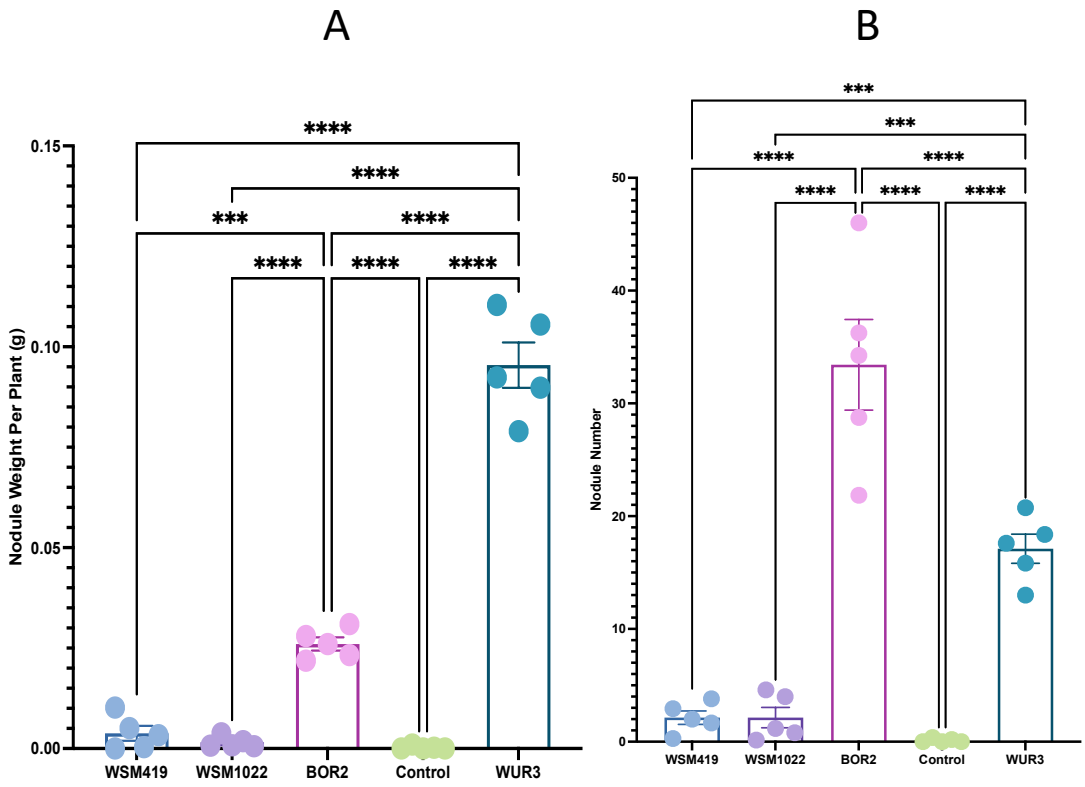


**Figure 3.6 Nodule weight per plant of *Parasponia andersonii* was significantly larger with *Bradyrhizobium elkanii* (WUR3), but *Mesorhizobium plurifarium* (BOR2) had the significantly highest number of nodules**
(A) Nodule weight per plant of *P. andersonii* inoculated with *Sinorhizobium medicae* (WSM419), *Sinorhizobium meliloti* (WSM1022), *Mesorhizobium plurifarium* (BOR2), *Bradyrhizobium elkanii* (WUR3). A significant difference was found between BOR2 and WUR3 and the other three treatments.
(B) Nodule number of *P. andersonii* inoculated with WSM419, WSM1022, BOR2, WUR3. A significant difference was found between BOR2 and WUR3 and the other three treatments. Significant differences found by a one-way ANOVA and a post-hoc Tukey test are indicated by *** = *P*-value ≤ 0.001 and **** = *P*-value ≤ 0.0001. There were five biological repeats (represented by the dots) with between 3 - 15 plants in each repeat. Error bars show ±SEM.

*P. andersonii* plants inoculated with WUR3 had significantly higher average nodule weight (avg. 0.095 g per plant) compared to WSM1022 (on avg. 0.002 g per plant), WSM419 (on avg. 0.004 g per plant), BOR2 (on avg. 0.026 g per plant) and the control (on avg. 0 g per plant) (Figure 3.6A). BOR2 had a significantly higher average nodule weight per plant compared to WSM419, WSM1022 and the control but was only around 30 % of the weight of the WUR3 average nodule weight per plant.

Despite having a smaller fresh weight of nodules, BOR2-inoculated nodules had on average 33 nodules per plant, compared to WUR3 that had 17 nodules per plant (Figure 3.6B). The BOR2-inoculated *P. andersonii* nodule number is similar to that previously found by (van Velzen et al., 2018) who also found around 32 nodules per plant. However, the WUR3-inoculated *P. andersonii* nodule numbers found by (van Velzen et al., 2018) were slightly lower with around 11 nodules per plant compared to this work with 17 nodules per plant. The other *P. andersonii* plants with rhizobial inoculants WSM1022 and WSM419 and the control only had between 0 - 2 nodules per plant (Figure 3.6B), which were significantly lower. In summary, BOR2-inoculation led to formation of a high number of small nodules on each plant whereas WUR3-inoculation led to fewer, larger nodules per plant.

Differences between nodule morphology could be seen. *P. andersonii* inoculated with BOR2 had nodules that were pale brown, hard and round (Figure 3.7). This small brown morphology of BOR2-inoculated *P. andersonii* nodule has been shown previously (Van Zeijl et al., 2018). WUR3 inoculation of *P. andersonii* led to the formation of large branched brown nodules, with white spots. On the rare occasion when *P. andersonii* nodules were formed with WSM419 inoculation, these were light brown and branched, and with WSM1022 inoculation the nodules were very small, round, and brown, with a dehydrated appearance.

Taken together, this shows that there is specificity in *P. andersonii* symbiosis as the nodule number and weight of WSM1022-inoculated and WSM419-inoculated plants were not significantly different to the control, but with BOR2 or WUR3 inoculation, *P. andersonii* plants produced many nodules. However, the extent of control *P. andersonii* has over regulation of symbiosis remains to be further investigated since, even when established, nodulation was not equal. BOR2-inoculation led to the greatest number of nodules being formed, with these being very small, and nodulation did not seem to lead to an increase in shoot or root biomass. In contrast, nodulation when inoculated with WUR3, which has also been established as an efficient nodulator of *P. andersonii,* led to formation of fewer nodules compared to BOR2, but nodulation that led to a significant increase in the

shoot and root biomass; the greatest compared to any other inoculant and the control.

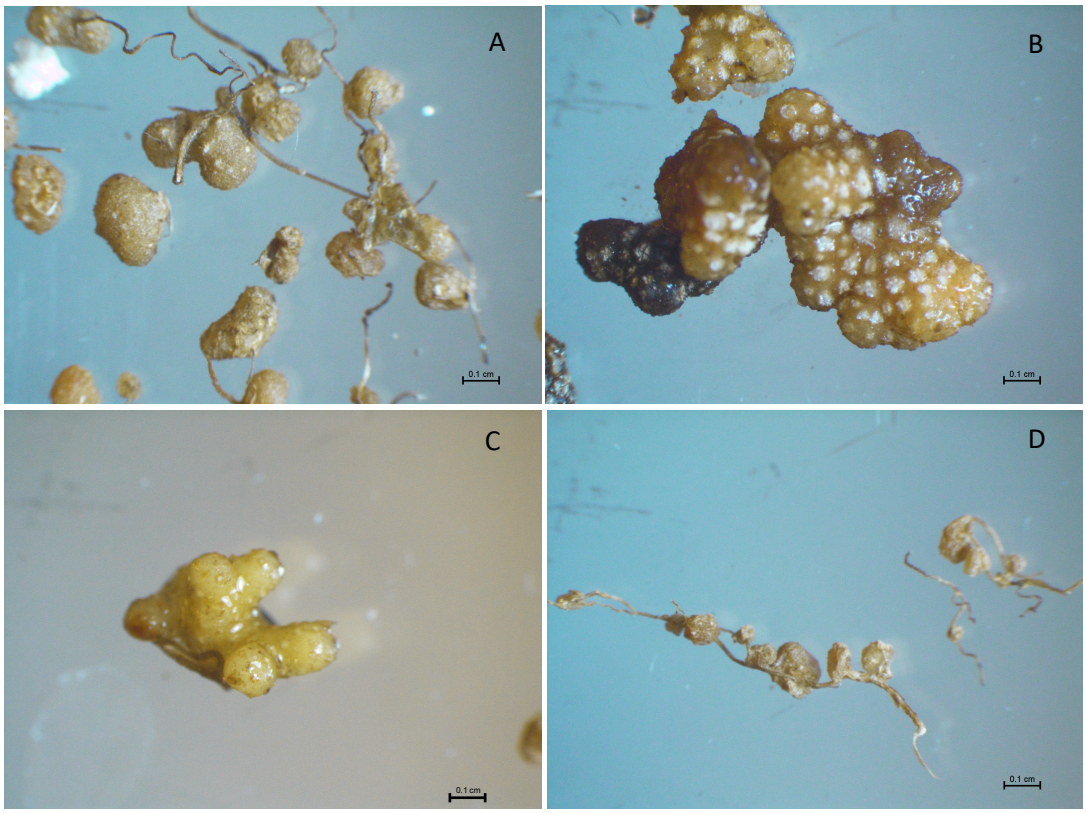


**Figure 3.7 *Parasponia andersonii* nodule phenotypes when inoculated with different rhizobial species**
(A) *Mesorhizobium plurifarium* (BOR2) inoculation led to formation of small round nodules. (B) *Bradyrhizobium elkanii* (WUR3) inoculation led to formation of large nodules with white dots all over. (C) For *Sinorhizobium medicae* (WSM419) inoculation, on the rare occasion nodules were produced they looked like undeveloped WUR3 nodules. (D) For *Sinorhizobium meliloti* (WSM1022) inoculation, in the rare occasion nodules were formed, these looked like dehydrated BOR2 nodules. Scale bar = 0.1 cm

## 3.3 Discussion

### 3.3.1 Specificity of nodulation in *Medicago truncatula*, as assessed in response to inoculation with different rhizobial strains

Investigating how different rhizobial species can impact the shoot and root biomass of nodulating plants can enable us to gain insight into the specificity and impact of symbiotic relationships. This is important to consider as the agricultural sector is looking to move away from nitrogen fertilisers due to the negative environmental impacts it can have. For instance, nitrate application through fertiliser was found to have a 92.7 % contribution to causing marine eutrophication (Balasuriya et al., 2022). Instead of a nitrate fertiliser, rhizobia can be used as a replacement source of nitrogen for crops, but choosing the right symbiotic partners is important because if they are incompatible or not efficient in partnership, the host plant will not be provided with the nitrogen it needs.

This research found that *M. truncatula* had two compatible symbiotic partners in WSM1022 and WSM419, as not only were nodules formed upon rhizobial inoculation, but these plants also had a significant increase in shoot biomass. Whilst WSM419 did not show a significant difference in number of nodules formed compared to the control like WSM1022 did, another biological repeat would most likely add the statistical power needed to show this significant difference. *M. truncatula* did not form a symbiotic partnership with BOR2 or WUR3 as no nodules were formed, indicating the specificity of rhizobial partner range. BOR2 and WUR3 inoculation not leading to nodule organogenesis could be due to *M. truncatula* not recognising the Nod Factors (NFs) that BOR2 and WUR3 express. As reviewed in (Lindström and Mousavi, 2020) there are NF biosynthesis genes named *nod*, *nol* and *noe* and some of these are commonly found in rhizobia whilst others are more specific to the rhizobia which allows for the specificity found in symbiotic nitrogen-fixing. For example, WUR3 (Op den Camp et al., 2012), WSM1022 and WSM419 (Baxter et al., 2021) share the commonly found NF biosynthesis genes *nodA/B/C* which are involved in the synthesis of the NF backbone. Whilst WUR3, WSM1022 and WSM419 also possess the commonly found *nodD* gene, which is involved in the recognition of plant flavonoids, WSM1022 and WSM419 possess three copies

(*nodD1/D2/D3*) and WUR3 only has one copy of *nodD*. WUR3 also possesses other NF biosynthesis genes that are the same in WSM1022 and WSM419 (*nod/I/J/L/P/Q*). However, WUR3 also has NF biosynthesis genes that WSM1022 and WSM419 do not possess (*nodS/U/Z*, *noIL*, *nolO*, *noeE/I*) and WSM1022 and WSM419 have NF biosynthesis genes that WUR3 does not possess (*nodE/F/H/M/N*, *nolF/G*, *syrM* and *noeA/B*) (Op den Camp et al., 2012, Baxter et al., 2021).

It would be interesting to determine if expressing *P. andersonii* NF receptor genes in *M. truncatula* would lead to nodule organogenesis in a similar way to how *M. truncatula* expressing *Lotus japonicus* NF receptor genes leads to increase of the host range of *M. truncatula* (Radutoiu et al., 2007). However, it must be noted that it may not be *M. truncatula* not responding to NFs, but also/or rhizobia are not responding to the plant exudates. Previous research has shown that not all rhizobia will respond to every flavonoid (Yokoyama, 2008) and perhaps BOR2 and WUR3 do not respond to *M. truncatula* flavonoids, or other root exudes, rather than *M. truncatula* not responding to the NFs. Comparative gene expression profiling of plant and rhizobia could be informative to study this further.

When *M. truncatula* was inoculated with WSM419, there were fewer nodules formed despite leading to the same significant increase in plant shoot yield as when *M. truncatula* was inoculated with WSM1022. This suggests that WSM419 is a more efficient symbiotic partner in comparison to WSM1022 for *M. truncatula*, due to *M. truncatula* having a higher yield of shoot biomass per nodule.

It has already been found that *M. truncatula* has a non-efficient symbiotic partner in the denoted model symbiont *Sinorhizobium meliloti* 1021 (Sm1021). When inoculated, nodules are still formed on *M. truncatula* and these do house bacteria that fix nitrogen, leading to higher mean nitrogen shoot compared to the control, but this increase is lower than that resulting from inoculation with WSM419 or WSM1022 (Beatriz Lagunas, Personal Communication). Sm1021-inoculated plants had less than 50 % of the shoot dry weight *M. truncatula* compared to WSM419 and WSM1022-inoculated plants, but still had significantly more than the non-inoculated control (Terpolilli et al., 2008). It would be interesting to evaluate the similarities and differences that there are between this inefficient symbiotic partnership, *M.*

*truncatula*-Sm1021 and the one possessed by *P. andersonii* and BOR2. If these symbionts are not providing nitrogen to allow for a significant increase in shoot biomass, are these inefficient symbiotic partnerships in *P. andersonii* providing something other than nitrogen? This could be in the form of providing defence priming and so, experiments that involve priming *P. andersonii* with a BOR2 inoculation before exposing *P. andersonii* to a pathogen could be conducted. This could be done in a similar way as (Smigielski et al., 2019) where *M. truncatula* gained added protection from the fungal pathogen *Erysiphe pisi* after an initial inoculation with *S. meliloti* Sm2011 (another inefficient partner of *M. truncatula*).

### 3.3.2 Variety of hosting of rhizobia in *Parasponia andersonii*

It has already been demonstrated that *P. andersonii* has a broad range of symbionts that can form nodules, even if they are inefficient partners due to lower rates of nitrogenase activity (Op den Camp et al., 2012). However, *P. andersonii* does also control the symbiont. When there are high amounts of available nitrogen, *P. andersonii* was found to have a decreased rhizobial population within formed nodules and produce less nodules once ammonium nitrate levels reached 3.75 mM (Dupin et al., 2020). This demonstrates that *P. andersonii* exhibits autoregulation of nodulation, as for other legumes where high amounts of nitrogen feed into a mechanism that prevents nodule formation (Dupin et al., 2020).

Plant NF receptors, such as *MtLYK3* in *M. truncatula* (Limpens et al., 2003), are essential for the process of nodulation to be initiated and *P. andersonii* has been shown to have an ortholog of *MtLYK3* in the forms of *PanLYK3* and *PanNFP2* (Rutten et al., 2020). It is possible the reason for WSM1022 and WSM419-inoculation not leading to nodule formation on *P. andersonii* is because the NFs they produce are not recognised by the NF receptors that *P. andersonii* possess. Despite *P. andersonii* being described as promiscuous, this shows that there is some level of control in the process of nodulation in *P. andersonii*. As previously suggested, expressing *M. truncatula* NF receptor genes in *P. andersonii* could be tested to ask if nodule organogenesis could be initiated when plants are inoculated with WSM1022 or

WSM419; and WSM1022 and WSM419 could be tested for their ability to recognise the exudates being produced by *P. andersonii*.

(Op den Camp et al., 2012) demonstrated that WUR3-inoculation can lead to formation of nodules on *P. andersonii* and (van Velzen et al., 2018) showed that BOR2-inoculation can lead to formation of nodules on *P. andersonii,* with these nodules housing bacteria. The (van Velzen et al., 2018) study found that WUR3 and BOR2 inoculation both led to nodulation of *P. andersonii*, but also found that BOR2 has nitrogenase activity (van Velzen et al., 2018). Despite this previous research, the output of these symbiotic relationships has not been previously tested in terms of shoot biomass. This is why WUR3 and BOR2 were investigated along with WSM419 and WSM1022 to test the symbiotic output and the limits of the promiscuity of *P. andersonii* with the symbiotic relationships.

Whilst (van Velzen et al., 2018) found nitrogenase activity, in this work BOR2-inoculation led to nodulation that did not lead to a significant increase of the shoot biomass of *P. andersonii* compared to the control. This lack of increase in shoot or root biomass resulting from BOR2 inoculation of *P. andersonii* has not been shown before alongside the significant increase in shoot and root biomass resulting from WUR3 inoculation *of P. andersonii*. Previous research on BOR2 inoculated plants was investigated at the early stages of nodulation in *P. andersonii* (four to six weeks old) (van Velzen et al., 2018) whereas this research was conducted after 12 weeks of growth. The nodules that were formed by BOR2 were also much smaller in size compared to WUR3. This leads to the conclusion that these BOR2 nodules are not fully formed and any nitrogen-fixing abilities they did have has eventually ceased. The underpinning molecular differences between BOR2-inoculated and WUR3-inoculated nodules will be investigated in Chapter 4.

Further investigation of the promiscuity of *P. andersonii* can also continue from this work. WUR3 was isolated from a nodule from the legume, *Chamaecrista fasciculata*, (Op den Camp et al., 2012) and BOR2 from the rhizosphere of non-nodulator *Trema orientalis* (van Velzen et al., 2018). This leads to an opportunity to isolate rhizobia from the nodules and rhizosphere of *P. andersonii* itself to investigate the naturally forming communties. By testing the extent of the different species

found and how they compare to the results found here by conducting the same experiments (recording shoot, root and nodule biomass and nodule number after 12 weeks), this will further help the understanding of which rhizobia are the best symbiotic partners for *P. andersonii*, and how promiscuious *P. andersonii* really is.

## 3.4 Conclusion

This chapter has shown that there is a phenotypic difference depending on the rhizobial partner, for both the legume *M. truncatula* and the non-legume *P. andersonii*. BOR2 inoculation leads to formation of many small nodules on *P. andersonii* but they do not provide a significant contribution of nitrogen to the plant, indicated by a lack of shoot biomass increase resulting from nodulation. This has suggested questions to further pursue, such as why BOR2 escapes the selection process in *P. andersonii* at first but then does not produce fully formed nodules as WUR3-inoculation leads to. This will be explored further in the subsequent chapters.

# Chapter 4: Analysing the differences in nodulation of *Parasponia andersonii* with *Mesorhizobium plurifarium* BOR2 compared to *Bradyrhizobium elkanii* WUR3

## 4.1 Introduction

### 4.1.1 Hormones and nodulation

As reviewed in (Velandia et al., 2022) hormones play an important role in nodulation as both positive and negative regulators. They also play roles at different stages of nodulation, from rhizobial infection all the way to nodule senescence. For instance, auxin has been found to be a positive regulator of nodulation whilst ethylene is a negative regulator of nodulation. Cytokinins, giberrelins and brassinosteroids have also been found to play a variety of roles in nodulation. For example, it was found that brassinosteroids are a negative regulator of rhizobial infection in *Pisum sativum* by preventing infection thread (IT) formation (McGuiness et al., 2020), however, they do have a positive role in nodule development. For instance, when Brassinazole Resistant 1 (*BZR1*), a key regulator of the brassinosterid pathway was mutated in *Medicago truncatula*, nodule development was partially impaired (Cui et al., 2019). Auxin and ethylene are also key positive and negative regulators of nodulation, as will be explored further below.

### 4.1.2 Auxin and nodulation: a positive regulator

Auxin is a well-studied hormone that is important for a variety of roles in plant development from seed development (Atif et al., 2013) to lateral root formation (Wilmoth et al., 2005). Auxin also has an important role in nodulation and has been found to be a positive regulator in rhizobial infection, nodule intiation and nodule development. Auxin Response Factors (ARFs) such as *ARF16a* has been found at infection sites in *M. truncatula* and mutating *ARF16a* was found to lead to reduced rhizobial infection (Breakspear et al., 2014). It has also been shown that *ARF2*, *ARF3*, *ARF4a*, and *ARF4b* are required for the infection threads to reach the cortex to infect the nodule primordia (Kirolinko et al., 2021).

Nodule primordium development involves similar signalling pathways as lateral root development including recruiting YUCCA and Stylish (*STY*) genes (involved in auxin biosynthesis) to promote cell devisions that form the developing nodule (Schiessl et al., 2019). Interestingly, auxin biosynthesis through YUCCA and *STY* genes acts via Lob-Domain Protein 16 (*LBD16*) which is activated via a cytokinin-reliant pathway (Schiessl et al., 2019), showing how the hormones interplay with each other during nodule organogenesis. In nodule development, it was found in *Glycine max* that YUCCA gene *YUC2a* was expressed in maturing nodules (Wang and Schippers, 2019), showing how auxin is important in not only initiating nodule formation, but regulating continued nodule formation and activity.

### 4.1.3 Ethylene and nodulation: a negative regulator

In opposition to auxin, ethylene has been found to be a negative regulator of nodulation and it was first found to act early in the signalling pathway (Oldroyd et al., 2001). Within six hours of inoculation of *Lotus japonicus* with *Mesorhizobium loti*, ethylene production was found to increase (Reid et al., 2018). Ethylene is required to control the level of nodulation occurring and when the gene responsible for controlling ethylene signalling, Ethylene Insensitive 2 (*EIN2*), is mutated, legumes such as *L. japonicus* hypernodulate and become hyperinfected (Reid et al., 2018). Ethylene is also important in activating defences and so must be controlled to allow compatible rhizobia not be recognised as pathogens, which requires the genes Defective in Nitrogen Fixation (*DNF2*) and *SymCRK* in *M. truncatula* (Berrabah et al., 2018). There has also been evidence to suggest that ethylene also has a role in some way in more mature nodules and nitrogen fixing capability. It was found that when *EIN2* in *L. japonicus* was mutated or had a double knockdown of Ethylene Response Factor 74 (*MtERF74*) and *MtERF75* in *M. truncatula* was generated nitrogen fixing activity was reduced (Rovere et al., 2023). This indicates that ethylene is needed not only at the start of nodulation, but also throughout nodulation progression.

### 4.1.4 Nodule senescence

Nodule senescence, where the nodule and rhizobia inside are degraded, is not only the natural end to an aging nodule (Van de Velde et al., 2006), but also can be used to sanction inefficient nodules. In *Pisum sativum* (pea), inefficient rhizobia can trigger higher levels of nodule senescence compared to the natural senescence that comes from aging (Serova et al., 2017). Nodule senescence can also occur as a means of removing the carbon sink that is the nodule during times of stress such as drought, but only as a last resort to get the maximum benefit from the nitrogen-fixing rhizobia (Dhanushkodi et al., 2018).

As well as having a role during nodule initation and nodule organogenesis, ethylene has also been found to be involved at the later stages of nodulation, nodule senescence. Nodule and leaf senescence have a high degree in overlap in terms of signalling, including ethylene having a role in *M. truncatula* nodule senescence (Van de Velde et al., 2006). This has also been shown in common bean where ethylene was found to be upregulated during nodule senescence (da Silva et al., 2019) and the ethylene precursor 1-aminocyclopropane-1-carboxylic acid (ACC) was found to be upregulated during nodule senescence in *P. sativum* L. (Serova et al., 2017).

Whilst auxin has been shown to be important in nodule formation, research on the role of auxin role in nodule senescence is limited. However, during the senescence of leaves (which has similar programming to nodule senescence) it was found that overexpressing *YUCCA6* (a gene involved in auxin biosynthesis) lead to a delayed senescent reponse (Kim et al., 2011). It was found in *Glycine max* senescing nodules that YUCCA gene *YUC2a* promotor activity was low, perhaps indicating that auxin biosynthesis is needed to be suppressed for senescence to occur (Wang et al., 2019).

During nodule senescene regulation of autophagic degradation can be seen. This is a process that found in all eukaryotes and is important for maintaining homeostasis by recycling cellular material that is damaged or no longer needed. *M. truncatula* has been found to have 39 Autophage-Related Genes (*ATGs*) and expression of each ATG varies dependent on the tissue. For instance, 34 of the 39 ATGs were tested and 13 ATGs were highly expressed in roots and 7 were high

expressed in leaves (Yang et al., 2021). The role of autophagy in senescence is still being unravelled, however, as reviewed in (Wang and Schippers, 2019), autophagy initially stalls senescence in leaves but once senescence commences, autophagy is needed to break down important components to be recycled by the plant.

### 4.1.5 Aims and objectives

*Mesorhizobium plurifari*um (BOR2) and *Bradyrhizobium elkanii* (WUR3) inoculation led to vastly different nodule phenotypes with *Parasponia andersonii.* BOR2 inoculation led to formation of many small nodules that did not lead to any increase in shoot weight whereas WUR3 inoculation led to fewer, larger nodules that did lead to a significantly increased shoot weight (see Chapter 3). To try to understand these differences, the nodules themselves were investigated at microscopic and molecular levels.

Firstly, due to the vastly different visible phenotypes of the nodules microscopy techniques were used to investigate the phenotypes of the rhizobia inside and whether their shape, amount or position are different between BOR2-harbouring nodules and WUR3-harbouring nodules. Secondly, molecular techniques were used to discover if the early nodulation signalling pathway was different upon inoculation and if there were any differences as the nodule is forming.

## 4.2 Results

### 4.2.1 Transmission electron microscopy of *Mesorhizobium plurifari*um (BOR2) and *Bradyrhizobium elkanii* (WUR3)-inoculated nodules

*Mesorhizobium plurifari*um (BOR2) and *Bradyrhizobium elkanii* (WUR3) inoculation led to vastly different nodule phenotypes and to investigate the nodule morphology and rhizobial morphology, electron microscopy was used to image inner nodule tissue. Four-week old *P. andersonii* plants from tissue culture were inoculated with 5 ml of either BOR2 or WUR3 ($OD_{600}$ = 0.05). This was a second inoculation of BOR2 and WUR3 due to an initial inoculation of 300 µl ($OD_{600}$ = 0.05) of BOR2 and WUR3 of one day old *P. andersonii* plants from tissue culture had not produced nodules after four weeks. The plants were left to grow at 28 °C in 16 hour

light/8 hour dark for seven weeks before the nodules were fixed in resin and sectioned for analysis for transmission electron microscopy. It was found that rhizobia was present in nodules from plants that had been inoculated with WUR3, whilst nodules from plants that had been inoculated with BOR2 did not appear to have any bacteria present (Figure 4.1).

These findings indicate that the BOR2 rhizobia may have ceased to grow and may have been lost from the nodule in later stages. BOR2 rhizobia have previously been found by (van Velzen et al., 2018) in *P. andersonii* six weeks old nodules using light microscopy; these plants were seven weeks old, which might represent a senescent state

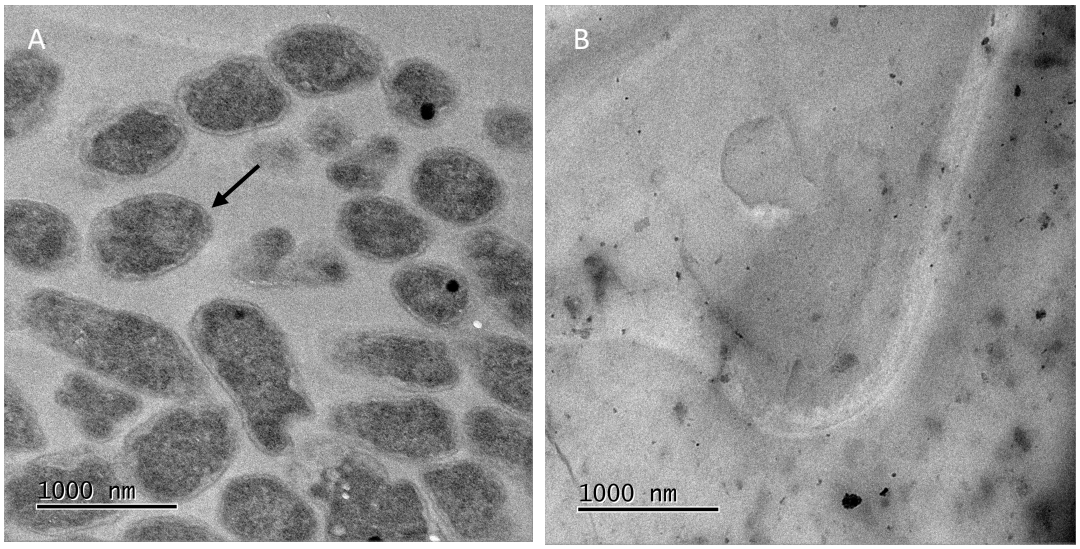


**Figure 4.1 Electron microscopy images of *Parasponia andersonii* nodules inoculated with either *Bradyrhizobium elkanii* (WUR3) or *Mesorhizobium plurifari*um (BOR2)**
Images show *Parasponia andersonii* nodules at seven weeks old after being inoculated with 5 ml of rhizobia ($OD_{600}$ = 0.05). (A) *Bradyrhizobium elkanii* (WUR3) rhizobia can be seen (arrow) inside a *P. andersonii* nodules. (B) *Mesorhizobium plurifari*um (BOR2) rhizobia were not found inside the *P. andersonii* nodules.

### 4.2.2 RNA-Seq identifies only one differentially expressed gene at the whole root level between *Mesorhizobium plurifari*um (BOR2) vs *Bradyrhizobium elkanii* (WUR3) vs control-inoculated *Parasponia andersonii* roots

To establish what the molecular differences are that underpin the previously found phenotypes of the *Mesorhizobium plurifari*um (BOR2) and *Bradyrhizobium elkanii* (WUR3) inoculated nodules (see Chapter 3), an experiment was carried out to establish the differences in gene expression in nodules between BOR2 and WUR3-

inoculated plants at early stages of symbiotic interaction, using RNA-Seq. *P. andersonii* was potted from three week old rooted *P. andersonii* tissue culture and grown at 28 °C in 16-hour light/ 8-hour dark for two weeks. The plants were then inoculated with 300 µl of BOR2 ($OD_{600}$ = 0.05), WUR3 ($OD_{600}$ = 0.05) or water as a mock and the roots were harvested for RNA extraction over a timecourse of 0 hours (mock only), 24 hours, and 7 days.

After extracting RNA with three repeats of each condition, it was sequenced with reactions for paired end, unstranded, 150 bp read length sequences with a depth of at least 20 million reads per sample (Novogene). For trimming, fastp was used (Chen et al., 2018) and the alignment and counts (the number of times the reads align to each gene) were generated using STAR (Dobin et al., 2013). The *P. andersonii* genome and genome annotation (NCBI BioProject number PRJNA272473) used for alignment was found on parasponia.org (van Velzen et al., 2018). DESeq2 (Love et al., 2014) was used to carry out differential expression analysis, including internal normalisation. The plotPCA function within DESeq2 was then used to produce a Principal Component Analysis (PCA) plot to ask if the RNA-Seq replicate samples clustered. PCA analysis showed that there was no clear clustering within replicates which indicates that Differentially Expressed Genes (DEGs) were unlikely to be found (Figure 4.2).

Initially, each timepoint for WUR3 and BOR2 inoculated nodules was compared to the mock at the corresponding time point to ask if there were any DEGs present. Using DESeq2, only one DEG found was between BOR2-inoculated roots at seven days versus the mock roots at seven days with a $\log_2$ fold change > 1 and padj < 0.05. This was a less strigent analysis compared to other methods using DESeq2 with where the $\log_2$ fold change requirement was > 2 (van Velzen et al., 2018), and yet only one DEG was found, PanWU01x14_324850, a cupredoxin.

The reason for the lack of within-replicate clustering and DEGs could be explained by the sampling technique. Spot inoculation of the rhizobia was carried out and the whole roots was sampled, which could have meant any differences that could have been found were diluted as the whole root would not be in contact with inoculant. The reason for taking the whole root was due to previous findings as BOR2-

harbouring nodules were found quite far down the root and not just at the top (see Chapter 3). This knowledge of nodule placement, combined with these being very young *P. andersonii* roots meaning there was not much material to harvest led to the decision to harvest the whole root for RNA extraction. Whilst this experiment did not provide insight into the early stages of nodulation in *P. andersonii*, it would be worth repeating with adjustments to the sampling technique. In this work, rather than analysing root-located responses, RNA expression differences in nodules were then pursued.

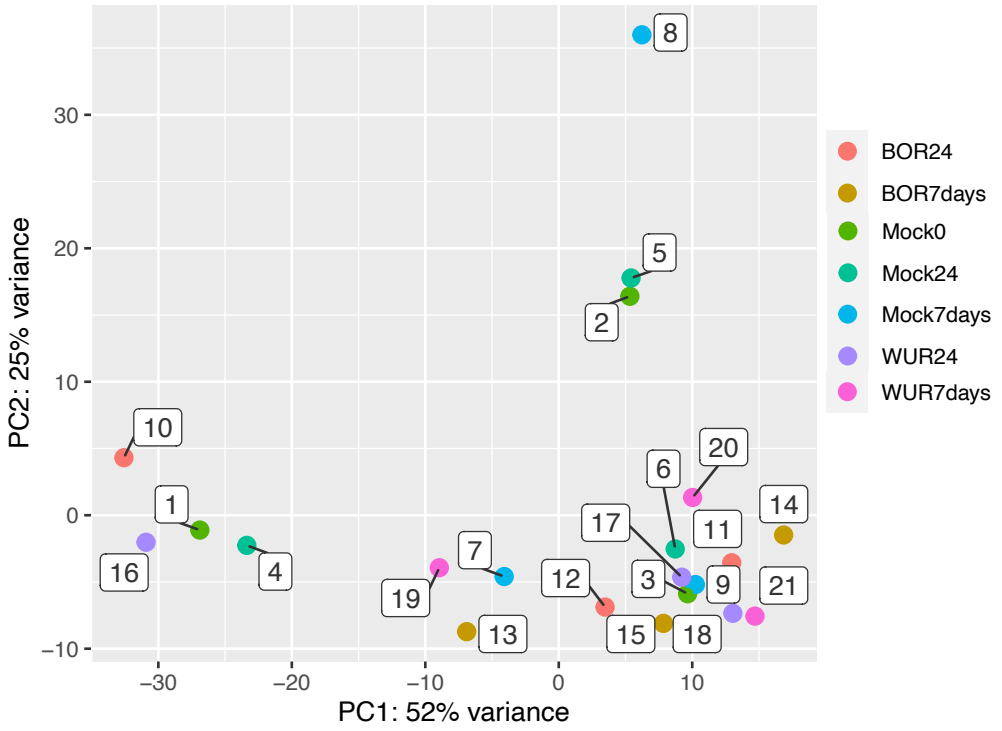


**Figure 4.2 Principal component analysis of RNAseq data from *Mesorhizobium plurifariu*m (BOR2) vs *Bradyrhizobium elkanii* (WUR3) vs mock inoculation in a time course of *Parasponia andersonii* roots**
PCA plot of *Parasponia andersonii* RNA-Seq counts did not find any clustering by sample type. *P. andersonii* plants were potted from rooted tissue culture and grown for two weeks at 28 °C in a 16-hour light/ 8- hour dark cycle. Plants were then inoculated with water and harvested at 0 hours (labels 1-3), 24 hours (labels 4-6) or 7 days (labels 7-9) (control samples). *P. andersonii* was also inoculated with *Mesorhizobium plurifariu*m (BOR2) rhizobia and harvested at 24 hours (labels 10-12) and 7 days (labels 13-15) or *Bradyrhizobium elkanii* (WUR3) rhizobia at 24 hours (labels 16-18) and 7 days (19-21). Roots from three plants wee included in each repeat. Samples from within each treatment type/timepoint are coloured the same, as shown in the key.

### 4.2.3 RNA-Seq of *Mesorhizobium plurifari*um (BOR2) vs *Bradyrhizobium elkanii* (WUR3) harbouring *Parasponia andersonii* nodules found 371 differentially expressed genes

To ask if there are any gene expression differences between BOR2 and WUR3-inoculated nodules to help explain the different nodule phenotypes, the nodules themselves were compared at the gene expression level. This involved extracting RNA from BOR2 and WUR3 inoculated *P. andersonii* nodules eight weeks after a 5 ml ($OD_{600}$ = 0.05) inoculation of four week old *P. andersonii* plants from tissue culture. This was a second inoculation of WUR3 or BOR2 due to an inoculation of 300 µl of BOR2 or WUR3 of one day old *P. andersonii* plants from tissue culture had not produced nodules after four weeks.

After extracting RNA from nodules of four plants in each repeat and two repeats of each condition, RNA was sequenced with reactions for paired end, unstranded, 150 bp read length sequences (Novogene). The depth of sequencing was determined to be at least 20 million reads per sample. For trimming, fastp was used (Chen et al., 2018) and the alignment and counts (the number of times the reads align to each gene) were generated using STAR (Dobin et al., 2013). The *P. andersonii* genome and genome annotation (NCBI BioProject number PRJNA272473) used for alignment was found on parasponia.org (van Velzen et al., 2018). DESeq2 (Love et al., 2014) was used to for differential expression analysis, including internal normalisation.

The plotPCA function within DESeq2 was used to produce a PCA plot to determine ask if the RNA-Seq samples clustered on a global level. It was found that the two repeats of each inoculant were clustered together (Figure 4.3 A), suggesting that there may be differentially expressed genes between rhizobial inoculant types. For this RNA-Seq analysis, BOR2-inoculated nodules were designated as the baseline when identifying differentially expressed genes (DEGs). Using DESeq2, a total of 371 DEGs were found between BOR2- and WUR3-harbouring nodules with a $\log_2$ fold change ≥ 1.5 and padj < 0.05. A heat map of the $\log_2$ transformed counts data of BOR2 and WUR3 inoculated nodules averaged across the two repeats was then

generated in order to visualise the extent of gene expression change between nodule samples (Figure 4.3 B).

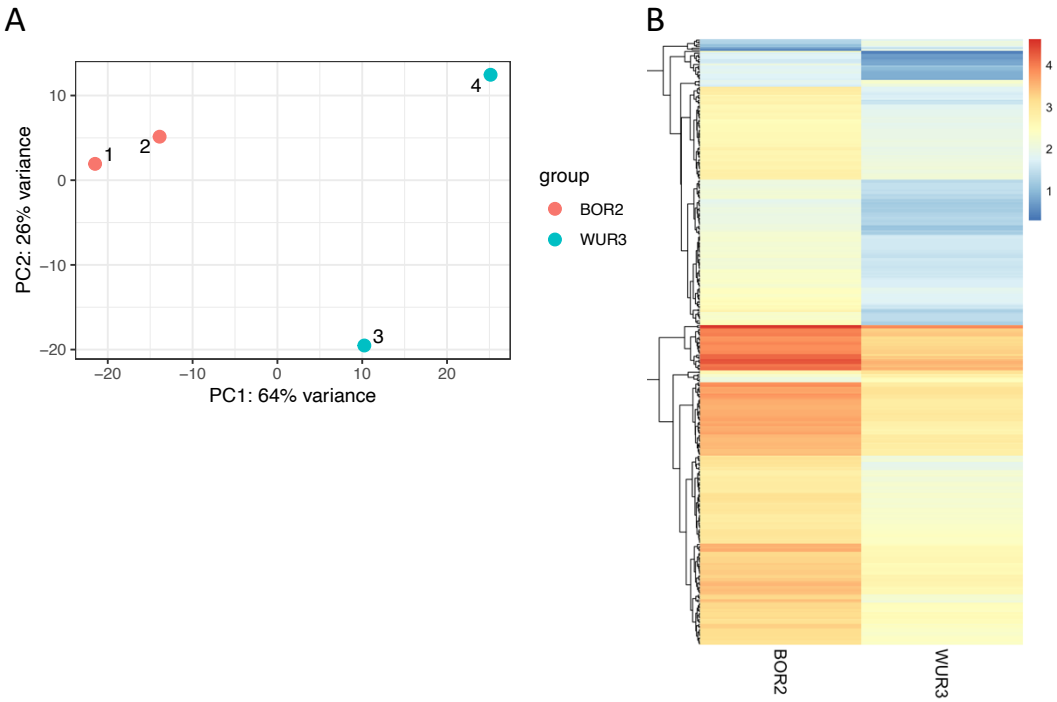


**Figure 4.3 PCA plot and heatmap visualising *Mesorhizobium plurifari*um (BOR2) vs *Bradyrhizobium elkanii* (WUR3) inoculated *Parasponia andersonii* nodules differential gene expression**
(A) A PCA plot showing the clustering of the two repeats of *Parasponia andersonii* nodules inoculated with *Mesorhizobium plurifarium* (BOR2) (red dots 1 and 2) or *Bradyrhizobium elkanii* (WUR3) (blue dots 3 and 4).
(B) A heatmap of normalised average counts of the 371 DEGs of BOR2 and WUR3-inoculated *P. andersonii* nodules. The scale bar represents the gene expression level from lowest (blue) to highest (red)

Out of the 371 DEGs, 18 of these DEGs were expressed at a higher level in WUR3-inoculated nodules than in BOR2 inoculated nodules and the other 318 DEGs were expressed at a lower level in WUR3 inoculated nodules compared to BOR2-inoculated nodules (Figure 4.4). Unexpectedly, this demonstrates that the nodules harbouring BOR2 were undergoing more substantial changes at the molecular level compared to nodules harbouring WUR3.

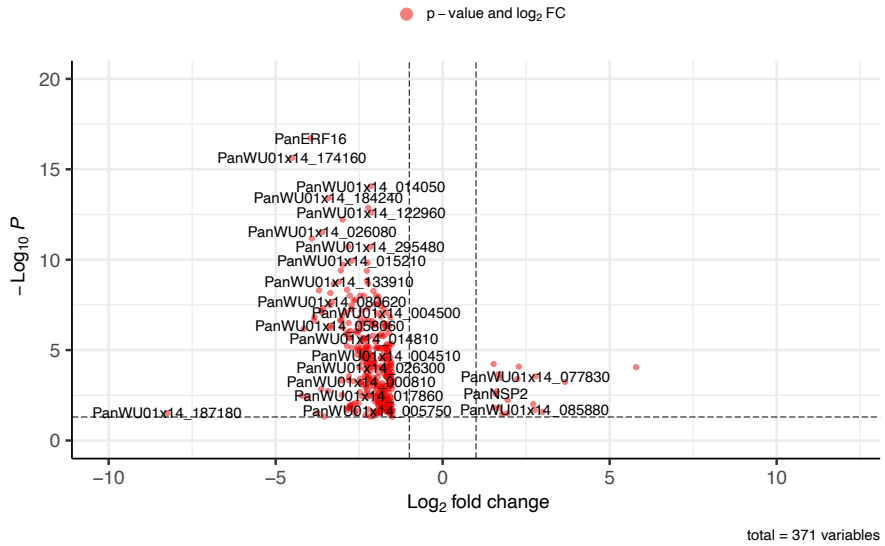


**Figure 4.4 An enhanced volcano plot showing the $log_2$ fold change of gene counts of *Mesorhizobium plurifari*um (BOR2) vs *Bradyrhizobium elkanii* (WUR3) inoculated *Parasponia andersonii* nodules versus the $log_{10}$ *P* -value**
371 DEGs were found between *Mesorhizobium plurifarium* (BOR2) and *Bradyrhizobium elkanii* (WUR3)-inoculated *Parasponia andersonii* nodules with $log_2$ fold change ≥ 1.5 and padj < 0.05. The majority of the DEGs were expressed at a lower level in WUR3-inoculated nodules compared to BOR2-inoculated nodules.

### 4.2.4 *Mesorhizobium plurifari*um (BOR2) vs *Bradyrhizobium elkanii* (WUR3) harbouring nodules DEGs can be grouped into four clusters

Hierarchical clustering of the RNA-Seq data was then used to group the DEGs found, with an elbow method used to determine the optimal number of clusters (Figure 4.5 A). Four clusters were determined to be optimal, based on where the "elbow" of the curve landed. Genes in five clusters were also investigated as it could also be seen as where the "elbow" of the curve is, however, this did not break up the large Cluster 1 and instead broke up the small Cluster 3, which did not add any biological value, and so it was considered than four clusters were optimal.

A heat map of the $log_2$ transformed counts data of BOR2 and WUR3 inoculated nodules was then generated within the four clusters in order to visualise the extent of gene expression change between nodule samples within each cluster (Figure 4.5 B). Cluster 1 contained 338 DEGs, Cluster 2 contained two DEGs

(PanWU01x14_014810 and PanWU01x14_152000), Cluster 3 contained 29 DEGs and Cluster 4 contained three DEGs (*PanZnF13*, PanWU01x14_082630 and PanWU01x14_333240).

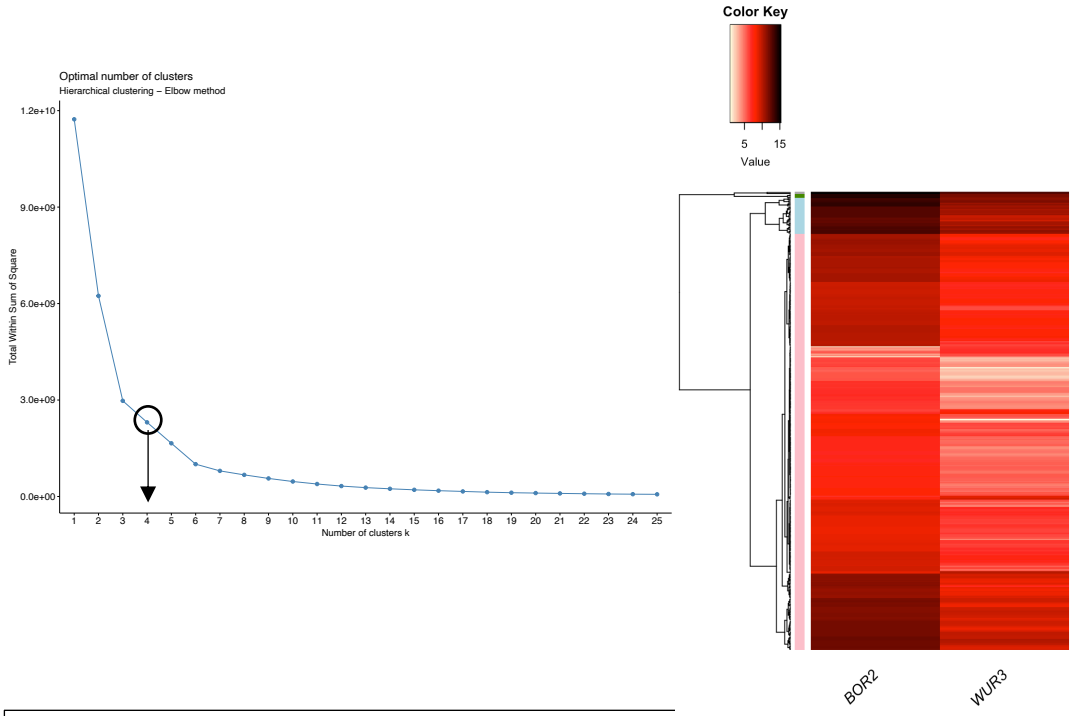


**Figure 4.5 Clustering of *Mesorhizobium plurifari*um (BOR2) vs *Bradyrhizobium elkanii* (WUR3) inoculated *Parasponia andersonii* DEGs, with a heatmap showing the DEGs within the four clusters**
(A) The optimal number of clusters was determined using heirachical clustering and the elbow method. This was determine to be 4 clusters where the elbow of the curve is (black arrow)
(B) A heatmap of normalised average counts of the 371 DEGs of *Mesorhizobium plurifarium* (BOR2) and *Bradyrhizobium elkanii* (WUR3)-inoculated *P. andersonii* nodules within the four clusters. Cluster 1 had 338 DEGs (pink), Cluster 2 had two DEGs (grey), Cluster 3 had 29 DEGs (blue) and Cluster 4 had three DEGs (green). The gradient bar shows the number of counts from lowest (pale yellow) to highest (black).

### 4.2.5 Cluster 1 includes highly expressed genes in *Mesorhizobium plurifari*um (BOR2) inoculated nodules that may be related to regulation of nodule senescence

In order to determine which processes were differentially expressed between BOR2 and WUR3 harbouring nodules a GO term enrichment analysis was conducted on each set of DEGs using a weighted Fisher statistic using the R package topGO (Alexa and Rahnenfugrer, 2022). The weighted Fisher test then calculates the

significance of the signifcant vs the expected numbers of genes within each GO term category and any GO terms with a *P*-value < 0.05 were considered enriched. The GO term annotations were mapped to the genome from a combination of UniProt submissions and InterProScan. The three categories of GO terms analysed were Biological Processes (BP), Molecular Function (MF) and Cellular Components (CC). Each cluster was then analysed for the enriched GO terms.

Cluster 1 was the largest cluster with 338 DEGs and includes all 18 DEGs that were more highly expressed in WUR3-harbouring nodules compred to BOR2-harbouring nodules. The GO term enrichment analysis showed that this cluster had nine enriched biological functions (BF), four enriched molecular functions (MF) and 17 enriched cellular components (CC) GO terms that were found to be *P*-value < 0.05 in the weighted Fisher test. GO Terms with *P*-value < 0.05 and at least five signifcant genes are presented in (Table 4.1).

One of the enriched BF GO terms of interest in Cluster 1 was the ethylene-activated signalling pathway (GO:0009873) that had ten significant genes with this GO term. Ethylene is a negative regulator of nodulation (Oldroyd et al., 2001) but it has also been found that ethylene was upregulated in nodule senescence in common bean (da Silva et al., 2019). This is interesting as all ten of the ethylene-activated signalling pathway genes are more highly expressed in BOR2-harbouring nodules compared to WUR3-harbouring nodules

Nine of the genes within the ethylene-activated signalling pathway are Apetala2 (AP2)/Ethylene Response Factors (ERF) transcription factors and all 10 of these genes are more highly expressed in BOR2-harbouring nodules compared to WUR3-harbouring nodules. The most highly expressed of these ten genes in BOR2-inoculated nodules compared to WUR3-inoculated nodules was *PanERF21* (Figure 4.6 A) which has an *M. truncatula* ortholog *MtERF109*. Whilst there is limited information on the *M. truncatula* ortholog of *PanERF21* (*MtERF109*), the *Arabidopsis thaliana* ortholog of *PanERF21* (*AtERF109* (previously known as *RRTf1*)) has been found to be upregulated in response to abiotic such as salt stess (Soliman and Meyer, 2019) and biotic stress (Vahabi et al., 2018). However, *AtERF109* has been found to have dual role, where *AtERF109* was found to induce senescence in older leaves

(Matsuo and Oelmüller, 2015). Perhaps this senescence-regulatory role *AtERF109* suggests that *PanERF21* plays a senescence-regulatory role in BOR2-harbouring nodules.

| GO.ID | Term | Annotated Genes | Significant Genes | Expected | Weight Fisher | Category |
|---|---|---|---|---|---|---|
| GO:0009873 | ethylene-activated signalling pathway | 45 | 10 | 4.80E-01 | 3.30E-11 | BP |
| GO:0006355 | regulation of transcription, DNA-templated | 922 | 30 | 9.94E+00 | 8.30E-09 | BP |
| GO:0010411 | xyloglucan metabolic process | 27 | 7 | 2.90E-01 | 1.00E-08 | BP |
| GO:0042546 | cell wall biogenesis | 56 | 9 | 6.00E-01 | 6.60E-08 | BP |
| GO:0071555 | cell wall organization | 166 | 9 | 1.79E+00 | 1.30E-05 | BP |
| GO:0005618 | cell wall | 27 | 7 | 3.00E-01 | 1.40E-08 | CC |
| GO:0048046 | apoplast | 124 | 8 | 1.40E+00 | 7.50E-05 | CC |
| GO:0005634 | nucleus | 2029 | 36 | 2.28E+01 | 0.0024 | CC |
| GO:0005886 | plasma membrane | 330 | 9 | 3.71E+00 | 0.0121 | CC |
| GO:0003700 | DNA-binding transcription factor activity | 605 | 28 | 5.57E+00 | 1.20E-12 | MF |
| GO:0016762 | Xyloglucan : xyloglucosyl transferase activity | 28 | 7 | 2.60E-01 | 4.90E-09 | MF |
| GO:0043565 | sequence-specific DNA binding | 233 | 10 | 2.14E+00 | 5.90E-05 | MF |
| GO:0004553 | hydrolase activity, hydrolysing O-glycosyl bond | 352 | 12 | 3.24E+00 | 0.00059 | MF |
| GO:0003677 | DNA binding | 1280 | 30 | 1.18E+01 | 0.00071 | MF |
| GO:0004674 | protein serine/threonine kinase activity | 697 | 12 | 6.41 | 0.02731 | MF |
| GO:0016757 | glycosyltransferase activity | 579 | 13 | 5.33 | 0.0397 | MF |

**Table 4.1 Enriched biological function (BP), molecular function (MF) and cellular component (CC) GO terms within the 318 genes in Cluster 1**
Enriched GO terms using TopGO with *P*-value < 0.05 using a weighted Fisher test for Cluster 1. Overall, Cluster 1 had nine enriched BFs, four enriched MFs and 17 enriched CCs but only GO terms with > 5 significant genes are presented here.
"Annotated" indicates how many GO terms are found throughout the genome (that are currently available through UniProt and InterProScan), "Significant" indicates how many of the genes in the cluster have the GO term and "Expected" indicates how many of the GO terms would be expected to be expressed.

One of the enriched MF GO terms in Cluster 1 was the protein serine/threonine kinase activity GO term (GO:0004674) associated with 12 genes. All 12 of these genes were more highly expressed in BOR2-harbouring nodules compared to WUR3-harbouring nodules. The most highly expressed gene in BOR2-inoculated genes was *PanWU01x14_277820* (Figure. 4.6 B), a G protein-coupled receptor (GPCR) kinase. BLASTp of *PanWU01x14_277820* against the *M. truncatula*

database (version r5.0), found an ortholog of *MtMAPKKK20* which had an 98 % query cover (E value = 5e-131) with a *M. truncatula* ortholog invovled in the Mitogen-Acitvaetd Protein Kinase (MAPK) pathway named *MtMAPKKK20*. The MAPK pathway has been shown to be involved in ethylene signalling (Ouaked et al., 2003). This adds more evidence to the finding that the ethylene signalling pathway is a key component that is alternatively regulated in BOR2-harbouring nodules.

It is also interesting that the seven genes associated with the enriched GO term xyloglucan metabolic process (GO:0010411) all encode xyloglucan endotransglucosylase/hydrolase (XTH) (EC 2.4.1.207) proteins. All seven are also associated with the enriched GO terms cell wall biogenesis (GO:0042546), cell wall organisation (GO:0071555) and hydrolase activity (GO:0004553). They were found to be expressed more highly in BOR2-harbouring nodules compared to WUR3-harbouring nodules. As reviewed in (Hofte and Voxeur, 2017), xyloglucan is found in cell walls and increases the rigity of the cell walls by holding the layers of cellulose microfibrils together, which makes it intriguing as to why the hydrolyases are highly expressed in BOR2-harbouring nodules. Whilst there is very limited information on the role of *XTH* genes, there is some information on them being involved in leaf senescence, which have similar ways of functioning. An *XTH* gene found in *Diospyros kaki L.* (persimmon fruit tree) called *DkXTH8* was found to promote leaf senescence (Han et al., 2016). When the *DkXTH8* sequence was used as a BLASTp query against the *P. andersonii* database, the *PanWU01x14_184290* gene, which is amongst the seven DEGs, was found to have an 90 % query cover (E value = 3e-139), suggesting the genes are orthologs (Figure 4.6 C). Further study of *PanWU01x14_184290* would be interesting. It has previously been found that *ERF* genes could activate another XTH *D. kaki* gene, *DkXTH9*, during fruit softening (Wang et al., 2017) and a BLASTp search against the *P. andersonii* database suggests that *DkXTH9* is an ortholog of *PanWU01x14_184240* with a 93 % query cover (E value = 7e-129), another member of the seven DEGs.

Whilst the phloem development pathway GO term (GO:0010088) was found to be enriched, there were only two significant DEGs associated with this. This makes it hard to generalise, but they are worth considering since these two DEGs were in

the top five most highly expressed genes in BOR2-harbouring nodules compared to WUR3-harbouring nodules, with *PanWU01x14_187180* having the largest $log_2$ fold change of all the DEGs at -8.252 (Figure 4.6 D). These genes encode proteins for sieve element occlusion which is involved in blocking the phloem, thus blocking nutrient transport. During severe nutritional restriction, callose can build up to block the sieve pores (sieve element occlusion) in order to redirect resources for the best chance of survival. This can be seen in other areas of plant biology such as in seed development where the phloem supply of nutrients to some seeds is blocked to redirect nutrients to other seeds in order to maximise the chances of some seeds surviving (Martínez-Barradas et al., 2019).

*Glycine max L.* (soybean) nodules have a continuous phloem connection around the nodule (Livingston et al., 2019) and *P. andersonii* nodles have more of a central vascular system within the nodule (Bu et al., 2020, Trinick, 1979). Unusually, the supply of water to the nodule is through plant phloem flow and not via the xylem, as reviewed in (Sinclair and Nogueria, 2018). It is possible that *PanWU01x14_187180* expression leads to water and nutrient supply shutdown of BOR2-harbouring nodules, as an early step in nodule senescence as suggested by expression of the *XTH* genes. Perhaps this could be *P. andersonii* responding to the restricted supply of nitrogen and so without BOR2 supplying the nitrogen needed, the phloem is being blocked in order to redirect any available nutrients to the rest of the plant.

Six of the 18 DEGs that were more highly expressed in WUR3-harbouring nodules compared to BOR2-harbouring nodules were linked to enriched GO terms. However, only four of them belonged to GO terms that had more than five significant genes. These were *PanNSP2* (Figure 4.6 E) and *PanWU01x14_222790* that had the nucleus GO Term (GO: 0005634), *PanWU01x14_262630* and *PanDVL11* had the plasma membrane GO Term (GO:0005886) and *PanWU01x14_057030* that had the hydrolyase activity GO Term (GO:0004553). *NSP2* is well known to activate Nodulation Inception (*NIN*) in legumes (Xiao et al., 2020) which is important as *NIN* is needed for co-ordinating the nodulation process (Vernie et al., 2015). *PanNSP2* has also been found to be essential for nodule formation in *P. andersonii* (Van Zeijl et al., 2018) and in *M. truncatula*, *MtNSP2* has also been found to be active in mature

nodules (Roux et al., 2014), and that it may function in nodule differentiation (Kovacs et al., 2021). This demonstrates that WUR3-harbouring nodules express *PanNSP2* in

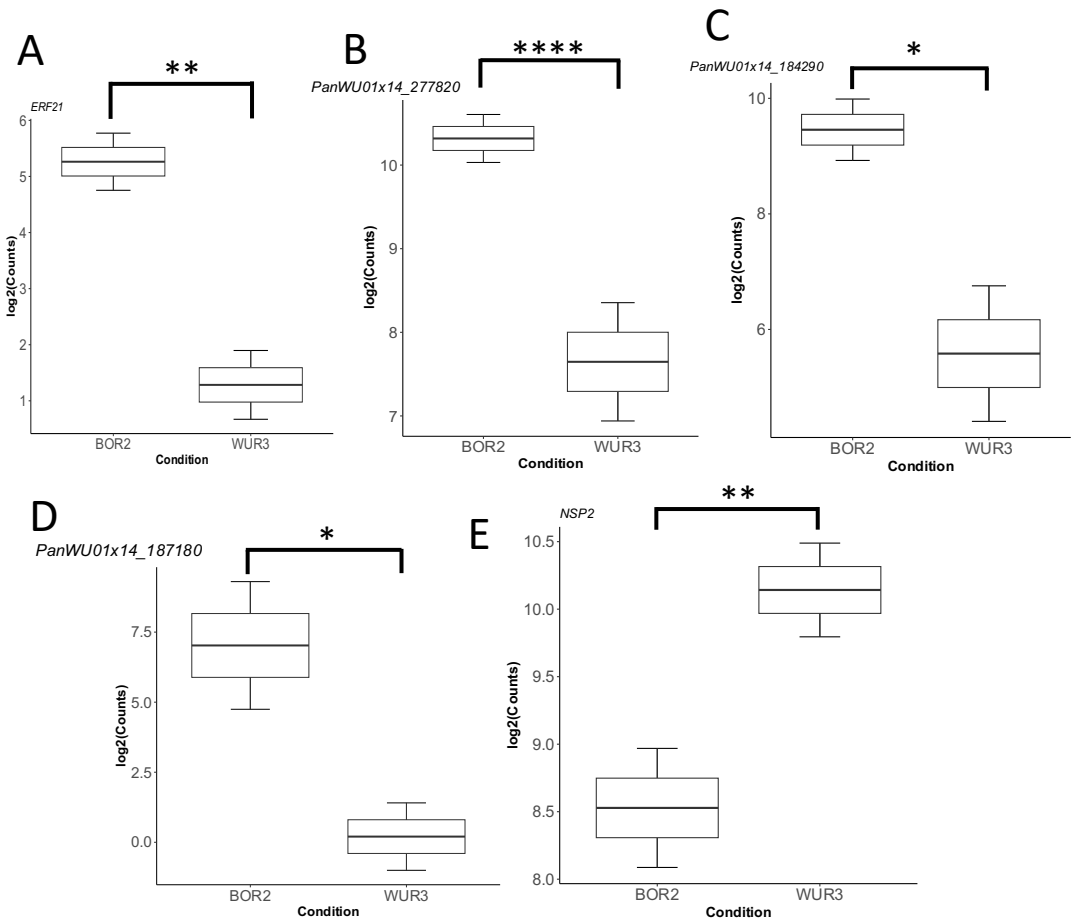


**Figure 4.6 Expression analysis of significant DEGs associated with enriched GO terms in *Mesorhizobium plurifari*um (BOR2) vs *Bradyrhizobium elkanii* (WUR3)-inoculated nodules**

(A) *PanERF21* that is annotated to the ethylene-activated signalling pathway GO term (GO:0009873) is significantly more highly expressed in *Mesorhizobium plurifari*um (BOR2) harbouring nodules compared to the *Bradyrhizobium elkanii* (WUR3) harbouring nodules

(B) *PanWU01x14_277820* that is a annotated to the GO term protein serine/threonine kinase activity GO term (GO:0004674) that has the *Medicago truncatula* ortholog *MtMAPKKK20*.

(C) *PanWU01x14_184290*, an endotransglucosylase/hydrolase (XTH) and has been annotated with the GO term xyloglucan metabolic process (GO:0010411).

(D) *PanWU01x14_187180*, annotated with the phloem development GO term (GO:0010088) is significantly more highly expressed in BOR2-harbouring nodules compared to WUR-harbouring nodules.

(E) *PanNSP2* that is annotated to the nucleus cellular component GO term (GO:0005634) that is one of the few DEGs to be more upregulated in WUR3-harbouring nodules compared to BOR2-harbouring nodules.

* = padj < 0.05, ** = padj < 0.01, **** = padj < 0.0001.

more mature nodules, and it would be interesting to see if a knockdown of *PanNSP2* would also cause a delay in nodulation as was seen in *M. truncatula* with a knockdown *MtNSP2* (Kovacs et al., 2021).

### 4.2.6 *PanWU01x14_152000* is a gene in Cluster 2 involved in abiotic stress response

Cluster 2 only contained two DEGs and the GO enrichment analysis found four enriched GO terms with a *P*-value < 0.05 (Table 4.1), however, due to there only being two DEGs, there is only limited ability to be generalist from this cluster. However, what is interesting is *PanWU01x14_152000*, a gene coding for a dehydrin protein was found to be highly expressed in BOR2 inoculated nodules compared to WUR3 and is associated with the enriched GO Terms related to response to water deprivation (GO:0009414) and response to cold (GO:0009409) (Figure 4.7). *PanWU01x14_152000* was found in previous reasearch to have an ortholog in the form of Cold-Acclimation-Specific 31 (*MtCAS31*) (Medtr6g084640) (van Velzen et al., 2018). In *M. truncatula*, *MtCAS31* is suspected to have different roles dependent on whether the abiotic stress is moderate or severe, as it was found to be expressed under drought stress. It was found to be expressed after two drought cycles (one drought cycle is seven days of drought followed by 100 ml of water) and it was suggested that *MtCAS31* protects nitrogen fixation as mutants had lower nitrogenase activity and increased expression of nodule senescence genes (Li et al., 2018). However, with three drought cycles *MtCAS31* was found to be involved in the autophaic degradation pathway (Li et al., 2020). Autophagic degradation is still being unravelled in terms of its role in senescence, however, as reviewed in (Wang and Schippers, 2019), autophagy initially stalls senescence in leaves but once senescence commences, autophagy is required to break down important components to be recycled by the plant. This could suggest a role for *PanWU01x14_152000* in BOR2-inoculated nodules that go through senescence, in that high levels of expression of *PanWU01x14_152000* may enable nutrient salvaging.

| GO.ID | Term | Annotated | Significant | Expected | Weighted Fisher Statistic | Category |
|---|---|---|---|---|---|---|
| GO:0009414 | response to water deprivation | 7 | 1 | 0 | 0.0013 | BP |
| GO:0009409 | response to cold | 19 | 1 | 0 | 0.0035 | BP |
| GO:0009737 | response to abscisic acid | 65 | 1 | 0.01 | 0.0119 | BP |
| GO:0046872 | metal ion binding | 2557 | 2 | 0.33 | 0.027 | MF |

**Table 4.2 Enriched biological function (BP), molecular function (MF) and cellular component (CC) GO terms within the two genes in Cluster 2**
Enriched GO terms using TopGO with *P*-value < 0.05 using a weighted Fisher test for Cluster 2. All GO terms found are presented here with three enriched BPs and two enriched MFs.

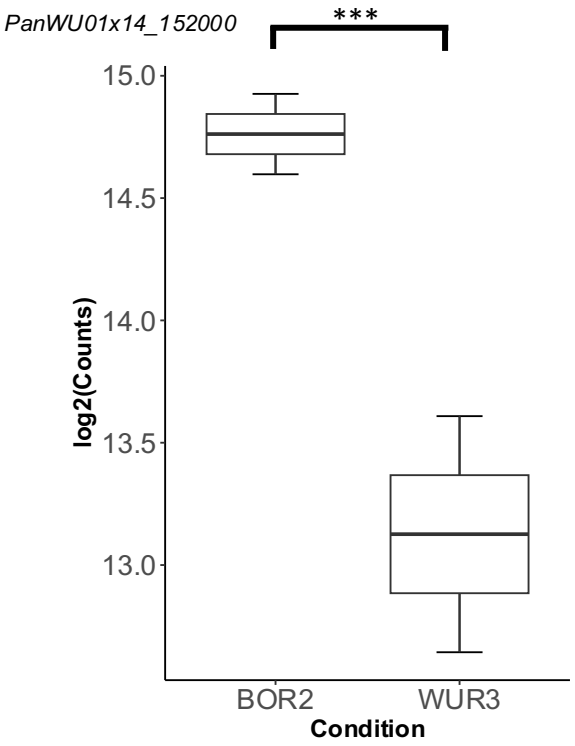


**Figure 4.7 Expression of a significant DEG (*PanWU01x14_152000*) found in Cluster 2 enriched GO terms**
*PanWU01x14_152000* that is annotated with response to water deprivation GO term (GO:0009414) and response to cold GO term (GO:0009409) is significantly more highly expressed in BOR2-harbouring nodules compared to WUR3-harbouring nodules
*** = padj < 0.001.

### 4.2.7 Cluster 3 contained genes potentially involved in nodule senescence

Cluster 3 contained 29 DEGs and the GO enrichment analysis found eight BP, nine MF and two CC GO terms with a *P*-value < 0.05. GO terms with at least seven significant genes are presented in (Table 4.3). Five of the DEGs in Cluster 3 were associated with three of the enriched GO terms, regulation of transcription (GO:0006355), DNA-binding transcription factor activity (GO:0003700) and nucleus (GO:0005634). These five DEGs are basic helix-loop-helix 102 (*PanbHLH102*), *PanWRKY37*, *WRKY50* and two AP2/ERF genes; *PanERF34*, *PanERF84*. All of these genes were found to be more highly expressed in BOR2 harbouring nodules compared to WUR3 harbouring nodules. *M. truncatula AP2/ERF*, *WRKY* and *bHLH* genes are all upregulated during age-dependent and dark-induced leaf senescence (Mahmood et al., 2022). As (Van de Velde et al., 2006) found, nodule and leaf senescence are very similar processes, and thus this expression analysis result could indicate that BOR2 is no longer found in the nodules is due to the nodule going through senescence.

| GO ID | Term | Annotated | Significant | Expected | Weighted Fisher Statistic | Category |
|---|---|---|---|---|---|---|
| GO:0006355 | regulation of transcription, DNA-templated transcription | 922 | 5 | 1.19 | 0.0046 | BP |
| GO:0003700 | DNA-binding transcription factor activity | 605 | 5 | 0.66 | 0.00036 | MF |
| GO:0046872 | metal ion binding | 2557 | 7 | 2.78 | 0.02413 | MF |
| GO:0005634 | nucleus | 2029 | 7 | 2.85 | 0.014 | CC |

**Table 4.3 Enriched biological function (BP), molecular function (MF) and cellular component (CC) GO terms within the two genes in Cluster 3**
Enriched GO terms using TopGO with *P*-value < 0.05 using a weighted Fisher test for Cluster 3. All GO terms found are presented here with one enriched BP and two enriched MFs and one enriched CC.

### 4.2.8 Cluster 4 contains a gene involved in senescence

Cluster 4 only contained three DEGs and the GO enrichment analysis found four enriched GO terms with a *P*-value < 0.05 (Table 4.1). However, due to there only being three DEGs, similiarly to Cluster 2 there is only limited generality to be gained

from this information. There was one GO term of interest enriched, GO:0098542 which is related to defence responses to other organism. The gene associated with this GO term was *PanWU01x14_082630*, which was more highly expressd in BOR2 inoculated nodules compared to WUR3 inoculated nodules. *PanWU01x14_082630* codes for a late embryogenesis abundant protein and was found to be a 100 % query match to the *A. thaliana* gene Yellow Leaf Specific 9 (*AtYLS9)* (E value = 5e-79), suggesting that the genes are orthologs. *AtYLS9* is expressed during leaf senescence, particularly during late stages (Yoshida et. al., 2001) and is also regularly used as a marker for leaf senescence in research in *A. thaliana* (Zhang et al., 2022). Although the finding of a single gene, this adds further evidence pointing towards BOR2-harbouring nodules being in the process of senescing.

| GO.ID | Term | Annotated | Significant | Expected | weightFisher | Category |
|---|---|---|---|---|---|---|
| GO:0098542 | defense response to other organism | 112 | 1 | 0.02 | 0.021 | BP |
| GO:0000272 | polysaccharide catabolic process | 118 | 1 | 0.02 | 0.022 | BP |
| GO:0016161 | beta-amylase activity | 8 | 1 | 0 | 0.001 | MF |
| GO:0102229 | amylopectin maltohydrolase activity | 8 | 1 | 0 | 0.001 | MF |

**Table 4.4 Enriched biological function (BP) and molecular function (MF)) GO terms within the two genes in cluster 4**
Enriched GO terms using TopGO with *P*-value < 0.05 using a weighted Fisher test for Cluster 3. All GO terms found are presented here with two enriched BP and two enriched MFs.

## 4.3 Discussion

When investigating new symbiotic relationships between a host and its symbiont, it is relevant to assess if they are not only efficiently initiated, but also sustained. This chapter has analysed potential reasons behind why *Mesorhizobium plurifari*um (BOR2) harbouring nodules were not leading to benefits for *P. andersonii* in terms of leading to an increase in shoot or root biomass (Chapter 3). This was especially puzzling as (van Velzen et al., 2018) found that there was nitrogenase activity ocurring within nodules containing BOR2.

Previous research on *P. andersonii* found live BOR2 inside *P. andersonii* nodules at six weeks when the nodule appeared to be active (van Velzen et al., 2018). However, at seven weeks, as in the experiments carried out here, BOR2 bacteria are no longer found inside nodules. Part of nodule senescence involves bacterial lysis and, as found by (Van de Velde et al., 2006), degradation of the symbiont partner happens before plant cell death occurs. This is in alignment with data in this chapter. The RNA-seq expression profiling analysis was conducted on eight week old nodules, and high expression of genes in relation to nodule senescence and cell wall degradation (e.g XTHs) found. This suggests that *P. andersonii* has potentially sanctioned BOR2 as is beginning to break down the nodule by eight weeks after inoculation, this sanctioning has been shown to happen in other legumes such as *L. japonicus* when inoculated with ineffective rhizobia (Regus et al., 2017).

*P. andersonii* has been shown to control its symbiotic relationships when enough nitrogen is available by not having unneeded symbiotic partners (Dupin et al., 2020). However, this work has shown that even once nodule organogenesis has begun, *P. andersonii* is still capable of controlling its symbionts by cutting off supply and killing off the bacteroids inside and the nodule as a whole (Figure 4.8). The reason why is currently unclear, perhaps BOR2 rhizobia are receiving more carbohydrates and not returning enough nitrogen to make the relationship sustainable. Perhaps future research can unravel this mechanism by using radiolabelled carbon to establish if there is a difference in carbon allocation when *P. andersonii* is inoculated with *Bradyrhizobium elkanii* (WUR3) rhizobia vs. BOR2 rhizobia. Using carbon tracers

has successfully been used before to show that carbon allocation in *Pisum sativum* (Pea) reduced by 40 % to nodules when nitrate was added (Metzner et al., 2022).

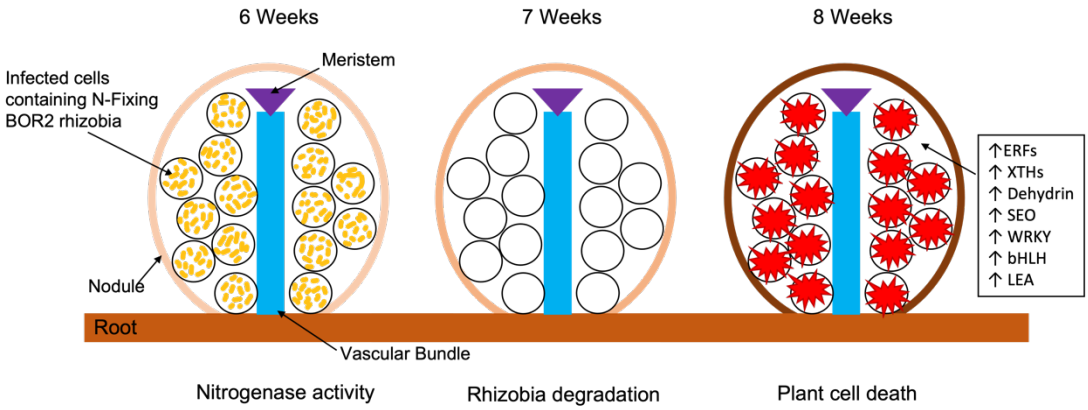


**Figure 4.8 An overview of the *Mesorhizobium plurifari*um (BOR2)-*Parasponia andersonii* nodule progression**
An overview of nodule progression when *Parasponia andersonii* is inoculated with *Mesorhizobium plurifari*um (BOR2). At six weeks, rhizobia can be seen within the nodule and nitrogenase activity is detected as found by (van Velzen et al., 2018). At seven weeks, the rhizobia are no longer present within *P. andersonii* nodules, indicating they have been degraded. At eight weeks, genes related to nodule senescence and potentially autphagic degradation are upregulated.
ERFs = Ethylene Response Factor, XTH = Xyloglucan endotransglucosylase/hydrolases, SEO = Sieve Element Occlusion, bHLH = basic helix-loop-helix and LEA = late embryogenesis abundant.

Analysis of RNA-Seq data between the BOR2 and WUR3 harbouring nodules is highly informative as it suggests that BOR2-harbouring nodules are potentially in the process of nodule senescence. Firstly, genes involved in the ethylene activated pathway are highly expressed in BOR2-harbouring nodules. Ethylene is not only a negative regulator throughout nodule organogenesis as reviewed in (Velandia et al., 2022) but it has also been found to be upregulated in nodule senescence (da Silva et al., 2019). A number of protein serine/threonine kinases were also found to be increased in expression in BOR2-harbouring nodules and MAPKs belong to this group and the MAPK pathway has also been shown to be involved in ethylene signalling (Ouaked et al., 2003). Xyloglucan endotransglucosylase/hydrolases (XTH) proteins were found to be highly expressed in BOR2-harbouring nodules and XTH orthologs in *Diosphyros kaki L.* (persimmon fruit tree) were found to promote leaf senescence

(Han et al., 2016). With all these genes being found to have some form of link to senescence, it supports the hypothesis that this may be the case for BOR-harbouring nodules. The most highly DEGs in BOR2-harbouring nodules are related to sieve element occlusion, suggesting that the supply of nutrients to nodules is being decreased in order to conserve the plant reserve of carbohydrates and nutrients.

*PanWU01x14_152000* found in Cluster 2 is a putative ortholog of *MtCAS31*, a gene found to be involved in the autophagic degradation pathway (Li et al., 2020). Whilst this is only one gene, it adds to the argument that BOR2-harbouring nodules are in the process of going through senescence and recycling the nodule components.

Overall, evidence from this chapter points towards *P. andersonii* being capable of controlling its endosymbiotic relatioships and sanctioning nodules that are potentially under performing.

## 4.4 Conclusion

This chapter has provided evidence that *P. andersonii* is able to control its symbiotic relationships even after nodule organogenesis. Despite nitrogenase activity being found when *P. andersonii* is inoculated with BOR2 at the beginning of the relationship (van Velzen et al., 2018) (and thus likely indicating active nodules), the rhizobia inside the nodule seem to be degraded when nodules mature, and the nodule tissue appear to senesce.

# Chapter 5: Developing genetic transformation in *Parasponia andersonii* and *Medicago truncatula* to enable cell-type investigation of nodule regulation

## 5.1 Introduction

As previously introduced (Chapter 1), nodulation requires coordinated signalling and development across many different root cell types. The epidermis is the site of initial plant-rhizobia interaction, where flavonoids (or perhaps another chemoattractant) are released by the plant which attract rhizobia and the rhizobia respond with Nod Factors (NF), leading to controlled bacterial entry (Figure 5.1; references for interactions within the text); this occurs concomitantly with division of the pericycle then cortex to form the nodule tissue.

### 5.1.1 Cell type location of the nodulation signalling pathway

The nodulation signalling pathway involved all the different tissue types found within the root (Figure 5.1). Within the epidermis, receptors that are expressed and localised on the plant membrane are involved in recognising the NFs the rhizobia produce. In *Medicago truncatula*, LysM Domain Receptor-Like Kinase 3 (*LYK3*) (Smit et al., 2007), Nod Factor Perception (*NFP*) (Arrighi et al., 2006), Does Not Make Infections 2 (*DMI2*) (Pan et al., 2018) are NF receptors and reception of NF initiates the process of nodulation. If a compatible plant-rhizobia interaction occurs, *DMI1* is then activated and is involved in regulating the calcium spiking which is essential in early signalling during nodule initiation (Liu et al., 2022a). The calcium spiking activates *DMI3* which is then required to activate Interacting Protein of *DMI3* (*IPD3*) expression which interprets the calcium spiking (Rival et al., 2012, Messinese et al., 2007). This forms the *DMI3*-*IPD3* complex which is linked to the Nodulation Signalling Pathway 1/2 (*NSP1* and *NSP2*) complex by DELLA proteins (Jin et al., 2016). *DMI3*/*IPD3*, alongside *NSP1* and *NSP2* within the DELLA linked complex, activates the expression one of the key regulators in nodulation, Nodule Inception (*NIN*) (Singh et al., 2014, Jin et al., 2016). *NSP1*/*NSP2* activates *NIN* expression with the help of

Interacting Protein of *NSP2* (*IPN2*) that enables the *NSP1/NSP2* complex to bind to the *NIN* promotor (Xiao et al., 2020).

*NIN* is involved in co-ordinating responses across the different root cell types and is important for not only bacterial infection but also nodule organogenesis. Within the epidermis, *NIN* inhibits Early Nodulin 11 (*ENOD11*), a marker gene for early responses to NFs, via competitive inhibition with Ethylene Response Factor Required for Nodulation 1 (*ERN1*) on the *ENOD11* promotor (Vernié et al., 2015).

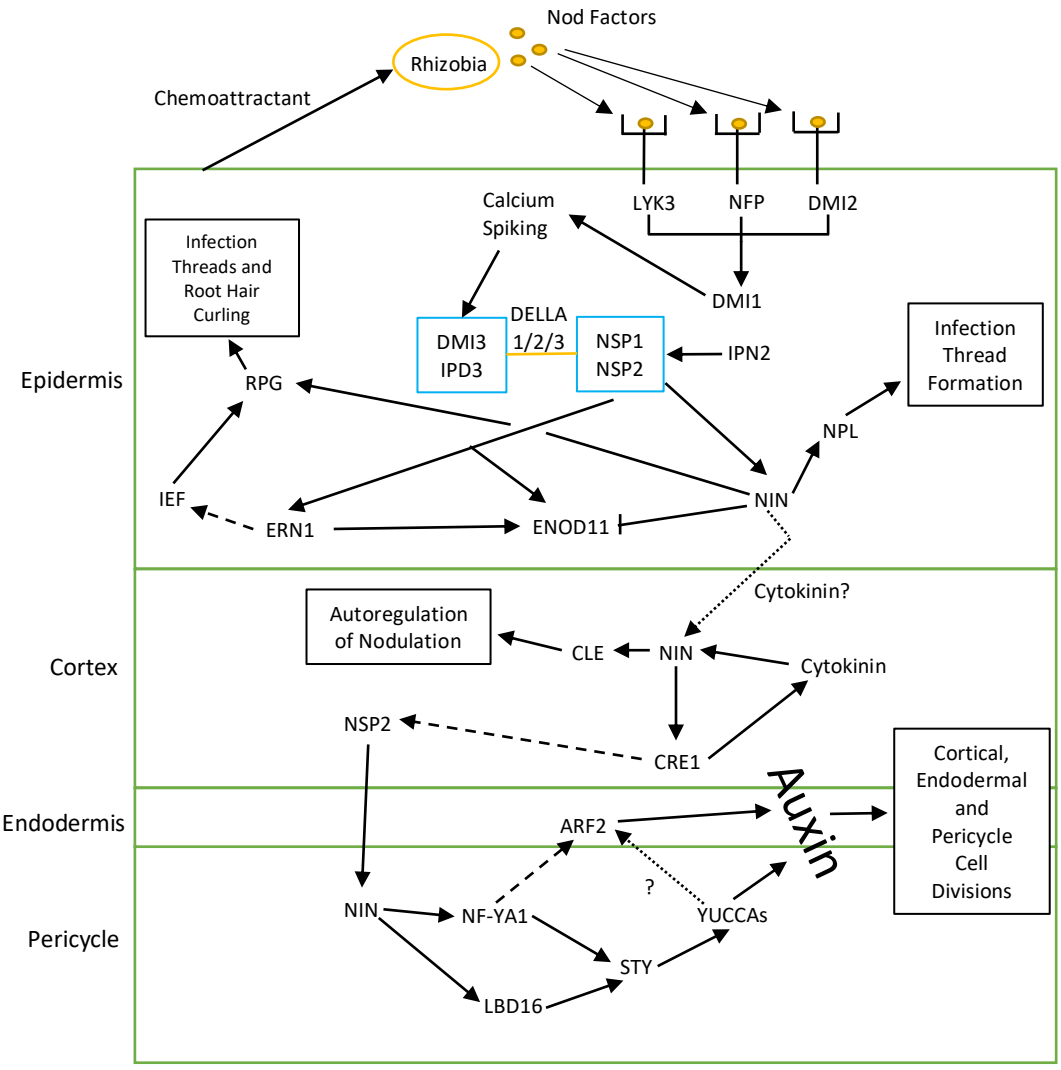


**Figure 5.1 Overview of the nodulation signalling pathway**
Chemoattractant and Nod factor signals are exchanged between the host plant and the rhizobia at the epidermis. This interaction initiates signalling within root tissue cell types and will eventually lead to infection threads being formed to allow the rhizobia to enter, at the same time as nodule organogenesis. Dashed line indicates indirect regulation; dotted line indicates a potential direct regulatory interaction. Yellow line = Link DELLA 1/2/3 provides between the *DMI3*/*IPD3* and *NSP1*/*NSP2* complexes.

*ERN1* and *ENOD11* expression have both also been shown to be induced by the *NSP1*/*NSP2* complex (Cerri et al., 2012).

Rhizobial travel through the root towards the nodule primordia via structures called infection threads. *NIN* has been shown another role as part of the infection thread development as it has been shown to promote Nodulation Pectate Lyase (*NPL*) expression which is required for remodelling the cell wall to allow for infection threads to form and elongate and therefore allowing for bacterial infection (Liu et al., 2019a). Rhizobium-directed Polar Growth (*RPG*) expression is also activated by *NIN* and is involved in root hair curling (needed to envelope the rhizobia in legumes that use root hair curling) and infection thread formation; *RPG* expression is also activated by Infection-related Epidermal Factor (*IEF*) which is downstream from *ERN1* (Kovács et al., 2022). It must be notated that there is another form of entry called crack entry, this is a method used by rhizobia for entry into *Parasponia andersonii* where the rhizobia enter through the literal cracks in the epidermis that formed through cell division in *P. andersonii* (Lancelle and Torey, 1984).

Following, although concomitant with all of these signalling interactions which are all located in the epidermis, there are a series of steps leading to nodule organogenesis which is essential to form the tissue that will the rhizobia. Epidermally-expressed *NIN* activates Cytokinin Response 1 (*CRE1*) expression, which is restricted to the cortex via a mobile signal that has suggested to be the plant hormone Cytokinin (Liu et al., 2019b). A positive feedback loop then occurs where *CRE1* triggers cytokinin signalling which then promotes further activation of *NIN* expression in the cortex (Vernié et al., 2015). Cortex-expressed *NSP2* is downstream of *CRE1* (Ariel et al., 2012) which then activates *NIN* expression in the pericycle (Liu et al., 2019b).

The pericycle-located *NIN* activates Nuclear Transcription Factor Y Subunit A-1 (*NF-YA1*) which is the one of the starting points for the signalling pathway towards cortical cell divisions and forming the nodule meristem. This is because *NF-YA1* directly controls Stylish (*STY*) transcription factors which in turn activate expression of YUCCA genes that are involved in auxin biosynthesis (Shrestha et al., 2021). Auxin biosynthesis is needed for the pericycle, endodermis and cortical cell divisions to start nodule organogenesis and to form the nodule primordium (Shrestha et al.,

2021). It has been shown that Auxin Response Factor 2 (*ARF2*) might act downstream of *NF-YA1*, but whether this is direct interaction or interaction through the YUCCA genes is currently unknown. *ARF2* is expressed in the endodermis and is also involved in triggering auxin biosynthesis, again being essential for those cortical, pericycle and endodermis cell divisions (Kirolinko et al., 2021, Cervantes-Pérez et al., 2022). *NIN* also activates Lob-Domain protein 16 (*LBD16*) expression, promoting the *STY* transcription factors (and therefore YUCCA genes) to trigger auxin biosynthesis again further (Schiessl et al., 2019).

*NIN* therefore has roles in three cell types: initial signalling in response to rhizobia within the epidermis, and initiation of nodule organogenesis in (i) the cortex and (ii) pericycle. Whilst *NIN* is found in all three of these tissue cell types, there is an order in which expression occurs: *NIN* cannot be expressed in the pericycle if *NIN* in the epidermis has not been expressed (Liu et al., 2019b). Of the different cell types that become mitotically active during nodule organogenesis, the pericycle cells are the first to divide, followed by the inner cortex (Timmers et al., 1999). This leads to cell division that is initiated at the pericycle, includes the endodermis and cortical layers, and ultimately leads to formation of a nodule primordium (Xiao et al., 2014).

Whilst legumes nodule formation is a benefit, there are also mechanisms to control how many nodules are being made, as part of a resource balancing mechanism. This is termed autoregulation of nodulation (AON) involving *NIN* activating CLAVATA3-like (CLE) gene expression (Laffont et al., 2020) which involves signalling between the root to shoot and shoot to root to regulate the number of nodules that are formed, as reviewed in (Li et al., 2022).

At the same time as the plant cells are dividing to form a nodule primordium, the infection threads form, enabling entrapped rhizobia via root hair curling to move towards the nodule (Figure 5.2). In *P. andersonii*, infection threads are only formed once the nodule primordium is forming to guide the rhizobia towards the nodule primordium cells which is controlled by *PanNIN* and *PanNF-YA1* (Bu et al., 2020). The rhizobia are then released into the nodule primordium cells, which is made up of the cortex cells, with the endodermis and pericycle cells remaining uninfected (Xiao et al., 2014). In *M. truncatula*, this rhizobial release is controlled by the Soluble N-Ethylmaleimide Sensitive Factor Attachment Protein Receptor (*SNARE*) Vesicle-

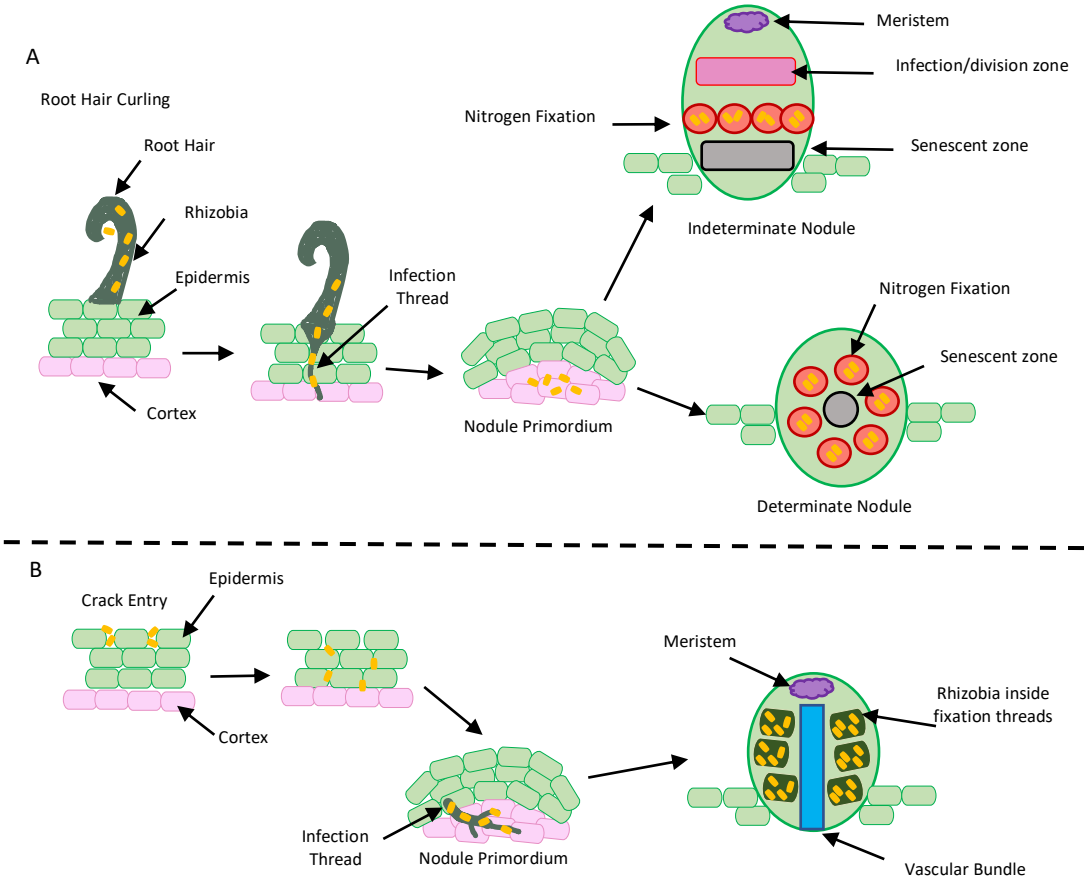


**Figure 5.2 Overview of rhizobia colonisation via root hair curling or crack entry to form nodules**
(A) Root hair curling entry that is found in both indeterminate (*Medicago truncatula*) and determinate (*Lotus japonicus*) nodulation. The infection thread guides the rhizobia towards the forming nodule primordium and the rhizobia are then released into the nodule primordium. The rhizobia then differentiate and are hosted within symbiosomes. (B) Crack entry of rhizobia as seen in *Parasponia andersonii*, cortical and epidermal cell division creates the gaps in the epidermis to allow colonisation by rhizobia. The rhizobia make their way towards the cortex, but infection threads need to form in order for the rhizobia to gain entry to the nodule primordium. The nodule matures and the rhizobia are housed in fixation threads on either side of the vascular bundle. Figure adapted from (Mendoza-Suárez et al., 2021).

Associate Membrane Protein (*VAMP72*) (Ivanov et al., 2012) and *NF-YA1* (Laporte et al., 2014). The rhizobia are hosted inside organelle-like structures called symbiosomes in legumes, in *P. andersonii* on the other hand, rhizobia are hosted within fixation threads (Op den Camp et al., 2011). It has been suggested that *NIN* is involved in the development of these symbiosomes in some way. Weak alleles of *NIN* were mutated (this allows for nodulation formation, but the nodules do not fix nitrogen), and it was found that symbiosome development was halted and early

senescence occurred (Liu et al., 2021). This highlights another potential role for *NIN* even after nodule organogenesis.

Inside the symbiosome, the rhizobia differentiate to be able to fix nitrogen; this differentiation is terminal in indeterminate nodules such as *M. truncatula*. Bacterial differentiation is controlled by defensin-like peptides that have antimicrobial properties termed nodule specific cysteine-rich (NCR) peptides (Van de Velde et al., 2010). *DNF1* is required in order for the NCRs to gain entry into the symbiosome (Wang et al., 2010). The symbiosome hosts a number of transporters to not only transport out the nitrogen produced by the rhizobial nitrogenase but also to transport the required nutrients to the symbiosome. For instance, Ferroporti2 (*FPN2*) is required to transport iron into the symbiosome and when the function of *FPN2* is lost, nitrogenase activity reduced (Escudero et al., 2020).

Overall, regulation of nodule formation involves a complex signalling pathway that is tissue specific, involves hormones, and in which all interactions are not yet elucidated (Figure 5.1).

### 5.1.2 Fluorescence-activated cell sorting can be used to isolate different cell types

As bacterial infection and nodule organogenesis involves distinct sets of interactions that are co-ordinated across the different root cell types, being able to separate the different root layers would allow a more in-depth view of the molecular mechanism occurring at each stage of nodulation, without the confabulating contents of many cell types. As previously introduced (see Section 1.12) This can be carried out by generating plant lines that express fluorescent markers in specific tissue types, and then using Fluorescence-Activated Cell Sorting (FACS) to separate the fluorescent cells and thus individual tissue type before sending for bulk RNA-seq. Whilst single cell RNA-seq (scRNA-seq) is a recently developed, powerful tool that can also show the transcriptome response happening within different tissue types without fluorescently labelled lines needing FACS, it is still much more expensive compared to bulk RNA-seq as reviewed in (Cole et al., 2021). In the context of this work, separating cell/tissue types during different stages of nodulation in *M. truncatula* and *P. andersonii* will allow an informative comparison to be made about the regulation of nodulation.

### 5.1.3 Aims and objectives

As mentioned previously (see Chapter 1), orthologs of key nodulation regulatory *M. truncatula* genes have been identified in *P. andersonii* and their role seems to be conserved. For instance, orthologs of *NIN* and *NF-YA1* have been found that are involved in nodule organogenesis and early symbiotic expression in both species (Bu et al., 2020). *P. andersonii* also has a *LYK3 M. truncatula* ortholog that recognises rhizobia NFs (Rutten, 2020). As previously found (see Chapter 3) *P. andersonii* is not necessarily as promiscuous as previously thought (Op den Camp et al., 2012) but not all rhizobial outcomes are the same as shown by the phenotypes presented by *Bradyrhizobium elkanii* (WUR3) and *Mesorhizobium plurifarium* (BOR2). Being able to compare and contrast the nodulation regulatory machinery of *P. andersonii* and *M. truncatula* at the cell type level could help to better elucidate how nodulation might be conserved. The aims of the work in this chapter were to generate stable cell type fluorescent lines of *M. truncatula* and *P. andersonii* to allow for further research into nodulation pathway signalling in the different root tissue types. This required plant transformation to insert a tissue-specifically-expressed fluorescent reporter into *M. truncatula* and *P. andersonii* and confirming the inserted sequence is present. It also involved adapting a protocol for protoplast generation for FACS from *Arabidopsis thaliana* (Birnbaum et al., 2005, Gifford et al, 2008) for use in *M. truncatula* and *P. andersonii*.

## 5.2 Results

### 5.2.1 Generating *Medicago truncatula* transiently expressing marker lines

Three-day old *M. truncatula* was transiently transformed with *Agrobacterium rhizogenes* containing a mCherry-Endoplasmic Reticulum (ER)-localised fluorescent protein under the control of the Expansin (EXPA) epidermal promoter, pEXPA (Figure 5.3). These transformed plants were then left for two weeks before the roots were cross-sectioned and analysed for mCherry fluorescence intensity and location using confocal microscopy. The pEXPA:mCherry-ER vector has already been shown to function in *M. truncatula* after transient transformation (Gaudioso-Pedraza et al., 2018) however, it was important to check the transient transformation within a different lab environment before moving onto a length stable transformation.

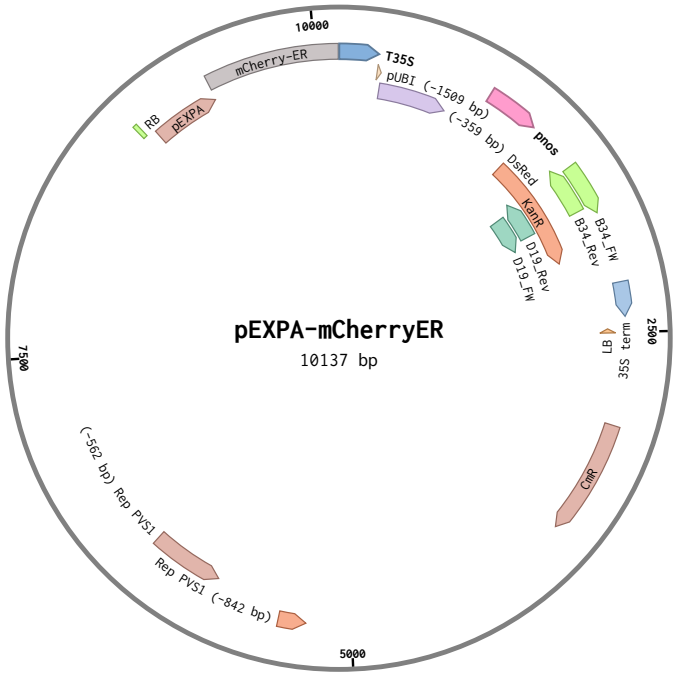


**Figure 5.3 Vector map of pEXPA:mCherry-ER used for plant transformation**
A pEXPA:mCherry-Endoplasmic Reticulum (ER)-localised fluorescent protein under the control of the Expansin (EXPA) epidermal promoter. Primers for the kanamycin gene for genotyping B34 (lime green) and D19 (teal) lines.

The epidermal vector was found to be successfully transformed into *M. truncatula* based on mCherry signal being detected with confocal microscopy (Figure 5.4). The signal was not particularly strong, but it did show that the signal was specific to the epidermis. This demonstrated that a generating a stable transformation line using this vector would be worthwhile; the ER tag aids in the cell type specificity (Lagunas et al., 2018).

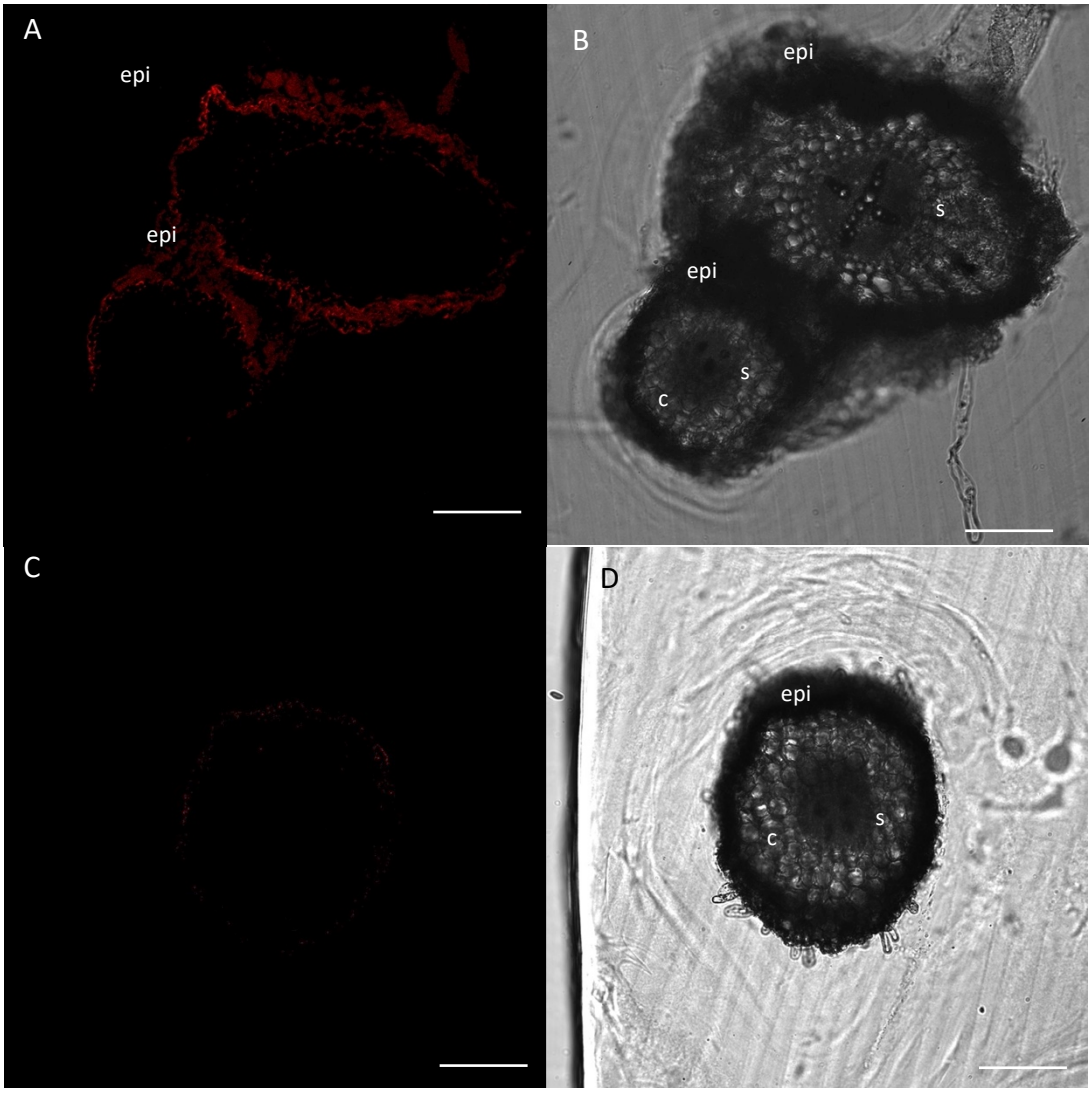


**Figure 5.4 *Medicago truncatula* transiently transformed with a pEXPA:mCherry-ER vector vs wild-type**
*Medicago truncatula* was transiently transformed with a pEXPA:mCherry-ER vector and imaged two weeks after transformation. (A) Two root sections showing a weak mCherry fluorescent signal was found in only the epidermis. (B) Brightfield image of the section of tissue in A. (C) Wild-type *M. truncatula* had no fluorescent signal when imaged in with the 561 nm laser and 578 – 696 wavelengths (D) wild-type section under brightfield. Scale bar = 100 µm. epi = epidermis, c = cortex and s = stele

### 5.2.2 Generating *Medicago truncatula* stable lines expressing a marker

The process of generating a stable *M. truncatula* line carrying an epidermal fluorescent vector is a lengthy process (almost two years from transformation to imaging) due to the tissue culture stages required, and a protocol for stable transformation here was adapted from (Zhou et al., 2004). The process began with transforming *Agrobacterium tumefaciens* with the pEXPA:mCherry-Endoplasmic Reticulum (ER) vector; this was determined to be successful by using specific primers to detect the mCherry fluorescent reporter sequence (Figure 5.5).

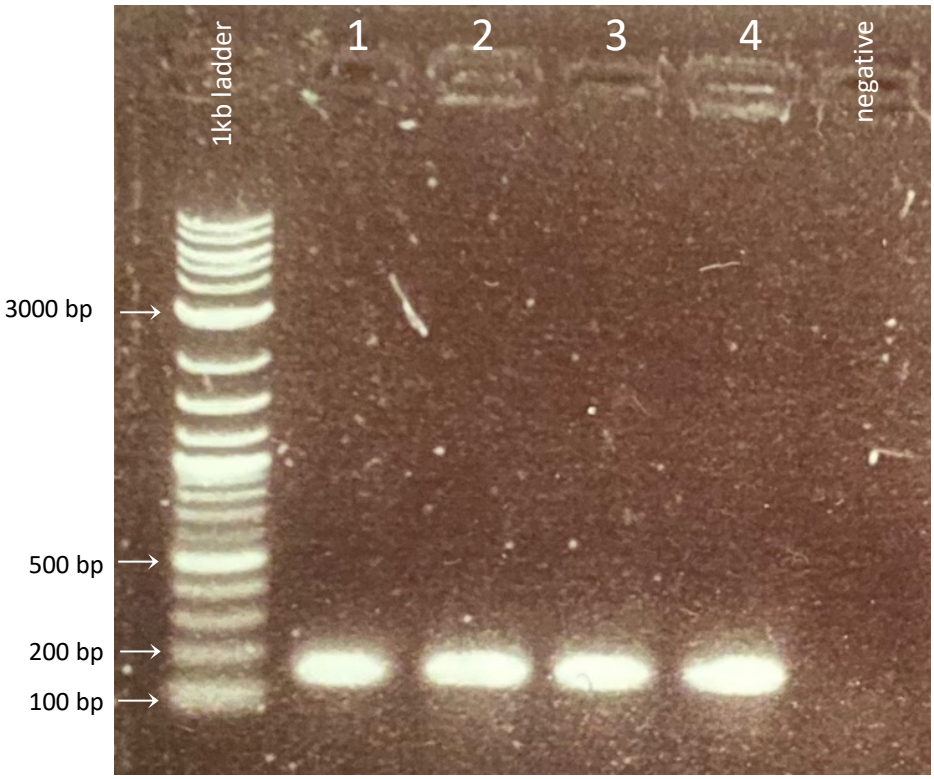


**Figure 5.5 pEXPA:mCherry-ER successfully transformed into *Agrobacterium tumefaciens.***
A gel showing an mCherry 155 bp PCR product from DNA extracted from four independent *Agrobacterium tumefaciens* colonies transformed with the pEXPA:mCherry-ER vector inserted (labelled 1 – 4) and a water negative control. Primers for the mCherry were used to locate the vector. A 1000 bp ladder was used.

The *A. tumefaciens* hosting the pEXPA:mCherry-ER vector was used to transform four-day old *M. truncatula* A17. *M. truncatula* was split 1 – 2 mm below the cotyledons and immersed in an *A. tumefaciens* solution ($OD_{600}$ = 0.8) and gently shaken for 30 minutes. There were dried on sterile filter paper and then left to grow on inoculation media for five days. The putatively transformed plants were then left

to shoot and *A. tumefaciens* growth was selected against using the addition of Timentin™ to media for 15 days. Putative transformants plants were selected via kanamycin antibiotic selection and then rooted; these were denoted as T0 plants, and they were left to grow and yield seed.

The seeds of T0 transformants (T1 generation) were then germinated and DNA from the T1 plant leaves was extracted and tested for presence of the vector. The original mCherry primers used to test for insertion in *A. tumefaciens* were not used as there was non-specific binding in *M. truncatula* which resulted in products for the wild type negative control and all the stable transformants, making it difficult to decide which transformants to send for sequencing. This led to the decision to use primers specific for the kanamycin resistance gene (355 bp product) (Figure 5.3). Plants A15, B34, B61, D19 were found to potentially be positive transformants (Figure 5.6) and so PCR products from these lines were sent for sequencing. In addition, there was a faint product in one of the wild type controls, so this was also sent for sequencing. B34 and D19 were subsequently confirmed to contain the kanamycin gene and thus were positive transformants, whereas the wild type 'product' was a non-kanamycin unrelated product (Figure 5.3).

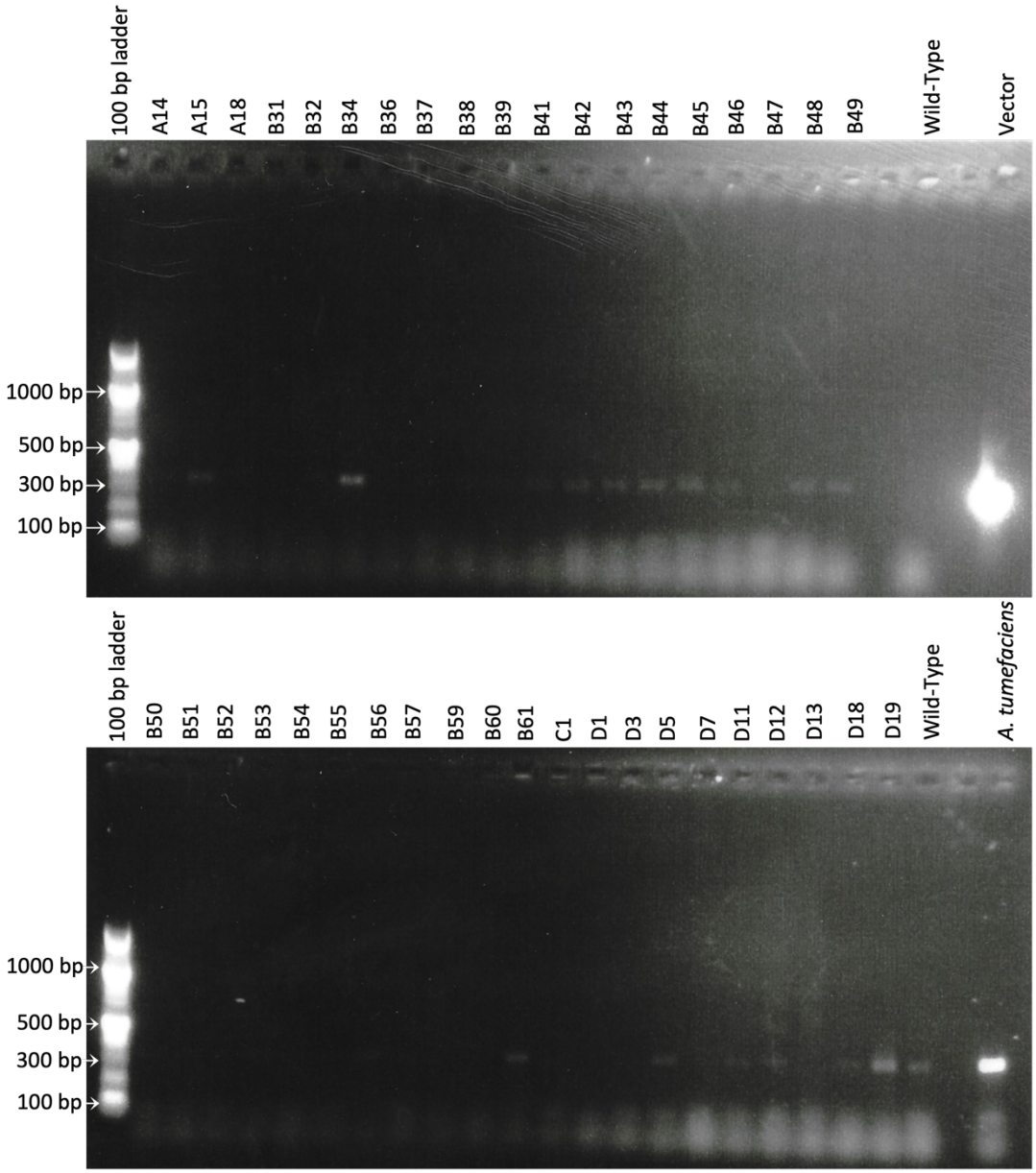


**Figure 5.6 PCR genotyping of pEXPA:mCherry-ER putative stable *Medicago truncatula* transformants**

DNA from 40 different stable transformant lines were tested with kanamycin resistance gene primers (355 bp fragment). The pEXPA:mCherry-ER vector and *Agrobacterium tumefaciens* containing pEXPA:mCherry-ER vector were used as positive controls. A15, B34, B42, B43, B44, B45, B46, B48, B49, B61, D5, D11, D12, D18 and D19 were potentially successful transformations as they were positive for this PCR product. A faint product was found in one of the wild type PCR reactions (lower gel) despite being a negative control, however, after sequencing it was determined that both of these wild types were in fact negative. A 100 bp ladder was used.

As plant B34 was one of transformant lines that was shown to have the insertion present, the seeds from this line (T2 generation) were germinated and seedlings screened after two weeks of growth using fluorescence then confocal

microscopy to ask if the fluorescence was (i) present and (ii) specific to the epidermis. Unfortunately, the signal was found to be throughout the different root tissue types (Figure 5.7). This was unexpected since these transformed plants carried the ER-tagged mCherry and samples were taken at a similar age to the transiently transformed plants (Figure 5.4). Despite this one line not being found to be epidermal-specific, there are other lines that can be tested in the future that express mCherry in an epidermal-specific manner, e.g. B61 (Figure 5.6).

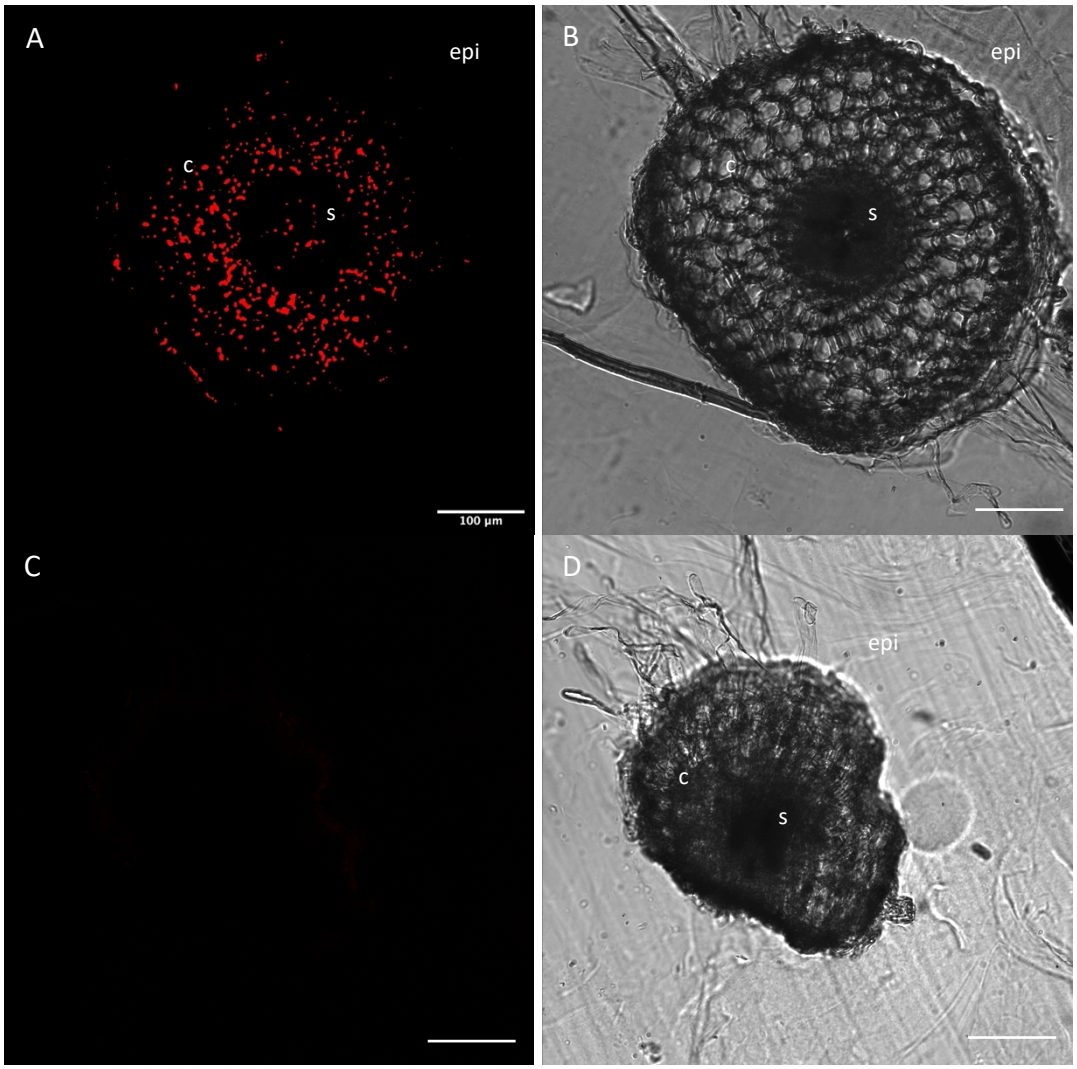


**Figure 5.7 Characterisation of fluorescence in *Medicago truncatula* stably transformed with a pEXPA:mCherry-ER vector**

(A) *Medicago truncatula* was stably transformed with a pEXPA:mCherry-ER vector was found to have strong fluorescent signal throughout the different root tissue types. (B) Brightfield image of the section in (A). (C) Wild-type *M. truncatula* showed no fluorescent signal and (D) wild type section under brightfield. Scale bar = 100 µm

epi = epidermis, c = cortex, s = stele

### 5.2.3 *Parasponia andersonii* leaves require different conditions compared to *Parasponia andersonii* stems for efficient transformation

In order to generate transgenic *P. andersonii* plants expressing tissue-specific fluorescence a variety of protocols were tested. There were two different protocols available to generate shoots from different *P. andersonii* tissues; from stems (Wardhani et al., 2019) and from leaves (Knyazev et al., 2018). There is also one published protocol for transforming *P. andersonii* shoots from stems (Wardhani et al., 2019) but no protocols available for the generation of transformed tissue from leaves.

Initially the (Wardhani et al., 2019) stem protocol was used due to the more detailed information available for the stem transformation protocol, but adult *P. andersonii* trees produce a limited number of young and green branches that can be used for propagation and any future transformation attempts. They do, however, produce a vast number of leaves, therefore the (Knyazev et al., 2018) protocol was attractive as it required fewer trees, and thus smaller growth space, yet should enable an abundance of material to be used to carry out transformation. This meant the shoots-from-leaves protocol also needed to be tested to establish its suitability for *P. andersonii* transformation within the lab, and details not available confirmed.

First, the protocols were tested for their ability to generate healthy wild-type *P. andersonii* shoots from leaves to ensure a successful starting point before starting transformations. Schenk-Hildebrandt (SH) media was chosen for establishing shoots from leaves as well as stems following (Wardhani et al., 2019) instead of the Gamborg's B5 and Woody Plant Medium (WPM) used in (Knyazev et al., 2018) to simplify methods for using both stems and leaves for tissue culture. The only differences in the types of media to establish new shoots in tissue culture that were required between leaves and stems were in the type and amount of hormone used. First, it was found that leaves cannot be placed straight onto 'propagation' media (1 mg/l Benzylaminopurine (BAP) and 0.1 mg/l Indole-3-Butyric Acid (IBA)) as shoots were not formed (Figure 5.8 A). However, it was confirmed that shoots did form when using stems as the starting material and placing stems straight onto 'propagation' media following the (Wardhani et al., 2019) protocol (Figure 5.8 B). Secondly, it was found that the leaves needed to be placed onto 'calli-induction'

media (0.05 mg/l 1-Naphthaleneacetic Acid (NAA) and 0.1 mg/l Thidiazuron (TDZ)) with the abaxial side touching the agar for four to six weeks for calli to establish first in continuous darkness at 28 °C. The established calli were then moved into the 16-hour light/8-hour dark 28 °C conditions onto 'TDZ propagation' media (0.2 mg/l TDZ and 0.05 mg/l IBA) with the adaxial side touching the agar (following the (Knyazev et al., 2018) protocol) (Figure 5.8 C - E).

Once the calli turned green the *P. andersonii* tissue could be moved onto 'propagation media' and shoots would eventually form (Figure 5.8 F). Once the starting leaf tissue is on 'propagation' media, the 'propagation' media can be refreshed monthly for long term tissue culture. This means that when using leaves or stems as starting material, they both eventually end up on propagation media during long term tissue culture maintenance making it simpler to maintain the tissue culture long term.

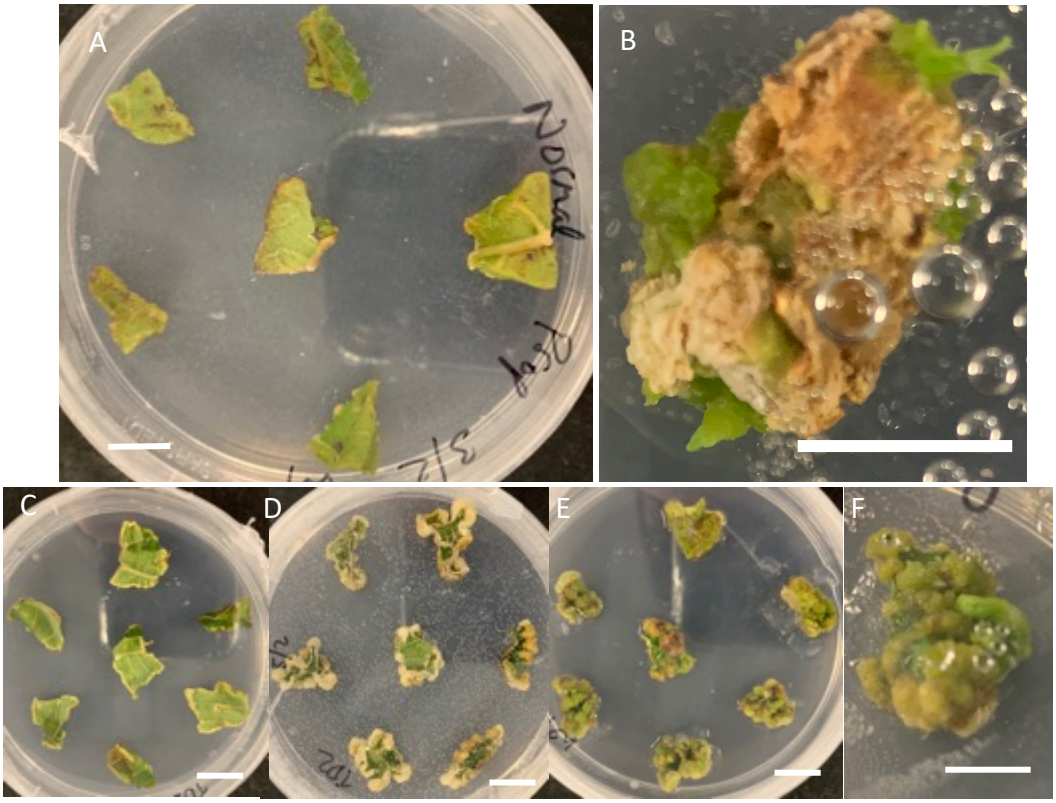


**Figure 5.8 Assessment of media requirements for induction of callus growth on *Parasponia andersonii* shoots on leaves.**

*Parasponia andersonii* leaves only produced callus and then shoots when media containing TDZ was used at the for establishing a new tissue culture (Knyazev et al., 2018). No callus or shoots were formed when using the (Wardhani et al., 2019) protocol for leaves which involves using 'propagation' media (1 mg/l BAP and 0.1 mg/l IBA), however shoots would form when using stems as a starting material. Shoots would only emerge on 'propagation' after green calli was established first when using leaves as a starting material.

(A) *P. andersonii* leaves on 'propagation' media after 34 days in continuous darkness at 28 °C where no calli or shoots developed.

(B) *P. andersonii* shoots form on stems on 'propagation' media at 28 °C under 16-hour light/8-hour dark conditions following the (Wardhani et al., 2019) protocol.

(C) 19-day old *P. andersonii* leaves on 'calli-induction' media (0.05 mg/l NAA and 0.1 mg/l TDZ) kept in continuous dark at 28 °C; small white calli began to form.

(D) 29-day old *P. andersonii* leaves on 'calli-induction' media kept in continuous dark at 28 °C. Large white calli formed and could be moved into 16-hour light/8-hour dark on 'TDZ propagation' media (0.05 mg/l IBA and 0.2 mg/l TDZ).

(E) 49-day old *P. andersonii* leaves on 'TDZ propagation' media at 28 °C under 16-hour light/8-hour dark conditions. The white calli turned green and shoots would eventually start forming.

(F) 60-day old *P. andersonii* leaves on 'propagation; media containing at 28 °C under 16-hour light/8-hour dark conditions.

Scale bars = 1 cm.

Whilst according the (Wardhani et al., 2019) protocol, stems for new tissue culture are stored in the light from the start, (Knyazev et al., 2018) had a four-to-six-week dark period whilst the leaves were on 'calli induction' media. To assess if the dark period was crucial for leaf formation (which is not the case for stems) two light conditions were trialled: keeping the leaves in the same condition in a 16-hour light/8-hour dark light cycle (as for stems) or in continuous darkness.

It was found that whilst wild type stems from an adult tree can be induced to form new shoots without a period in the dark (Wardhani et al., 2019), leaves need to be in the dark for four to six weeks whilst on 'calli-induction' media to generate calli before being moved into the light on 'TDZ propagation' media to allow for new shoots to form. If they are not kept in the dark for four to six weeks, they suffer from light damage and die (Figure 5.9).

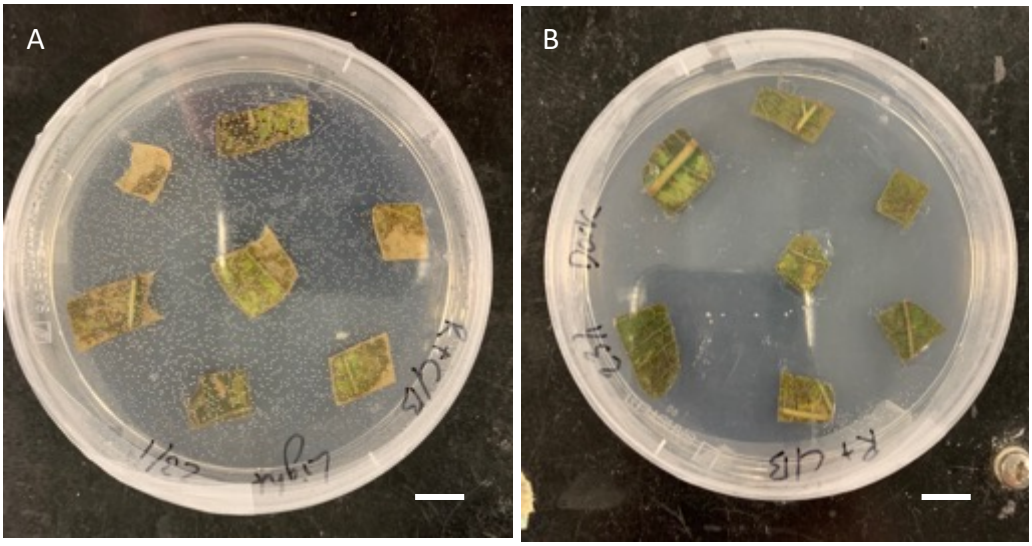


**Figure 5.9 *Parasponia andersonii* leaves must be kept in the dark until a callus has been formed.**
*Parasponia andersonii* leaf sections on 'calli-induction' media (0.05 mg/l NAA and 0.1 mg/l TDZ) will show bleaching and eventually die when kept in 16-hour light/8-hour dark light cycles (A) but continuously in the dark they do not suffer damage and will eventually form calli (B). Assessment of the images suggest that a light/dark cycle leads to damage to the leaf sections or tissue degradation (A) and so leaves must be kept in the dark until callus has been formed. Scale bars = 1 cm.

These experiments demonstrate the importance of TDZ and including a dark stage during the formation of calli from leaves in order to be used for new tissue culture or any future transformation attempts.

### 5.2.4 *Parasponia andersonii* may be resistant to glufosinate

Any natural antibiotic resistance that *P. andersonii* possesses needed to be determined before use of antibiotics for transformation selection. The vector chosen for transformation carried a GFP gene that would be expressed specifically in the cortex via the Endopeptidase (PEP) promotor, enabling future research in tissue specific gene expression in *P. andersonii* during nodulation (Figure 5.10). This vector included a glufosinate resistance gene to enable selection of newly transformed shoots.

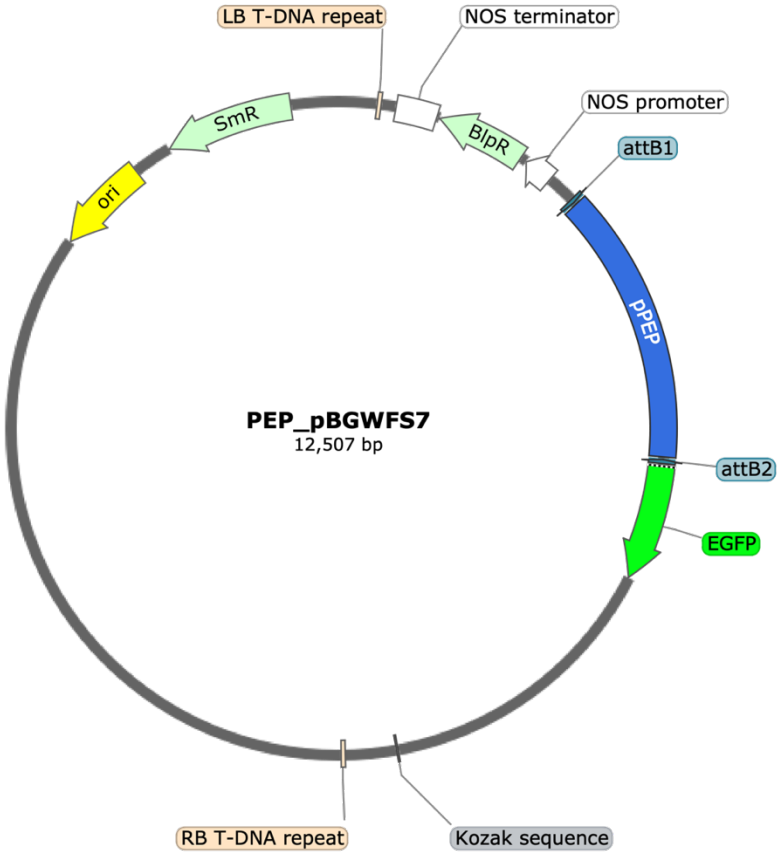


**Figure 5.10 Vector map of PEP_pBFWFS7 used for plant transformation**
A pBFWFS7 vector with a GFP gene that would be expressed specifically in the cortex via the PEP promotor. This particular vector has a glufosinate resistance gene (BlpR) that would be needed for selected successful *Parasponia andersonii* transformants.

As there was no information available on whether *P. andersonii* had any natural resistance to glufosinate, it was not clear if this vector would be suitable for plant transformation, and therefore tests were carried out. By growing *P. andersonii* on a range of different glufosinate concentrations (from 0 µg/ml to 50 µg/ml) and in the

same conditions for transformation (light levels and nutrient/hormone levels), the threshold concentration of glufosinate to select transformed *P. andersonii* was tested for. As transformation of *P. andersonii* was to include using stems and leaf tissue, both stems and leaves were tested for natural glufosinate tolerance.

Tests for wild-type *P. andersonii* stem tissue involved placing wild-type *P. andersonii* stems onto 'propagation media' (1 mg/l BAP and 0.1 mg/l IBA) for 14 days at a 16-hour light/8-hour dark cycle at 28 °C with the different concentrations of glufosinate. The level of *P. andersonii* resistance to glufosinate was however not possible to determine for shoots as all stems turned brown (indicating cell and tissue death) and stem segments had stopped producing shoots after 14 days on all levels of glufosinate, including 0 µg/ml (Figure 5.11).

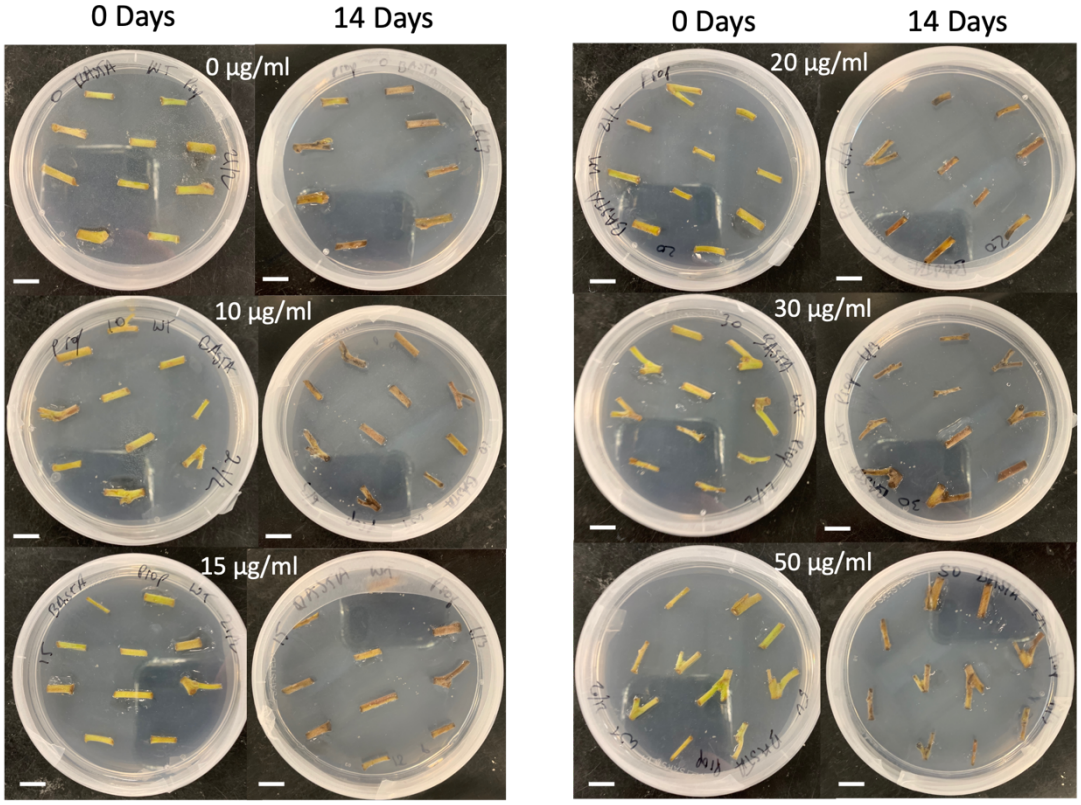


**Figure 5.11 Tests for natural resistance to glufosinate in *Parasponia andersonii* stems remain inconclusive.**
Sections of *Parasponia andersonii* stems on varying concentrations of glufosinate at 0 days and then the same stems at 14 days on 'propagation' media (1 mg/l BAP and 0.1 mg/l IBA) kept at 28 °C in a 16-hour light/8-hour dark cycle. All stems turned brown with not shoot formation after 14 days and thus the experiment was inconclusive.
Scale bar = 1 cm.

Tests for wild-type plant resistance to glufosinate in leaves were then carried out by placing leaves on 'calli induction' media (0.05 mg/l NAA and 0.1 mg/l TDZ) with four different concentrations of glufosinate (from 0 µg/ml to 50 µg/ml) and kept in continuous dark at 28 °C for 14 days. Leaves were either place abaxial side touching the agar or adaxial side touching the agar, as the *P. andersonii* leaves requires flipping the leaves over after calli have formed and the antibiotic selection will therefore need to be consistent on both sides. Results suggested sensitivity to glufosinate when the adaxial side of the leaf was touching the agar, and at glufosinate concentrations as low as 10 µg/ml (Figure 5.12). Leaves placed on the abaxial side turned brown in a similar way that stems the stems did (indicating tissue death), thus making it difficult to conclude if the plants were glufosinate resistant or not, and to what extent.

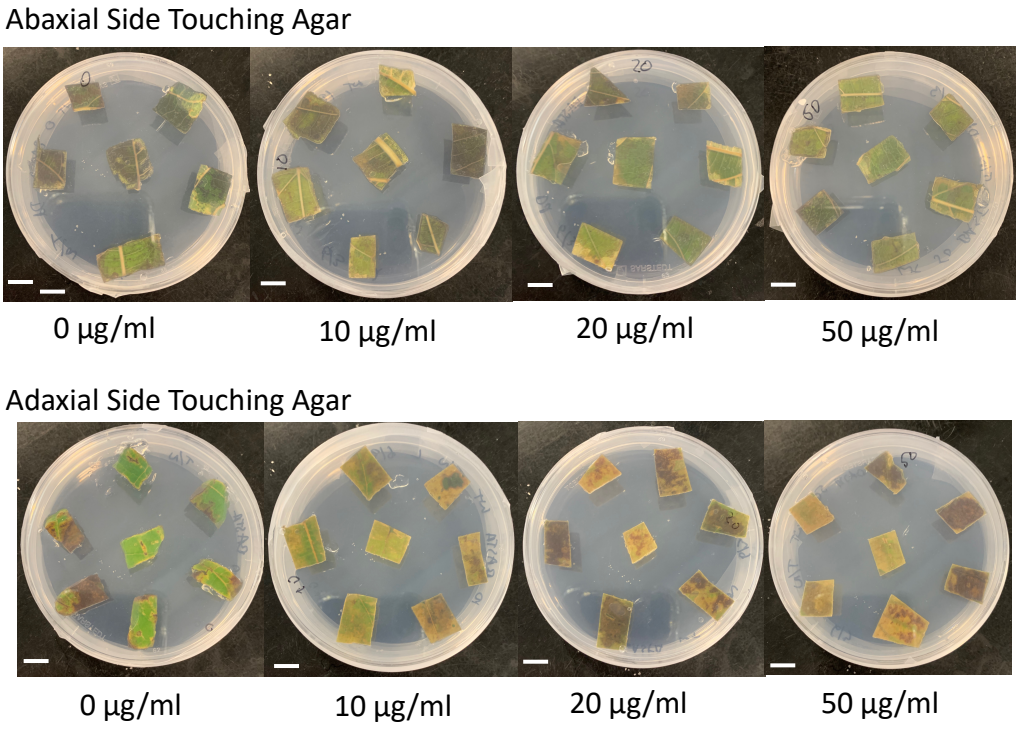


**Figure 5.12 *Parasponia andersonii* is more resistance to glufosinate on the abaxial side of the leaf, compared to when the leaves adaxial side.**
*Parasponia andersonii* leaf sections kept in continuous dark at 28 °C after 14 days on 'calli-induction' media (0.05 mg/l NAA and 0.1 mg/l TDZ) containing concentrations of glufosinate between (0 µg/ml and 50 µg/ml). The leaves were left either abaxial (A) or adaxial (B) side down on the agar. With the abaxial side down it is difficult to determine the tolerance level since all leaves on agar turned brown. With the adaxial side down the tolerance seems to be up to 10 µg/ml glufosinate. Scale bars = 1 cm.

These tests could be repeated to try to determine the sensitivity of growing plants to glufosinate resistance. For example, allowing more time calli to develop and then varying glufosinate concentration could provide a clearer of an indication of the level of natural resistance that *P. andersonii* has to glufosinate, and the potential to use this antibiotic in further research.

### 5.2.5 Transforming *Parasponia andersonii* with a kanamycin resistance-harbouring vector, following an existing protocol

(Wardhani et al., 2019) generated a protocol for transforming stable lines that had a variety of nodulation genes knocked out using CRISPR/Cas-9-mediated mutagenesis using vectors conveying kanamycin resistance. As the glufosinate tests were not conclusive and (Wardhani et al., 2019) had already shown kanamycin can be used for selection of transformed *P. andersonii* tissue, this suggested that transforming plants with the pEXPA:mCherry-ER vector (provided by (Gaudioso-Pedraza et al., 2018) previously used for *M. truncatula* conferring kanamycin resistance in plants would be an effective approach (see Section 5.2.2).

Stems and leaves from mature *P. andersonii* trees were surface sterilised and transformation attempted involved following the (Wardhani et al., 2019) protocol exactly for stems. There were slight adjustments for leaves due to the earlier findings that leaves need an adjusted protocol to be used in tissue culture (see Section 5.2.3). The surface sterilised leaf and stem tissue were infiltrated with *A. tumefaciens* containing the pEXPA:mCherry-ER vector before stems were placed on 'rooting' media (IBA 1 mg/ml and NAA 0.1 mg/ml) and leaves were placed on 'calli-induction' (0.05 mg/l NAA and 0.1 mg/l TDZ) media both with 20 mg/l acetosyringone and kept in the dark at 21 °C for two days. The leaf and stem tissue were cleaned via a washing stage and placed on either 'propagation' (1 mg/l BAP and 0.1 mg/l IBA) media (stems) back onto calli-induction media (leaves) with kanamycin selection for positive transformants and cefotaxime to prevent *A. tumefaciens* growth.

However, fungal contamination and *A. tumefaciens* overgrowth issues occurred which led to the first attempted transformation material not surviving. These issues of contamination and overgrowth were solved by replacing cefotaxime from the (Wardhani et al., 2019) protocol with 500 mg/ml Timentin™ as well as

changing the washing stage of removing the *A. tumefaciens* by increasing the three washes to one hour each with 500 mg/ml Timentin™ added to each wash. This allowed for further attempts of the transformation without the contamination setback. The leaves survived long enough to be moved onto 'TDZ-propagation' (0.2 mg/l TDZ and 0.05 mg/l IBA) media into a 16-hour light/8-hour dark cycle after four weeks and the stems were left on propagation media refreshed every two weeks. However, the stems and leaves and any shoots that emerged eventually turned brown and die once placed onto 'propagation' or 'TDZ-propagation' media in the kanamycin selection step using 50 µg/ml kanamycin (Figure 5.13). Any shoots that

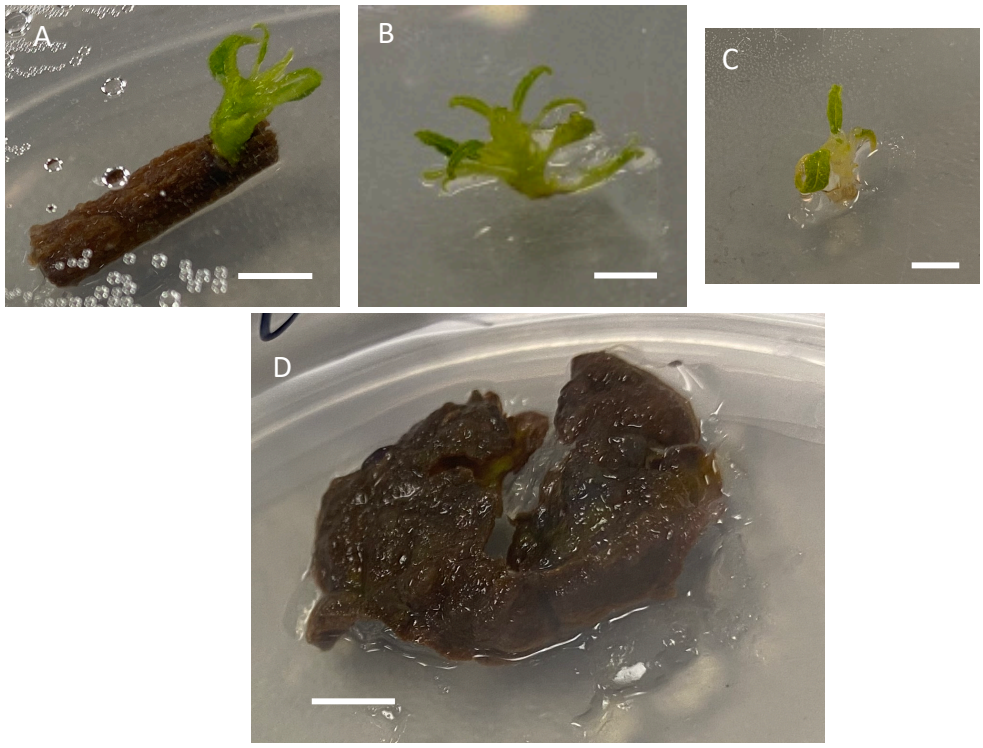


**Figure 5.13 *Parasponia andersonii* tissue did not survive the stable transformation selection process**
Whilst following the (Wardhani et al., 2019) protocol by infecting the tissue with *Agrobacterium tumefaciens* with a PEXPA:mCherry-ER vector did not produce successful transformants, despite putatively transformed tissue being produced.
(A) A shoot that has formed on a *Parasponia andersonii* stem after transformation with a pEXPA:mCherry-ER vector whilst on 50 µg/ml kanamycin 'propagation' (1 mg/l BAP and 0.1 mg/l IBA) plates. Tissue was kept at 28 °C in a 16-hour light/8-hour dark cycle.
(B) When taken off the stems, the shoots remained green whilst on 50 µg/ml kanamycin propagation plates, however these green shoots eventually turned yellow and died.
(C) The yellow tissue of (B) 40 days after being taken from the stem in (A).
(D) After transforming *P. andersonii* leaves and left in the dark on 'calli-induction' (0.05 mg/l NAA and 0.1 mg/l TDZ) media in continuous dark at 28 °C, the leaf would quickly turn brown indicating the tissue had not survived the 50 µg/ml kanamycin selection.
Scale bars = 5 mm.

did form (around 3 % of stems would produce shoots) would slowly yellow and die once placed directly onto the agar containing the 50 µg/ml kanamycin selection, which suggests these shoots were escaping the selection process as they were not kanamycin resistant. As this transformation protocol was not successful, a new method of transforming *P. andersonii* was attempted.

### 5.2.6 Progress towards a new protocol to transform *Parasponia andersonii* leaves and stems

Due to a lack of progress using the (Wardhani et al., 2019) protocol, a new method was developed to transform *P. andersonii* calli formed from leaves instead of transforming the tissue straight after cutting from the trees. Leaves were removed from wild-type trees and placed onto 'calli-induction' (0.05 mg/l NAA and 0.1 mg/l TDZ) media for four weeks in the dark at 28 °C following the (Knyazev et al., 2018) protocol. The calli produced on the leaves were then infiltrated with *A. tumefaciens* containing the pEXPA:mCherry-ER vector before being left on 'calli-induction' media for two days in the dark at 21 °C. The tissue was then washed and placed back onto 'calli-induction' with 500 mg/l Timentin™ and 50 µg/ml kanamycin selection and left in the dark at 28 °C for one week. Tissue was then moved onto 'TDZ propagation' (0.2 mg/l TDZ and 0.05 mg/l IBA) media with 500 mg/l Timentin™ with 50 µg/ml kanamycin with a 16-hour light/ 8-hour dark cycle at 28 °C and refreshed every two weeks.

Around 2 % of the leaves transformed had shoots form after 10 days (Figure 5.14). However, even though the shoots would remain green even after 30 days from inoculation with the 50 µg/ml kanamycin they again slowly turn brown and die within 58 days from inoculation.

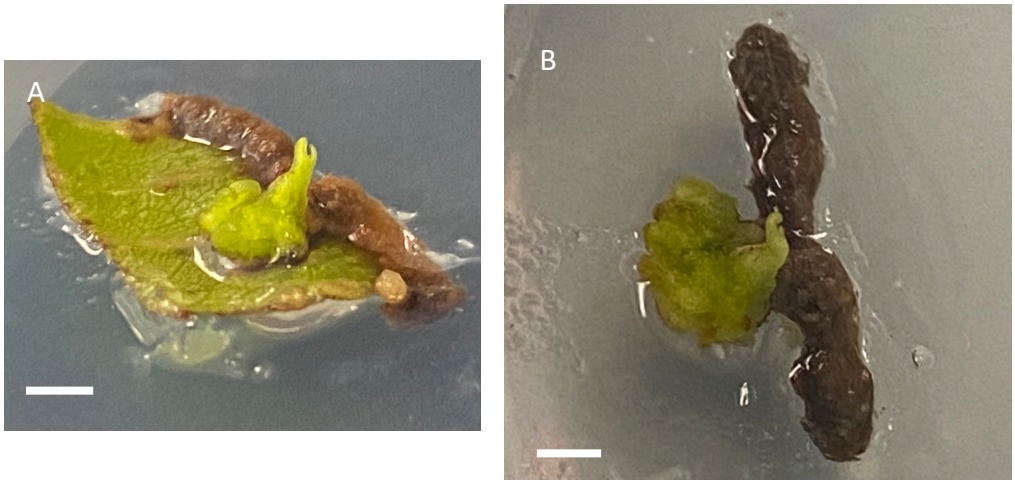


**Figure 5.14 Green *Parasponia andersonii* tissue on a kanamycin selection**
*Parasponia andersonii* leaves were left for four weeks on 'calli-induction' (0.05 mg/l NAA and 0.1 mg/l TDZ) media in continuous dark at 28 °C and then transformed with *Agrobacterium tumefaciens* containing a pEXPA:mCherry-ER vector. The tissue was then washed and placed back onto 'calli-induction' media with the 500 mg/l Timentin™ and 50 µg/ml kanamycin selection in continuous dark at 28 °C for one week. The tissue was then moved onto 'TDZ propagation' (0.2 mg/l TDZ and 0.05 mg/l IBA) media with 500 mg/l Timentin™ with 50 µg/ml kanamycin with a 16-hour light/ 8-hour dark cycle at 28 °C.
(A) A shoot formed on a *P. andersonii* leaf 10 days after being inoculated with *A. tumefaciens*.
(B) The shoot from (A) 30 days after inoculation with *A. tumefaciens* where dead leaf tissue surrounded the green calli and shoot had been taken off. Despite initial promising results, this shoot eventually turned brown and died. Scale bars = 2.5 mm.

Whilst a successful transformation may have not been completed in this research, this work has pushed forward a protocol for successful transformation of *P. andersonii* in the future. For instance, it was found that Timentin™ may be a better antibiotic to use against *A. tumefaciens* overgrowth compared to cefotaxime (see Section 5.3.6). As well as this, leaves could be potentially a better starting material for stable transformation for research groups who lack the space to maintain many trees, as one tree produces more usable leaf tissue for transformation compared to young green stems once a successful leaf transformation has taken place.

### 5.2.7 Protoplasts can be generated from *Parasponia andersonii* roots

Whilst a protocol has already been established for generation of protoplasts from *A. thaliana* (Birnbaum et al., 2005; Gifford et al., 2008), an efficient protocol for generating protoplasts had not yet been established for *P. andersonii*. Being able to

generate protoplasts is essential for FACS and other experiments such as single cell RNA-seq (scRNA-seq) to be conducted and so the possibility to characterise a protocol for protoplast generation of *P. andersonii* roots was tested. For the *P. andersonii* roots, the *A. thaliana* method was followed where the enzymes Macerozyme R10, Cellulase RS and Pectinase was used (see Section 2.4.5 for further details). The sample was viewed with microscopy to check for the presence of intact protoplasts, then the protoplast yield measured using a hemacytometer.

The method used was successful as protoplasts were generated (Figure 5.15), however the protocol needs further optimisation as there were only ~5000 protoplasts/ml which is a fraction of the number of cells needed for further experiments such as scRNA-seq or FACS assuming that only a few % will be cells of interest (if seeking to isolate just one cell type) and then take material forward for 'omics analysis. This does give a starting point for future optimisation to further improve the amount of cells/ml when generating *P. andersonii* protoplasts, such as modulating the concentration or type of enzymes. In addition, filtering to remove debris would be recommended.

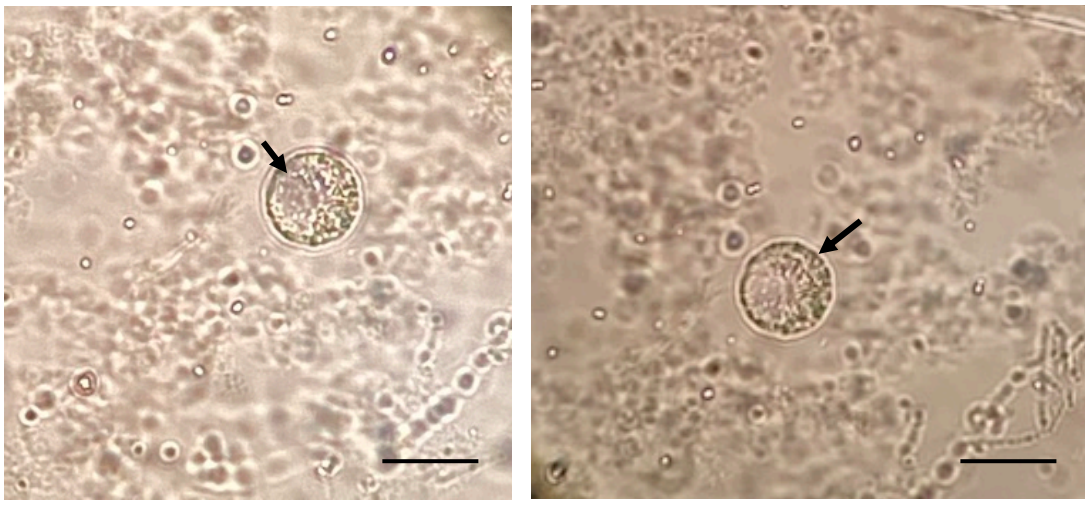

**Figure 5.15 *Parasponia andersonii* protoplasts generated from root material.**
After generating *Parasponia andersonii* root protoplasts, only ~5000 cells/ml of protoplasts was generated, and cell debris surrounded the protoplasts. Arrows indicate protoplasts found in a 0.1 ml of sample.
Scale bars = 5 µm.

## 5.3 Discussion

Substantial progress in understanding the genetic pathways underlying nodulation has been made in the last 20 years as reviewed in (Roy et al., 2020b), but there is still much to be discovered and understood. One of the ways to help add to our understanding is by investigating cell-type mechanism underpinning nodulation, and this can be done by carrying out FACS of tissue-specific fluorescent lines to separate cell types. Generating stable transformed lines in *M. truncatula* and *P. andersonii* is important as it would allow not only for the study of nodulation signalling within the different tissue types of each species, but also how this differs between species.

Firstly, this research has produced a working protocol by combining (Wardhani et al., 2019) and (Knyazev et al., 2018) that will make experimenting with *P. andersonii* more accessible to different research groups. This has been achieved by using leaves and stems as a starting material, which requires less trees to be kept. The same base media will also be used with both leaves and branches, with different hormone additions, which simplifies the process of *P. andersonii* tissue culture.

*P. andersonii* is one of five non-legumes that is able to form an interaction with rhizobia, and the presence of orthologous genes with *M. truncatula* that are known to control nodulation in legumes, such as *NIN* and *NF-YA1* (Bu et al., 2020), suggests that the regulatory machinery is conserved. This supports the view that nodulation was gained in a common ancestor and then lost in other species (van Velzen et al., 2018), and study of *P. andersonii* provides an exciting opportunity to determine how the genetic networks might have evolved or been conserved from a common ancestor (van Velzen et al., 2018). The work on *P. andersonii* has only just scratched the surface and determining whether the orthologous genes in *P. andersonii* are expressed in the same location or at the same time as *M. truncatula* is yet to be carried out. Once this can be carried out, it may also be possible to determine how responses to compatible rhizobia, incompatible rhizobia and pathogens are mediated between two distinct nodulators and pinpoint the location of these responses. This could be linked to how the symbiont or pathogen interacts

by using fluorescent bacterial lines at the same time as the plant fluorescent lines to analyse the plant-microbe interaction even further.

Not only will generation of fluorescent reporter lines help analyse the nodulation signalling pathway, but it could also help analyse how nodulation evolved. *Trema tomentosa* is a non-nodulating close relative of *P. andersonii* (van Velzen et al., 2018) and analysing how each tissue type reacts to the surrounding soil bacteria could possibly uncover which gene functions were lost from nodulator to non-nodulator over evolutionary time. Despite being a non-nodulator, *T. tomentosa* will still likely have some form of response to surrounding microbes in the environment. Therefore, questions can be posed such as, what are the difference between *T. tomentosa* and *P. andersonii* at the cell type level? For instance, *P. andersonii* haemoglobin needed to transport oxygen to the nitrogen-fixing rhizobia is 93 % identical in amino acids to the haemoglobin in *T. tomentosa*, and yet they function differently (Sturms et al., 2010); are there differences at the molecular level between these two species that can be uncovered using different fluorescent tissue reporter lines?

As introduced previously, single cell RNA-seq (scRNA-seq) is a powerful tool that can show the transcriptome response happening within different tissue types, it is still much more expensive compared to bulk RNA-seq as reviewed in (Cole et al., 2021). This means that the progress made to generate stable *M. truncatula* lines in this research will allow for tissue specific analysis by use of FACS whilst the costs for scRNA-seq currently remain high. Positive *M. truncatula* transformants were identified (including line B34), although the mCherry fluorescence was not specific to the epidermis. However, other lines can be screened that could have the epidermal fluorescence specificity required. In the short term, transient transformation could be used, but as this work shows, transiently transformed *M. truncatula* plants only had a weak mCherry signal.

In this work, significant progress has been made with the stable transformation of both *M. truncatula* and *P. andersonii* with the pEXPA:mCherry-ER vector used in this study. This has been a long process as the only protocol for *P. andersonii* transformation available from (Wardhani et al., 2019) required major changes to move closer to generating a stably transformed line. This has involved

devising a new protocol using more readily available *P. andersonii* leaves, and pinpointing conditions (using Timentin™) to repress *A. tumefaciens* overgrowth. Whilst a successfully transformed line has not yet been generated in *P. andersonii*, the progress shown here will allow this. The work presented also shows that protoplast generation from *P. andersonii* is possible, enabling subsequent FACS and thus cell type work to be carried out. The generation of protoplasts is also important for technology such as scRNA-seq as reviewed in (Denyer et al., 2022), which will allow *P. andersonii* to be ready for this type of analysis once the costs become more accessible.

## 5.4 Conclusion

Overall, this work has provided a strong foundation to be moved forward in the future towards generating stably transformed *M. truncatula* and *P. andersonii* lines. This provides an exciting future to compare nodulation between the model legume and the new model non-legume nodulator.

# Chapter 6: Discussion

## 6.1 Importance of research on scope of legume-rhizobia interactions

As introduced in Chapter 1, the population is expanding and is predicted to reach 9.7 billion people by 2050 as predicted in the latest United Nations report (United Nations, 2022). Nitrogen fertilisers that have been used to increase crop yield to feed this expanding population are huge contributors to $CO_2$ emissions (Menegat et al., 2022). Investigating ways to increase yields to feed the population whilst minimising the environmental damage caused by intensifying agriculture is essential. One of these ways is by investigating nitrogen fixing in nodulating legumes and the non-legume *Parasponia andersonii*. Analysing these relationships through phenotyping on a whole plant level in combination with determining the molecular changes occurring during nodulation helps add to the knowledge of nitrogen-fixing interactions. With *P. andersonii* being a non-legume capable of nitrogen-fixing with rhizobia, it helps examine the evolutionary timeline of how nodulation developed and could help researchers translate nodulation to important non-legume crops.

## 6.2 *Sinorhizobium medicae* WSM419 is an efficient symbiotic partner for *Medicago truncatula*

One of the aims of Chapter 3 was to explore the nodulation phenotypes of *Medicago truncatula* with *Sinorhizobium meliloti* (WSM1022), *Sinorhizobium medicae* (WSM419), *Mesorhizobium plurifarium* (BOR2) and *Bradyrhizobium elkanii* (WUR3) in order to ask how broad the symbiotic partner range is. Asking this question can help establish whether a host plant has more of a chance to establish symbiotic relationships in new habitats due to a higher chance of compatibility. However, it needs to be balanced by being selective of only highly efficient nodulators to avoid a high carbon input with low nitrogen reward for the plant. This is a question (Zarrabian et al., 2022) had in mind when investigating *Lotus japonicus* and *Lotus burttii* and found that *L. burttii* was far more promiscuous than *L. japonicus*.

In this research it was discovered that *M. truncatula* did not form nodules when inoculated with BOR2 or WUR3, which are two strains that are known

symbionts of *P. andersonii* (van Velzen et al., 2018, Op Den Camp et al., 2012). When *M. truncatula* was inoculated with known *M. truncatula* symbionts WSM419 or WSM1022 (Terpolilli et al., 2008), nodules were formed, suggesting there is quite a narrow rhizobial range for *M. truncatula* nodulation. Inoculation of *M. truncatula* with WSM419 or WSM1022 resulted in a significantly higher fresh shoot weight compared to the control, showing the impact of nodulation on the plant.

Determining nodulation efficiency has previously been shown by measuring the amount of nitrogen fixed per unit of plant mass (Irisarri et al., 2019) and through measuring nodule number, nodule mass and leaf nitrogen content (Athul et al., 2022). The research conducted here took a simple approach by noting that when *M. truncatula* was inoculated with WSM419, fewer nodules were formed and yet and had the same significantly higher shoot biomass compared to the control as WSM1022. However, this work still demonstrates the importance of phenotyping the root and shoot systems to fully understand the efficiency of the nodulation relationship. Even if a more simplistic approach is used to determine nodule efficiency, determining what the phenotypic consequences are from a symbiotic relationship provides context for investigating nodulation at a molecular level.

## 6.3 The promiscuity of *Parasponia andersonii* is not coupled with nodule efficiency

Chapter 3 not only analysed the phenotypes of different rhizobia with *M. truncatula*, but another aim of Chapter 3 was to explore the phenotypes of *P. andersonii* with WSM1022, WSM419, BOR2 and WUR3. Despite nodules being initiated with all four strains, *P. andersonii* did not produce a significant number of nodules when inoculated with WSM419 or WSM1022 compared to the control, which demonstrates the limitations of the promiscuity of *P. andersonii* as not every symbiont is compatible for successful nodulation. To demonstrate promiscuity in *P. andersonii,* (Op den Camp et al., 2012) showed that *P. andersonii* can host rhizobia that have low nitrogen fixation levels such as *Rhizobium tropici* WUR1 had 1/10 of the nitrogen fixation activity (acetylene reduction assay = 0.29 ± 0.17 µmol $C_2H_4$/h/g fresh weight) compared to WUR3 (acetylene reduction assay = 2.88 ± 1.39 µmol

$C_2H_4$/h/g fresh weight). However, these tests were only done on nodules that were four weeks old and so whether these nodules would eventually be sanctioned and degraded as was seen with BOR2 (see Section 4.2.1) is unknown.

*P. andersonii* formed nodules when inoculated with WUR3 and BOR2, but they differ in that a significantly larger number of nodules are formed with BOR2-inoculation, but that on the WUR3-harbouring nodules were maintained over a long period. Early stages of plant-rhizobial interactions depend on molecular signalling to determine outcome but also the extent of nodulation over a long period. Whilst certain legumes can form a symbiotic relationship that are nod factor (NF) independent, such as *Aeschynomene evenia* spp. *serrulata* and *Bradyrhizobium* sp. ORS278 (Gully et al., 2018), this is not the case for *P. andersonii*, despite nodules being initiated using the same crack-entry system as *A. evenia* spp. *serrulata* instead of root hair curling. WUR3 (Op den Camp et al., 2012), WSM1022 and WSM419 (Baxter et al., 2021) share the commonly found NF biosynthesis genes *nodA/B/C* as well as the nod genes *nod/I/J/L/P/Q* but do not share the nod genes *nodS/U/Z*, *noIL*, *nolO*, *and noeE/I* that WUR3 possesses. BOR2 NF biosynthesis genes are currently unknown; however, it would be interesting to see how similar or how different they are to the WUR3 NF biosynthesis genes as *P. andersonii* forms a significant number of nodules with BOR2 compared to the control and WUR3, which suggests there may be some altered NF signalling between these strains with *P. andersonii*.

At which point in plant-rhizobia interactions *P. andersonii* blocks rhizobial entry or nodule formation with incompatible rhizobia is unknown. Whilst it is very likely that the lack of recognition of the NFs being produced (or the rhizobia not recognising *P. andersonii* exudates) means this occurs at the recognitions stage, imaging *P. andersonii* fluorescently labelled rhizobia over a time course experiment could determine whether WSM419 or WSM1022 invade the *P. andersonii* epidermal cracks. This will then allow identification of the point at which nodulation with WSM419 or WSM1022 is blocked, even if nodulation does not begin in the first place. (Granqvist et al., 2015) found that NFs from *Sinorhizobium fredii* NGR234 led to calcium oscillations in *P. andersonii*, which is typically an indicator of symbiosis being initiated. Using calcium reporters in the plant and fluorescently labelled rhizobia

could be used to determine which NFs *P. andersonii* responds to with calcium oscillation responses. Experiment such as these will help determine which rhizobia are likely to be compatible with *P. andersonii*.

Overall, there are many avenues to take this research on *P. andersonii* promiscuity vs. nodule efficiency, and this research adds evidence to better understand the broad rhizobial symbiotic range of *P. andersonii*.

## 6.4 *Parasponia andersonii* has control over the symbiosis even after nodule organogenesis has commenced

Chapter 3 demonstrated that *P. andersonii* is prevented from forming nodules with incompatible rhizobia and (Dupin et al., 2020) found that *P. andersonii* can prevent unneeded nodule formation when enough nitrogen is available in the surrounding environment. This led to the aims of Chapter 4 that were to analyse the differences between BOR2 and WUR3-harbouring nodules using microscopy techniques as well as molecular techniques. These techniques were used to determine if the early nodulation signalling pathway was different upon inoculation and if there were any differences as the nodule is forming. This resulted in this work demonstrating for the first time that *P. andersonii* can control its symbiotic relationships even after nodule organogenesis has been initiated.

As found in Chapter 4, *P. andersonii* inoculated with BOR2 no longer had rhizobia present within the nodules at seven weeks after inoculation. This contrasted with findings of (van Velzen et al., 2018) showing BOR2 rhizobia in *P. andersonii* nodules, although they analysed younger (six-week post-inoculation) nodules. At eight weeks old, *P. andersonii* nodules inoculated with BOR2 appear to have started the process of autophagic degradation as the first step of nodule senescence. This follows what was found by (Van de Velde et al., 2006) in *M. truncatula*, where there is degradation of the symbiont partner first (through bacterial lysis) before plant cell death occurs during natural nodule senescence.

This research is pointing towards *P. andersonii* being able to sanction ineffective symbionts with bacterial degradation and early nodule senescence. Sanctions against rhizobia has been found in *L. japonicus* where ineffective rhizobial

resulted in accelerated nodule senescence (Regus et al., 2017). What was also found is this sanctioning can be selective within *L. japonicus* nodules, where a mixed population of efficient and inefficient rhizobia within one nodule resulted in only the cells containing the inefficient rhizobia being target for programmed cell death (Regus et al., 2017). This sanctioning can also be found in indeterminate nodules such as *Pisum sativum* and *Medicago sativa* where the undifferentiated rhizobia are sanctioned when their differentiated counterparts are not fixing nitrogen (Oono et al., 2011). This sanctioning can also be found through early nodule senescence when ineffective nodules are formed in *P. sativum* (Serova et al., 2018). What the threshold is for a host plant to sanction its symbionts and how this is regulated is still under investigation but may be linked to conditional decisions that combine global cues with nitrogen output (Westhoek et al., 2021). My work builds upon this nodule sanctioning by showing that a non-legume also has the potential to sanction its nodules, perhaps showing an evolutionary link.

As discussed previously, the reason why these BOR2-harbouring nodules are senescing still needs further research. This could be in the form of using carbon tracers (Metzner et al., 2022) to track how much carbon is used by BOR2 from the plant compared to how much WUR3 takes from the plant, since carbon usage is an important element in nodule surveillance mechanisms which regulate nodule activity.

The fact that the BOR2 rhizobia are being degraded by *P. andersonii* after nodule organogenesis demonstrates the importance of understanding the real term consequences of a symbiotic relationship. Using BOR2 inoculation to study nodulation in *P. andersonii* may act as a suitable system to study the nodulation capacity of *P. andersonii* as mature, functioning nodules are not formed. WUR3, therefore, may be a better candidate for studying *P. andersonii* for normal nodulation signalling, as nodules are maintained, and it leads to increased shoot and root fresh weight (as found in Chapter 3). This will allow for a compare and contrast between a fully functioning nodulation mechanism and a non-efficient one.

## 6.5 Progress towards future tools for analysing symbiosis in legumes and non-legumes

For nodulation to occur, the nodulation signalling pathway requires co-ordination across the different root tissue types, from the epidermis, to the pericycle and cortex (and back), as introduced in Chapter 5. Being able to individually analyse each tissue individually will greatly expand the knowledge of the nodulation signalling pathway. Chapter 5 aimed to generate stable cell type fluorescent lines of *M. truncatula* and *P. andersonii* to allow for further research into nodulation pathway signalling in the different root tissue types. Whilst a fully usable stable line has not yet been established, Chapter 5 has pushed progress towards generating epidermal-fluorescent stable lines for both *M. truncatula* and *P. andersonii*. As well as this, a foundation has been established for generating *P. andersonii* protoplasts with a protocol that can be built upon for future Fluorescence Activated Cell Sorting (FACS) or single cell RNA-seq (scRNA-seq) using *P. andersonii*.

Not only has this work helped establish epidermal fluorescent lines, but it could also be expanded into generating stable lines that have fluorescence in other root tissue types, such as cortex or pericycle. Not only this, but any future tissue-specific stable lines can be combined with using either fluorescently labelled rhizobia or pathogens so that many aspects of plant-microbe interactions can be studied, both symbiotic and pathogenic, and from plant and microbe sides.

## 6.6 Future directions for this research

This research has pinpointed many avenues to go down to further analyse *M. truncatula* and *P. andersonii* symbiosis efficiency with rhizobia. This includes investigating the initiation of nodulation through analysing the NFs produced by the rhizobia and the plant NF receptors, and the response of different species of rhizobia to *M. truncatula* and *P. andersonii* exudates. Further analysing why BOR2-inoculated nodules are being sanctioned by *P. andersonii* through the use of carbon radiolabelling and nodule senescence as a whole in *P. andersonii* nodulation will be very informative. Generating a range of stable lines for both *P. andersonii* and *M. truncatula* of different fluorescent root tissue types will benefit the research community greatly, particularly those interested in coordination of signalling pathways over space and time.

Overall, this work has pushed forward research into nodulation in the legume *M. truncatula* and in the non-legume *P. andersonii*, and comparative understanding of nitrogen-fixing symbiosis (Figure 6.1).

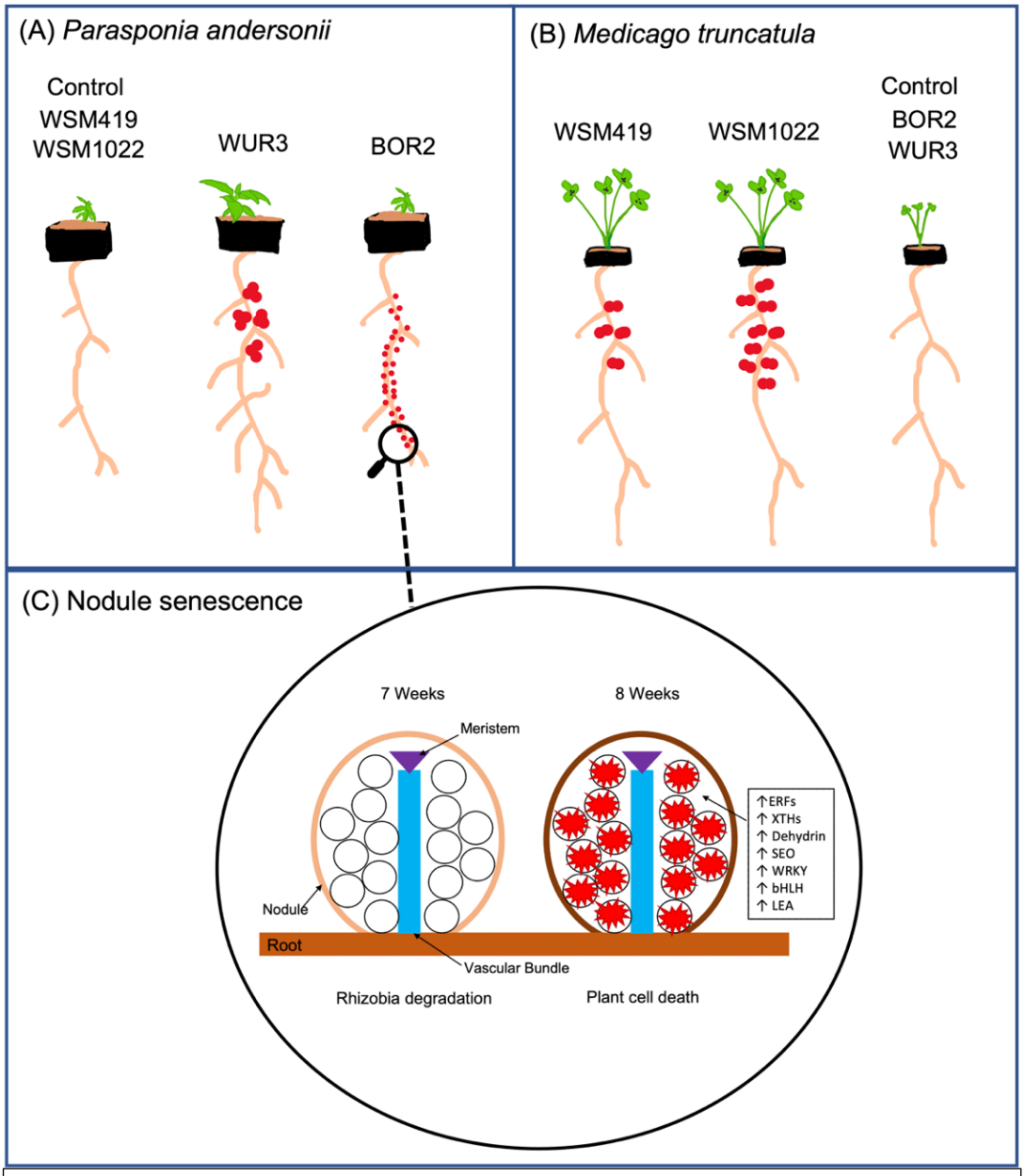


**Figure 6.1 An overview of the key findings in this work**
(A) *Parasponia andersonii* has a significant increase in shoot and root biomass when inoculated with *Bradyrhizobium elkanii* (WUR3). There was no significant difference when P. andersonii was inoculated with *Sinorhizobium meliloti* (WSM1022), *Sinorhizobium medicae* (WSM419) or BOR2. However, *Mesorhizobium plurifari*um (BOR2) produced a significant number of small nodules.
(B) *Medicago truncatula* formed nodules that had a significant increase in shoot fresh weight when inoculated with WSM419 or WSM1022 but not when inoculated with BOR2 or WUR3. Due to WSM419 needing less nodules to have the same increase in shoot fresh weight, this was deemed to be a more efficient rhizobial partner for M. truncatula.
(C) The nodule phenotype shown by *P. andersonii* when inoculated with BOR2 was likely due to *P. andersonii* degrading the rhizobia within the nodule at seven weeks (as shown with the microscopy images) and by eight weeks old, *P. andersonii* nodules inoculated with BOR2 are going through nodule senescence. This shows that *P. andersonii* is capable of sanctioning unproductive rhizobial partners.

# References


ALEXA, A. & RAHNENFUHRER, J. 2022. topGO: enrichment analysis for gene ontology. *R package version.*

ARIEL, F., BRAULT-HERNANDEZ, M., LAFFONT, C., HUAULT, E., BRAULT, M., PLET, J., MOISON, M., BLANCHET, S., ICHANTÉ, J. L. & CHABAUD, M. 2012. Two direct targets of cytokinin signaling regulate symbiotic nodulation in *Medicago truncatula*. *The Plant Cell,* 24**,** 3838-3852.

ARRIGHI, J.-F., BARRE, A., BEN AMOR, B., BERSOULT, A., SORIANO, L. C., MIRABELLA, R., DE CARVALHO-NIEBEL, F., JOURNET, E.-P., GHÉRARDI, M. & HUGUET, T. 2006. The *Medicago truncatula* lysine motif-receptor-like kinase gene family includes *NFP* and new nodule-expressed genes. *Plant Physiology,* 142**,** 265-279.

ATHUL, P. P., PATRA, R. K., SETHI, D., PANDA, N., MUKHI, S. K., PADHAN, K., SAHOO, S. K., SAHOO, T. R., MANGARAJ, S. & PRADHAN, S. R. 2022. Efficient native strains of rhizobia improved nodulation and productivity of French bean (*Phaseolus vulgaris* L.) under rainfed condition. *Frontiers in Plant Science,* 13.

ATIF, R. M., BOULISSET, F., CONREUX, C., THOMPSON, R. & OCHATT, S. J. 2013. In vitro auxin treatment promotes cell division and delays endoreduplication in developing seeds of the model legume species *Medicago truncatula*. *Physiologia Plantarum,* 148**,** 549-559.

BALASURIYA, B. T. G., GHOSE, A., GHEEWALA, S. H. & PRAPASPONGSA, T. 2022. Assessment of eutrophication potential from fertiliser application in agricultural systems in Thailand. *Science of The Total Environment,* 833**,** 154993.

BARGMANN, B. O. & BIRNBAUM, K. D. 2010. Fluorescence activated cell sorting of plant protoplasts. *JoVE (Journal of Visualized Experiments)***,** e1673.

BAXTER, L., ROY, P., PICOT, E., WATTS, J., JONES, A., WILKINSON, H., SCHÄFER, P., GIFFORD, M. & LAGUNAS, B. 2021. Comparative Genomics across Three Ensifer Species Using a New Complete Genome Sequence of the *Medicago* Symbiont *Sinorhizobium* (*Ensifer*) *meliloti* WSM1022. *Microorganisms,* 9**,** 2428.

BEHM, J. E., GEURTS, R. & KIERS, E. T. 2014. *Parasponia*: a novel system for studying mutualism stability. *Trends in Plant Science,* 19**,** 757-763.

BERRABAH, F., BALLIAU, T., AÏT-SALEM, E. H., GEORGE, J., ZIVY, M., RATET, P. & GOURION, B. 2018. Control of the ethylene signaling pathway prevents plant defenses during intracellular accommodation of the rhizobia. *New Phytologist,* 219**,** 310-323.

BERTRAND, A., BIPFUBUSA, M., DHONT, C., CHALIFOUR, F.-P., DROUIN, P. & BEAUCHAMP, C. J. 2016. Rhizobial strains exert a major effect on the amino acid composition of alfalfa nodules under NaCl stress. *Plant Physiology and Biochemistry,* 108**,** 344-352.

BERTRAND, A., DHONT, C., BIPFUBUSA, M., CHALIFOUR, F.-P., DROUIN, P. & BEAUCHAMP, C. J. 2015. Improving salt stress responses of the symbiosis in alfalfa using salt-tolerant cultivar and rhizobial strain. *Applied Soil Ecology,* 87**,** 108-117.

BHAR, A., CHATTERJEE, M., GUPTA, S. & DAS, S. 2018. Salicylic acid regulates systemic defense signaling in chickpea during *Fusarium oxysporum* f. sp. *ciceri* race 1 infection. *Plant Molecular Biology Reporter,* 36**,** 162-175.

BIRNBAUM, K., JUNG, J. W., WANG, J. Y., LAMBERT, G. M., HIRST, J. A., GALBRAITH, D. W. & BENFEY, P. N. 2005. Cell type–specific expression profiling in plants via cell sorting of protoplasts from fluorescent reporter lines. *Nature Methods,* 2**,** 615-619.

BREAKSPEAR, A., LIU, C., ROY, S., STACEY, N., ROGERS, C., TRICK, M., MORIERI, G., MYSORE, K. S., WEN, J. & OLDROYD, G. E. 2014. The root hair "infectome" of *Medicago truncatula* uncovers changes in cell cycle genes and reveals a requirement for auxin signaling in rhizobial infection. *The Plant Cell,* 26**,** 4680-4701.

BU, F., RUTTEN, L., ROSWANJAYA, Y. P., KULIKOVA, O., RODRIGUEZ-FRANCO, M., OTT, T., BISSELING, T., VAN ZEIJL, A. & GEURTS, R. 2020. Mutant analysis in the nonlegume *Parasponia andersonii* identifies NIN and NF-YA1 transcription factors as a core genetic network in nitrogen-fixing nodule symbioses. *New Phytologist,* 226**,** 541-554.

BUER, C. S. & MUDAY, G. K. 2004. The transparent testa4 mutation prevents flavonoid synthesis and alters auxin transport and the response of *Arabidopsis* roots to gravity and light. *The Plant Cell,* 16**,** 1191-1205.

BURNAT, M., HERRERO, A. & FLORES, E. 2014. Compartmentalized cyanophycin metabolism in the diazotrophic filaments of a heterocyst-forming cyanobacterium. *Proceedings of the National Academy of Sciences,* 111**,** 3823-3828.

CAI, J., ZHANG, L.-Y., LIU, W., TIAN, Y., XIONG, J.-S., WANG, Y.-H., LI, R.-J., LI, H.-M., WEN, J. & MYSORE, K. S. 2018. Role of the Nod factor hydrolase MtNFH1 in regulating Nod factor levels during rhizobial infection and in mature nodules of *Medicago truncatula*. *The Plant Cell,* 30**,** 397-414.

CANNON, S. B., MCKAIN, M. R., HARKESS, A., NELSON, M. N., DASH, S., DEYHOLOS, M. K., PENG, Y., JOYCE, B., STEWART JR, C. N. & ROLF, M. 2015. Multiple polyploidy events in the early radiation of nodulating and nonnodulating legumes. *Molecular Biology and Evolution,* 32**,** 193-210.

CAPOEN, W., DEN HERDER, J., ROMBAUTS, S., DE GUSSEM, J., DE KEYSER, A., HOLSTERS, M. & GOORMACHTIG, S. 2007. Comparative transcriptome analysis reveals common and specific tags for root hair and crack-entry invasion in *Sesbania rostrata*. *Plant Physiology,* 144**,** 1878-1889.

CÁRDENAS, L., MARTÍNEZ, A., SÁNCHEZ, F. & QUINTO, C. 2008. Fast, transient and specific intracellular ROS changes in living root hair cells responding to Nod factors (NFs). *The Plant Journal,* 56**,** 802-813.

CARLIER, A., FEHR, L., PINTO-CARBÓ, M., SCHÄBERLE, T., REHER, R., DESSEIN, S., KÖNIG, G. & EBERL, L. 2016. The genome analysis of *Candidatus Burkholderia crenata* reveals that secondary metabolism may be a key function of the *Ardisia crenata* leaf nodule symbiosis. *Environmental Microbiology,* 18**,** 2507-2522.

CARLIER, A. L., OMASITS, U., AHRENS, C. H. & EBERL, L. 2013. Proteomics analysis of *Psychotria* leaf nodule symbiosis: improved genome annotation and metabolic predictions. *Molecular Plant-Microbe Interactions,* 26**,** 1325-1333.

CERRI, M. R., FRANCES, L., LALOUM, T., AURIAC, M.-C., NIEBEL, A., OLDROYD, G. E., BARKER, D. G., FOURNIER, J. & DE CARVALHO-NIEBEL, F. 2012. *Medicago truncatula* ERN transcription factors: regulatory interplay with NSP1/NSP2 GRAS factors and expression dynamics throughout rhizobial infection. *Plant Physiology,* 160**,** 2155-2172.

CERVANTES-PÉREZ, S. A., THIBIVILLIERS, S., LAFFONT, C., FARMER, A. D., FRUGIER, F. & LIBAULT, M. 2022. Cell-specific pathways recruited for symbiotic nodulation in the *Medicago truncatula* legume. *Molecular Plant*.

CHAINTREUIL, C., GULLY, D., HERVOUET, C., TITTABUTR, P., RANDRIAMBANONA, H., BROWN, S. C., LEWIS, G. P., BOURGE, M., CARTIEAUX, F. & BOURSOT, M. 2016. The evolutionary dynamics of ancient and recent polyploidy in the African semiaquatic species of the legume genus *Aeschynomene*. *New Phytologist,* 211**,** 1077-1091.

CHANG, A. C. G., CHEN, T., LI, N. & DUAN, J. 2019. Perspectives on endosymbiosis in coralloid roots: association of cycads and cyanobacteria. *Frontiers in Microbiology,* 10**,** 1888.

CHEN, S., ZHOU, Y., CHEN, Y. & GU, J. 2018. fastp: an ultra-fast all-in-one FASTQ preprocessor. *Bioinformatics,* 34**,** i884-i890.

CHOI, H.-K., MUN, J.-H., KIM, D.-J., ZHU, H., BAEK, J.-M., MUDGE, J., ROE, B., ELLIS, N., DOYLE, J. & KISS, G. B. 2004. Estimating genome conservation between crop and model legume species. *Proceedings of the National Academy of Sciences,* 101**,** 15289-15294.

CHOI, I.-Y., HYTEN, D. L., MATUKUMALLI, L. K., SONG, Q., CHAKY, J. M., QUIGLEY, C. V., CHASE, K., LARK, K. G., REITER, R. S. & YOON, M.-S. 2007. A soybean transcript map: gene distribution, haplotype and single-nucleotide polymorphism analysis. *Genetics,* 176**,** 685-696.

COMPAORÉ, J. & STAL, L. J. 2010. Oxygen and the light–dark cycle of nitrogenase activity in two unicellular cyanobacteria. *Environmental Microbiology,* 12**,** 54-62.

COMPTON, K. K., HILDRETH, S. B., HELM, R. F. & SCHARF, B. E. 2020. An updated perspective on *Sinorhizobium meliloti* chemotaxis to alfalfa flavonoids. *Frontiers in Microbiology,* 11**,** 581482.

COOK, D. R. 1999. *Medicago truncatula*-a model in the making! *Current Opinion in Plant Biology,* 2**,** 301-304.

CORWIN, D. L. 2021. Climate change impacts on soil salinity in agricultural areas. *European Journal of Soil Science,* 72**,** 842-862.

CUI, X., YAN, Q., GAN, S., XUE, D., WANG, H., XING, H., ZHAO, J. & GUO, N. 2019. *GmWRKY40*, a member of the WRKY transcription factor genes identified from *Glycine max* L., enhanced the resistance to Phytophthora sojae. *BMC Plant Biology,* 19**,** 1-15.

DA SILVA, H. A. P., CAETANO, V. S., PESSOA, D. D. V., PACHECO, R. S. & SIMOES-ARAUJO, J. L. 2019. Molecular and biochemical changes of aging-induced nodules senescence in common bean. *Symbiosis,* 79**,** 33-48.

DAWSON, J. 2007. Ecology of actinorhizal plants. *Nitrogen-Fixing Actinorhizal Symbioses.* Springer.

DE MEYER, F., DANNEELS, B., ACAR, T., RASOLOMAMPIANINA, R., RAJAONAH, M. T., JEANNODA, V. & CARLIER, A. 2019. Adaptations and evolution of a heritable

leaf nodule symbiosis between *Dioscorea sansibarensis* and *Orrella dioscoreae*. *The ISME Journal,* 13**,** 1831-1844.

DEAN, J. M., MESCHER, M. C. & DE MORAES, C. M. 2014. Plant dependence on rhizobia for nitrogen influences induced plant defenses and herbivore performance. *International Journal of Molecular Sciences,* 15**,** 1466-1480.

DHANUSHKODI, R., MATTHEW, C., MCMANUS, M. T. & DIJKWEL, P. P. 2018. Drought-induced senescence of *Medicago truncatula* nodules involves serpin and ferritin to control proteolytic activity and iron levels. *New Phytologist,* 220**,** 196-208.

DIAGNE, N., ARUMUGAM, K., NGOM, M., NAMBIAR-VEETIL, M., FRANCHE, C., NARAYANAN, K. K. & LAPLAZE, L. 2013. Use of *Frankia* and actinorhizal plants for degraded lands reclamation. *BioMed Research International,* 2013.

DÍAZ-VALLE, A., LÓPEZ-CALLEJA, A. C. & ALVAREZ-VENEGAS, R. 2019. Enhancement of Pathogen Resistance in Common Bean Plants by Inoculation With *Rhizobium etli*. *Frontiers in Plant Science,* 10.

DOBIN, A., DAVIS, C. A., SCHLESINGER, F., DRENKOW, J., ZALESKI, C., JHA, S., BATUT, P., CHAISSON, M. & GINGERAS, T. R. 2013. STAR: ultrafast universal RNA-seq aligner. *Bioinformatics,* 29**,** 15-21.

DONG, W. & SONG, Y. 2020. The significance of flavonoids in the process of biological nitrogen fixation. *International Journal of Molecular Sciences,* 21**,** 5926.

DUPIN, S. E., GEURTS, R. & KIERS, E. T. 2020. The non-legume *Parasponia andersonii* mediates the fitness of nitrogen-fixing rhizobial symbionts under high nitrogen conditions. *Frontiers in Plant Science,* 10**,** 1779.

ECHBAB, H., ARAHOU, M., DUCOUSSO, M., NOURISSIER-MOUNTOU, S., DUPONNOIS, R., LAHLOU, H. & PRIN, Y. 2007. Successful nodulation of *Casuarina* by *Frankia* in axenic conditions. *Journal of Applied Microbiology,* 103**,** 1728-1737.

EDMONDS, D. A., CALDWELL, R. L., BRONDIZIO, E. S. & SIANI, S. M. 2020. Coastal flooding will disproportionately impact people on river deltas. *Nature Communications,* 11**,** 1-8.

EHINGER, M., MOHR, T. J., STARCEVICH, J. B., SACHS, J. L., PORTER, S. S. & SIMMS, E. L. 2014. Specialization-generalization trade-off in a *Bradyrhizobium* symbiosis with wild legume hosts. *BMC Ecology,* 14**,** 1-19.

EPIHOV, D. Z., SALTONSTALL, K., BATTERMAN, S. A., HEDIN, L. O., HALL, J. S., VAN BREUGEL, M., LEAKE, J. R. & BEERLING, D. J. 2021. Legume–microbiome interactions unlock mineral nutrients in regrowing tropical forests. *Proceedings of the National Academy of Sciences,* 118**,** e2022241118.

ESCUDERO, V., ABREU, I., TEJADA-JIMÉNEZ, M., ROSA-NÚÑEZ, E., QUINTANA, J., PRIETO, R. I., LARUE, C., WEN, J., VILLANOVA, J. & MYSORE, K. S. 2020. *Medicago truncatula* Ferroportin2 mediates iron import into nodule symbiosomes. *New Phytologist,* 228**,** 194-209.

FAO. 2022. *FAOSTAT: Fertilizers by Nutrient* [Online]. fao.org: License: CC BY_NC_SA 3.0 IGO. Available: ww.fao.org/faostat/en/#data/RFN [Accessed 09-02-2023 2023].

FLEISCHMAN, D. & KRAMER, D. 1998. Photosynthetic rhizobia. *Biochimica et Biophysica Acta (BBA)-Bioenergetics,* 1364**,** 17-36.

FOURNIER, J., TEILLET, A., CHABAUD, M., IVANOV, S., GENRE, A., LIMPENS, E., DE CARVALHO-NIEBEL, F. & BARKER, D. G. 2015. Remodeling of the infection

chamber before infection thread formation reveals a two-step mechanism for rhizobial entry into the host legume root hair. *Plant Physiology,* 167**,** 1233-1242.

GASSER, M., ALLOISIO, N., FOURNIER, P., BALMAND, S., KHARRAT, O., TULUMELLO, J., CARRO, L., HEDDI, A., DA SILVA, P. & NORMAND, P. 2022. A Nonspecific Lipid Transfer Protein with Potential Functions in Infection and Nodulation. *Molecular Plant-Microbe Interactions,* 35**,** 1096-1108.

GAUDIOSO-PEDRAZA, R., BECK, M., FRANCES, L., KIRK, P., RIPODAS, C., NIEBEL, A., OLDROYD, G. E., BENITEZ-ALFONSO, Y. & DE CARVALHO-NIEBEL, F. 2018. Callose-regulated symplastic communication coordinates symbiotic root nodule development. *Current Biology,* 28**,** 3562-3577. e6.

GAVRIN, A., CHIASSON, D., OVCHINNIKOVA, E., KAISER, B. N., BISSELING, T. & FEDOROVA, E. E. 2016. VAMP721a and VAMP721d are important for pectin dynamics and release of bacteria in soybean nodules. *New Phytologist,* 210**,** 1011-1021.

GIFFORD, M. L., DEAN, A., GUTIERREZ, R. A., CORUZZI, G. M. & BIRNBAUM, K. D. 2008. Cell-specific nitrogen responses mediate developmental plasticity. *Proceedings of the National Academy of Sciences,* 105**,** 803-808.

GOORMACHTIG, S., CAPOEN, W., JAMES, E. K. & HOLSTERS, M. 2004. Switch from intracellular to intercellular invasion during water stress-tolerant legume nodulation. *Proceedings of the National Academy of Sciences,* 101**,** 6303-6308.

GRANQVIST, E., SUN, J., OP DEN CAMP, R., PUJIC, P., HILL, L., NORMAND, P., MORRIS, R. J., DOWNIE, J. A., GEURTS, R. & OLDROYD, G. E. 2015. Bacterial-induced calcium oscillations are common to nitrogen-fixing associations of nodulating legumes and non-legumes. *New Phytologist,* 207**,** 551-558.

GULLY, D., CZERNIC, P., CRUVEILLER, S., MAHÉ, F., LONGIN, C., VALLENET, D., FRANÇOIS, P., NIDELET, S., RIALLE, S. & GIRAUD, E. 2018. Transcriptome profiles of Nod factor-independent symbiosis in the tropical legume *Aeschynomene evenia*. *Scientific Reports,* 8**,** 10934.

GUTIÉRREZ-GARCÍA, K., BUSTOS-DÍAZ, E. D., CORONA-GÓMEZ, J. A., RAMOS-ABOITES, H. E., SÉLEM-MOJICA, N., CRUZ-MORALES, P., PÉREZ-FARRERA, M. A., BARONA-GÓMEZ, F. & CIBRIÁN-JARAMILLO, A. 2019. Cycad coralloid roots contain bacterial communities including cyanobacteria and *Caulobacter* spp. that encode niche-specific biosynthetic gene clusters. *Genome Biology and Evolution,* 11**,** 319-334.

HAN, Y., BAN, Q., LI, H., HOU, Y., JIN, M., HAN, S. & RAO, J. 2016. DkXTH8, a novel xyloglucan endotransglucosylase/hydrolase in persimmon, alters cell wall structure and promotes leaf senescence and fruit postharvest softening. *Scientific Reports,* 6**,** 39155.

HARRISON, T. L., SIMONSEN, A. K., STINCHCOMBE, J. R. & FREDERICKSON, M. E. 2018. More partners, more ranges: generalist legumes spread more easily around the globe. *Biology Letters,* 14**,** 20180616.

HASHIDOKO, Y., NISHIZUKA, H., TANAKA, M., MURATA, K., MURAI, Y. & HASHIMOTO, M. 2019. Isolation and characterization of 1-palmitoyl-2-linoleoyl-sn-glycerol as a hormogonium-inducing factor (HIF) from the coralloid roots of *Cycas revoluta* (*Cycadaceae*). *Scientific Reports,* 9**,** 1-12.

HÖFTE, H. & VOXEUR, A. 2017. Plant cell walls. *Current Biology,* 27**,** R865-R870.

HOOVER, T. R., IMPERIAL, J., LUDDEN, P. W. & SHAH, V. K. 1989. Homocitrate is a component of the iron-molybdenum cofactor of nitrogenase. *Biochemistry,* 28**,** 2768-2771.

HUSSAIN, S., ZHANG, J.-H., ZHONG, C., ZHU, L.-F., CAO, X.-C., YU, S.-M., BOHR, J. A., HU, J.-J. & JIN, Q.-Y. 2017. Effects of salt stress on rice growth, development characteristics, and the regulating ways: A review. *Journal of Integrative Agriculture,* 16**,** 2357-2374.

IRISARRI, P., CARDOZO, G., TARTAGLIA, C., REYNO, R., GUTIÉRREZ, P., LATTANZI, F. A., REBUFFO, M. & MONZA, J. 2019. Selection of competitive and efficient rhizobia strains for white clover. *Frontiers in Microbiology,* 10**,** 768.

IVANOV, S., FEDOROVA, E. E., LIMPENS, E., DE MITA, S., GENRE, A., BONFANTE, P. & BISSELING, T. 2012. Rhizobium–legume symbiosis shares an exocytotic pathway required for arbuscule formation. *Proceedings of the National Academy of Sciences,* 109**,** 8316-8321.

IWANYCKI AHLSTRAND, N. & STEVENSON, D. W. 2021. Retracing origins of exceptional cycads in botanical collections to increase conservation value. *Plants, People, Planet,* 3**,** 94-98.

JIN, Y., LIU, H., LUO, D., YU, N., DONG, W., WANG, C., ZHANG, X., DAI, H., YANG, J. & WANG, E. 2016. DELLA proteins are common components of symbiotic rhizobial and mycorrhizal signalling pathways. *Nature communications,* 7**,** 1-14.

JOHNSON, M., ZARETSKAYA, I., RAYTSELIS, Y., MEREZHUK, Y., MCGINNIS, S. & MADDEN, T. L. 2008. NCBI BLAST: a better web interface. *Nucleic Acids Research,* 36**,** W5-W9.

KALLONIATI, C., KROMPAS, P., KARALIAS, G., UDVARDI, M. K., RENNENBERG, H., HERSCHBACH, C. & FLEMETAKIS, E. 2015. Nitrogen-fixing nodules are an important source of reduced sulfur, which triggers global changes in sulfur metabolism in *Lotus japonicus*. *The Plant Cell,* 27**,** 2384-2400.

KANESAKI, Y., HIROSE, M., HIROSE, Y., FUJISAWA, T., NAKAMURA, Y., WATANABE, S., MATSUNAGA, S., UCHIDA, H. & MURAKAMI, A. 2018. Draft genome sequence of the nitrogen-fixing and hormogonia-inducing cyanobacterium *Nostoc cycadae* strain WK-1, isolated from the coralloid roots of *Cycas revoluta*. *Genome Announcements,* 6**,** e00021-18.

KARMARKAR, V. 2014. Transcriptional regulation of nodule development and senescence in *Medicago truncatula*, Wageningen University and Research.

KAZMIERCZAK, T., YANG, L., BONCOMPAGNI, E., MEILHOC, E., FRUGIER, F., FRENDO, P., BRUAND, C., GRUBER, V. & BROUQUISSE, R. 2020. Legume nodule senescence: a coordinated death mechanism between bacteria and plant cells. *Advances in Botanical Research,* 94**,** 181-212.

KEET, J.-H., ELLIS, A. G., HUI, C. & LE ROUX, J. J. 2017. Legume–rhizobium symbiotic promiscuity and effectiveness do not affect plant invasiveness. *Annals of Botany,* 119**,** 1319-1331.

KIM, J. I., MURPHY, A. S., BAEK, D., LEE, S.-W., YUN, D.-J., BRESSAN, R. A. & NARASIMHAN, M. L. 2011. YUCCA6 over-expression demonstrates auxin function in delaying leaf senescence in *Arabidopsis thaliana*. *Journal of Experimental Botany,* 62**,** 3981-3992.

KIROLINKO, C., HOBECKER, K., WEN, J., MYSORE, K. S., NIEBEL, A., BLANCO, F. A. & ZANETTI, M. E. 2021. Auxin Response Factor 2 (ARF2), ARF3, and ARF4 mediate both lateral root and nitrogen fixing nodule development in *Medicago truncatula*. *Frontiers in Plant Science,* 12**,** 659061.

KITAEVA, A. B., DEMCHENKO, K. N., TIKHONOVICH, I. A., TIMMERS, A. C. & TSYGANOV, V. E. 2016. Comparative analysis of the tubulin cytoskeleton organization in nodules of *Medicago truncatula* and *Pisum sativum*: bacterial release and bacteroid positioning correlate with characteristic microtubule rearrangements. *New Phytologist,* 210**,** 168-183.

KLOCK, M. M., BARRETT, L. G., THRALL, P. H. & HARMS, K. E. 2016. Differential plant invasiveness is not always driven by host promiscuity with bacterial symbionts. *AoB Plants,* 8.

KLOCK, M. M., URBINA, H. G., BARRETT, L. G., THRALL, P. H. & HARMS, K. E. 2022. Provenance of rhizobial symbionts is similar for invasive and noninvasive acacias introduced to California. *FEMS Microbiology Ecology,* 98.

KNYAZEV, A., KULUEV, B., VERSHININA, Z. & CHEMERIS, A. 2018. Callus Induction and Plant Regeneration from Leaf Segments of Unique Tropical Woody Plant *Parasponia andersonii* Planch. *Plant Tissue Culture and Biotechnology,* 28**,** 45-55.

KOHLEN, W., NG, J. L. P., DEINUM, E. E. & MATHESIUS, U. 2018. Auxin transport, metabolism, and signalling during nodule initiation: indeterminate and determinate nodules. *Journal of Experimental Botany,* 69**,** 229-244.

KOVACS, S., FODOR, L., DOMONKOS, A., AYAYDIN, F., LACZI, K., RÁKHELY, G. & KALO, P. 2021. Amino acid polymorphisms in the VHIID conserved motif of Nodulation Signaling Pathways 2 distinctly modulate symbiotic signaling and nodule morphogenesis in *Medicago truncatula*. *Frontiers in Plant Science***,** 2473.

KOVÁCS, S., KISS, E., JENEI, S., FEHÉR-JUHÁSZ, E., KERESZT, A. & ENDRE, G. 2022. The *Medicago truncatula* IEF Gene Is Crucial for the Progression of Bacterial Infection During Symbiosis. *Molecular Plant-Microbe Interactions,* 35**,** 401-415.

LAFFONT, C., IVANOVICI, A., GAUTRAT, P., BRAULT, M., DJORDJEVIC, M. A. & FRUGIER, F. 2020. The NIN transcription factor coordinates CEP and CLE signaling peptides that regulate nodulation antagonistically. *Nature Communications,* 11**,** 3167.

LAGUNAS, B., WALKER, L., HUSSAIN, R. M. F., HANDS-PORTMAN, I., WOOLLEY-ALLEN, K. & GIFFORD, M. L. 2018. Histological Profiling Over Time to Optimize Root Cell Type-Specific Reporter Lines for Cell Sorting. *Root Development.* Springer.

LANCELLE, S. A. & TORREY, J. 1984. Early development of Rhizobium-induced root nodules of *Parasponia rigida*. I. Infection and early nodule initiation. *Protoplasma,* 123**,** 26-37.

LAPORTE, P., LEPAGE, A., FOURNIER, J., CATRICE, O., MOREAU, S., JARDINAUD, M.-F., MUN, J.-H., LARRAINZAR, E., COOK, D. R. & GAMAS, P. 2014. The CCAAT box-binding transcription factor NF-YA1 controls rhizobial infection. *Journal of Experimental Botany,* 65**,** 481-494.

LE ROUX, M. M., MILLER, J. T., WALLER, J., DÖRING, M. & BRUNEAU, A. 2022. An expert curated global legume checklist improves the accuracy of occurrence, biodiversity and taxonomic data. *Scientific Data,* 9**,** 708.

LEMAIRE, B., SMETS, E. & DESSEIN, S. 2011. Bacterial leaf symbiosis in *Ardisia* (Myrsinoideae, Primulaceae): molecular evidence for host specificity. *Research in Microbiology,* 162**,** 528-534.

LESK, C., ROWHANI, P. & RAMANKUTTY, N. 2016. Influence of extreme weather disasters on global crop production. *Nature,* 529**,** 84-87.

LI, X., FENG, H., WEN, J., DONG, J. & WANG, T. 2018. MtCAS31 aids symbiotic nitrogen fixation by protecting the leghemoglobin MtLb120-1 under drought stress in *Medicago truncatula*. *Frontiers in plant science,* 9**,** 633.

LI, X., LIU, Q., FENG, H., DENG, J., ZHANG, R., WEN, J., DONG, J. & WANG, T. 2020. Dehydrin MtCAS31 promotes autophagic degradation under drought stress. *Autophagy,* 16**,** 862-877.

LI, Y., PEI, Y., SHEN, Y., ZHANG, R., KANG, M., MA, Y., LI, D. & CHEN, Y. 2022. Progress in the self-regulation system in legume nodule development-AON (autoregulation of nodulation). *International Journal of Molecular Sciences,* 23**,** 6676.

LIMPENS, E., FRANKEN, C., SMIT, P., WILLEMSE, J., BISSELING, T. & GEURTS, R. 2003. LysM domain receptor kinases regulating rhizobial Nod factor-induced infection. *Science,* 302**,** 630-633.

LINDSTRÖM, K. & MOUSAVI, S. A. 2020. Effectiveness of nitrogen fixation in rhizobia. *Microbial Biotechnology,* 13**,** 1314-1335.

LIU, C.-W., BREAKSPEAR, A., GUAN, D., CERRI, M. R., JACKSON, K., JIANG, S., ROBSON, F., RADHAKRISHNAN, G. V., ROY, S. & BONE, C. 2019a. NIN acts as a network hub controlling a growth module required for rhizobial infection. *Plant Physiology,* 179**,** 1704-1722.

LIU, H., LIN, J.-S., LUO, Z., SUN, J., HUANG, X., YANG, Y., XU, J., WANG, Y.-F., ZHANG, P. & OLDROYD, G. E. 2022a. Constitutive activation of a nuclear-localized calcium channel complex in *Medicago truncatula*. *Proceedings of the National Academy of Sciences,* 119**,** e2205920119.

LIU, J., RASING, M., ZENG, T., KLEIN, J., KULIKOVA, O. & BISSELING, T. 2021. NIN is essential for development of symbiosomes, suppression of defence and premature senescence in *Medicago truncatula* nodules. *New Phytologist,* 230**,** 290-303.

LIU, J., RUTTEN, L., LIMPENS, E., VAN DER MOLEN, T., VAN VELZEN, R., CHEN, R., CHEN, Y., GEURTS, R., KOHLEN, W. & KULIKOVA, O. 2019b. A remote cis-regulatory region is required for NIN expression in the pericycle to initiate nodule primordium formation in *Medicago truncatula*. *The Plant Cell,* 31**,** 68-83.

LIU, Y., GUO, Z. & SHI, H. 2022b. Rhizobium Symbiosis Leads to Increased Drought Tolerance in Chinese Milk Vetch (*Astragalus sinicus* L.). *Agronomy,* 12**,** 725.

LIU, Y., LIU, X., DONG, X., YAN, J., XIE, Z. & LUO, Y. 2022c. The effect of *Azorhizobium caulinodans* ORS571 and γ-aminobutyric acid on salt tolerance of *Sesbania rostrata*. *Frontiers in Plant Science,* 13.

LIVINGSTON, D., TUONG, T., NOGUEIRA, M. & SINCLAIR, T. 2019. Three-dimensional reconstruction of soybean nodules provides an update on vascular structure. *American Journal of Botany,* 106**,** 507-513.

LODWIG, E., LEONARD, M., MARROQUI, S., WHEELER, T., FINDLAY, K., DOWNIE, J. & POOLE, P. 2005. Role of polyhydroxybutyrate and glycogen as carbon storage compounds in pea and bean bacteroids. *Molecular plant-microbe interactions,* 18**,** 67-74.

LOVE, M. I., HUBER, W. & ANDERS, S. 2014. Moderated estimation of fold change and dispersion for RNA-seq data with DESeq2. *Genome biology,* 15**,** 1-21.

MAHMOOD, K., TORRES-JEREZ, I., KROM, N., LIU, W. & UDVARDI, M. K. 2022. Transcriptional Programs and Regulators Underlying Age-Dependent and Dark-Induced Senescence in *Medicago truncatula*. *Cells,* 11**,** 1570.

MALVIYA, M. K., SOLANKI, M. K., LI, C.-N., WANG, Z., ZENG, Y., VERMA, K. K., SINGH, R. K., SINGH, P., HUANG, H.-R. & YANG, L.-T. 2021. Sugarcane-legume intercropping can enrich the soil microbiome and plant growth. *Frontiers in Sustainable Food Systems,* 5**,** 606595.

MANGAL, V., LAL, M. K., TIWARI, R. K., ALTAF, M. A., SOOD, S., KUMAR, D., BHARADWAJ, V., SINGH, B., SINGH, R. K. & AFTAB, T. 2022. Molecular insights into the role of reactive oxygen, nitrogen and sulphur species in conferring salinity stress tolerance in plants. *Journal of Plant Growth Regulation***,** 1-21.

MARINKOVIĆ, J., BJELIĆ, D., ĐORĐEVIĆ, V., BALEŠEVIĆ-TUBIĆ, S., JOŠIĆ, D. & VUCELIĆ-RADOVIĆ, B. 2019. Performance of different *Bradyrhizobium* strains in root nodule symbiosis under drought stress. *Acta Physiologiae Plantarum,* 41**,** 1-13.

MARTÍNEZ-BARRADAS, V., BERNAL, L., LÓPEZ-BALTAZAR, J., COELLO, P., CRUZ-GARCÍA, F., MÁRQUEZ, J. & MARTÍNEZ-BARAJAS, E. 2019. Nutritional restriction triggers callose accumulation on the sieve plates of the funiculus of developing bean seeds. *South African Journal of Botany,* 121**,** 549-557.

MATSUO, M. & OELMÜLLER, R. 2015. REDOX RESPONSIVE TRANSCRIPTION FACTOR1 is involved in age-dependent and systemic stress signaling. *Plant Signaling & Behavior,* 10**,** e1051279.

MCGUINESS, P. N., REID, J. B. & FOO, E. 2020. Brassinosteroids play multiple roles in nodulation of pea via interactions with ethylene and auxin. *Planta,* 252**,** 1-8.

MEESTERS, T. M., VAN VLIET, W. M. & AKKERMANS, A. D. 1987. Nitrogenase is restricted to the vesicles in *Frankia* strain EAN1pec. *Physiologia Plantarum,* 70**,** 267-271.

MENDOZA-SUÁREZ, M., ANDERSEN, S. U., POOLE, P. S. & SÁNCHEZ-CAÑIZARES, C. 2021. Competition, nodule occupancy, and persistence of inoculant strains: Key factors in the Rhizobium-legume symbioses. *Frontiers in Plant Science,* 12**,** 690567.

MENEGAT, S., LEDO, A. & TIRADO, R. 2022. Greenhouse gas emissions from global production and use of nitrogen synthetic fertilisers in agriculture. *Scientific Reports,* 12**,** 14490.

MERGAERT, P., UCHIUMI, T., ALUNNI, B., EVANNO, G., CHERON, A., CATRICE, O., MAUSSET, A.-E., BARLOY-HUBLER, F., GALIBERT, F. & KONDOROSI, A. 2006. Eukaryotic control on bacterial cell cycle and differentiation in the

Rhizobium–legume symbiosis. *Proceedings of the National Academy of Sciences,* 103**,** 5230-5235.

MESSINESE, E., MUN, J.-H., YEUN, L. H., JAYARAMAN, D., ROUGÉ, P., BARRE, A., LOUGNON, G., SCHORNACK, S., BONO, J.-J. & COOK, D. R. 2007. A novel nuclear protein interacts with the symbiotic DMI3 calcium-and calmodulin-dependent protein kinase of *Medicago truncatula*. *Molecular Plant-Microbe Interactions,* 20**,** 912-921.

METZNER, R., CHLUBEK, A., BÜHLER, J., PFLUGFELDER, D., SCHURR, U., HUBER, G., KOLLER, R. & JAHNKE, S. 2022. In vivo imaging and quantification of carbon tracer dynamics in nodulated root systems of pea plants. *Plants,* 11**,** 632.

MNASRI, B., AOUANI, M. E. & MHAMDI, R. 2007. Nodulation and growth of common bean (*Phaseolus vulgaris*) under water deficiency. *Soil Biology and Biochemistry,* 39**,** 1744-1750.

MOHR, W., LEHNEN, N., AHMERKAMP, S., MARCHANT, H. K., GRAF, J. S., TSCHITSCHKO, B., YILMAZ, P., LITTMANN, S., GRUBER-VODICKA, H. & LEISCH, N. 2021. Terrestrial-type nitrogen-fixing symbiosis between seagrass and a marine bacterium. *Nature,* 600**,** 105-109.

NGUYEN, T. V., WIBBERG, D., VIGIL-STENMAN, T., BERCKX, F., BATTENBERG, K., DEMCHENKO, K. N., BLOM, J., FERNANDEZ, M. P., YAMANAKA, T. & BERRY, A. M. 2019. *Frankia*-enriched metagenomes from the earliest diverging symbiotic *Frankia* cluster: they come in teams. *Genome Biology and Evolution,* 11**,** 2273-2291.

NOUIOUI, I., CORTÉS-ALBAYAY, C., CARRO, L., CASTRO, J. F., GTARI, M., GHODHBANE-GTARI, F., KLENK, H.-P., TISA, L. S., SANGAL, V. & GOODFELLOW, M. 2019. Genomic insights into plant-growth-promoting potentialities of the genus *Frankia*. *Frontiers in Microbiology,* 10**,** 1457.

OLDROYD, G. E., ENGSTROM, E. M. & LONG, S. R. 2001. Ethylene inhibits the Nod factor signal transduction pathway of *Medicago truncatula*. *The Plant Cell,* 13**,** 1835-1849.

OLDROYD, G. E. & LONG, S. R. 2003. Identification and characterization of nodulation-signaling pathway 2, a gene of *Medicago truncatula* involved in Nod factor signaling. *Plant Physiology,* 131**,** 1027-1032.

OONO, R., ANDERSON, C. G. & DENISON, R. F. 2011. Failure to fix nitrogen by non-reproductive symbiotic rhizobia triggers host sanctions that reduce fitness of their reproductive clonemates. *Proceedings of the Royal Society B: Biological Sciences,* 278**,** 2698-2703.

OONO, R., MULLER, K. E., HO, R., JIMENEZ SALINAS, A. & DENISON, R. F. 2020. How do less-expensive nitrogen alternatives affect legume sanctions on rhizobia? *Ecology and Evolution,* 10**,** 10645-10656.

OP DEN CAMP, R., STRENG, A., DE MITA, S., CAO, Q., POLONE, E., LIU, W., AMMIRAJU, J. S., KUDRNA, D., WING, R. & UNTERGASSER, A. 2011. LysM-type mycorrhizal receptor recruited for rhizobium symbiosis in nonlegume *Parasponia*. *Science,* 331**,** 909-912.

OP DEN CAMP, R. H., POLONE, E., FEDOROVA, E., ROELOFSEN, W., SQUARTINI, A., OP DEN CAMP, H. J., BISSELING, T. & GEURTS, R. 2012. Nonlegume *Parasponia andersonii* deploys a broad rhizobium host range strategy resulting in largely

variable symbiotic effectiveness. *Molecular Plant-Microbe Interactions,* 25**,** 954-963.

OUAKED, F., ROZHON, W., LECOURIEUX, D. & HIRT, H. 2003. A MAPK pathway mediates ethylene signaling in plants. *The EMBO Journal,* 22**,** 1282-1288.

PAN, H., STONOHA-ARTHER, C. & WANG, D. 2018. Medicago plants control nodulation by regulating proteolysis of the receptor-like kinase DMI2. *Plant Physiology,* 177**,** 792-802.

PARSONS, R., RAVEN, J. & SPRENT, J. 1992. A simple open flow system used to measure acetylene reduction activity of *Sesbania rostrata* stem and root nodules. *Journal of Experimental Botany,* 43**,** 595-604.

PARSONS, R., SILVESTER, W. B., HARRIS, S., GRUIJTERS, W. & BULLIVANT, S. 1987. *Frankia* vesicles provide inducible and absolute oxygen protection for nitrogenase. *Plant Physiology,* 83**,** 728-731.

PAWLOWSKI, K. & DEMCHENKO, K. N. 2012. The diversity of actinorhizal symbiosis. *Protoplasma,* 249**,** 967-979.

PEDROSA, A., SANDAL, N., STOUGAARD, J., SCHWEIZER, D. & BACHMAIR, A. 2002. Chromosomal map of the model legume *Lotus japonicus*. *Genetics,* 161**,** 1661-1672.

PELEG-GROSSMAN, S., VOLPIN, H. & LEVINE, A. 2007. Root hair curling and Rhizobium infection in *Medicago truncatula* are mediated by phosphatidylinositide-regulated endocytosis and reactive oxygen species. *Journal of Experimental Botany,* 58**,** 1637-1649.

PINTO-CARBÓ, M., GADEMANN, K., EBERL, L. & CARLIER, A. 2018. Leaf nodule symbiosis: function and transmission of obligate bacterial endophytes. *Current Opinion in Plant Biology,* 44**,** 23-31.

POKHREL, Y., FELFELANI, F., SATOH, Y., BOULANGE, J., BUREK, P., GÄDEKE, A., GERTEN, D., GOSLING, S. N., GRILLAKIS, M. & GUDMUNDSSON, L. 2021. Global terrestrial water storage and drought severity under climate change. *Nature Climate Change,* 11**,** 226-233.

RADUTOIU, S., MADSEN, L. H., MADSEN, E. B., JURKIEWICZ, A., FUKAI, E., QUISTGAARD, E. M., ALBREKTSEN, A. S., JAMES, E. K., THIRUP, S. & STOUGAARD, J. 2007. LysM domains mediate lipochitin–oligosaccharide recognition and Nfr genes extend the symbiotic host range. *The EMBO Journal,* 26**,** 3923-3935.

RANI, L., THAPA, K., KANOJIA, N., SHARMA, N., SINGH, S., GREWAL, A. S., SRIVASTAV, A. L. & KAUSHAL, J. 2021. An extensive review on the consequences of chemical pesticides on human health and environment. *Journal of Cleaner Production,* 283**,** 124657.

REGUS, J. U., QUIDES, K. W., O'NEILL, M. R., SUZUKI, R., SAVORY, E. A., CHANG, J. H. & SACHS, J. L. 2017. Cell autonomous sanctions in legumes target ineffective rhizobia in nodules with mixed infections. *American journal of botany,* 104**,** 1299-1312.

REID, D., LIU, H., KELLY, S., KAWAHARADA, Y., MUN, T., ANDERSEN, S. U., DESBROSSES, G. & STOUGAARD, J. 2018. Dynamics of ethylene production in response to compatible Nod factor. *Plant Physiology,* 176**,** 1764-1772.

RIVAL, P., DE BILLY, F., BONO, J.-J., GOUGH, C., ROSENBERG, C. & BENSMIHEN, S. 2012. Epidermal and cortical roles of NFP and DMI3 in coordinating early steps of nodulation in *Medicago truncatula*. *Development,* 139**,** 3383-3391.

ROUX, B., RODDE, N., JARDINAUD, M. F., TIMMERS, T., SAUVIAC, L., COTTRET, L., CARRÈRE, S., SALLET, E., COURCELLE, E. & MOREAU, S. 2014. An integrated analysis of plant and bacterial gene expression in symbiotic root nodules using laser-capture microdissection coupled to RNA sequencing. *The Plant Journal,* 77**,** 817-837.

ROVERE, M., PUCCIARIELLO, C., CASTELLA, C., BERGER, A., FORGIA, M., GUYET, T. A., BOSSENO, M., PACOUD, M., BROUQUISSE, R. & PERATA, P. 2023. Group VII Ethylene Response Factors, MtERF74 and MtERF75, sustain nitrogen fixation in *Medicago truncatula* microoxic nodules. *Plant, Cell & Environment,* 46**,** 607-620.

ROY, R., REINDERS, A., WARD, J. M. & MCDONALD, T. R. 2020a. Understanding transport processes in lichen, Azolla–cyanobacteria, ectomycorrhiza, endomycorrhiza, and rhizobia–legume symbiotic interactions. *F1000Research,* 9.

ROY, S., LIU, W., NANDETY, R. S., CROOK, A., MYSORE, K. S., PISLARIU, C. I., FRUGOLI, J., DICKSTEIN, R. & UDVARDI, M. K. 2020b. Celebrating 20 years of genetic discoveries in legume nodulation and symbiotic nitrogen fixation. *The Plant Cell,* 32**,** 15-41.

RUTTEN, L. 2020. Evolution of nitrogen-fixing root nodules; Analysis of conserved signalling pathways in Legumes and *Parasponia.* PhD, Wageningen University.

SAHRUZAINI, N. A., REJAB, N. A., HARIKRISHNA, J. A., KHAIRUL IKRAM, N. K., ISMAIL, I., KUGAN, H. M. & CHENG, A. 2020. Pulse crop genetics for a sustainable future: Where we are now and where we should be heading. *Frontiers in plant science,* 11**,** 531.

SASKI, C., LEE, S.-B., DANIELL, H., WOOD, T. C., TOMKINS, J., KIM, H.-G. & JANSEN, R. K. 2005. Complete chloroplast genome sequence of *Glycine max* and comparative analyses with other legume genomes. *Plant Molecular Biology,* 59**,** 309-322.

SATO, S., NAKAMURA, Y., KANEKO, T., ASAMIZU, E., KATO, T., NAKAO, M., SASAMOTO, S., WATANABE, A., ONO, A. & KAWASHIMA, K. 2008. Genome structure of the legume, *Lotus japonicus*. *DNA Research,* 15**,** 227-239.

SAYERS, E. W., CAVANAUGH, M., CLARK, K., PRUITT, K. D., SHERRY, S. T., YANKIE, L. & KARSCH-MIZRACHI, I. 2023. GenBank 2023 update. *Nucleic Acids Research,* 51**,** D141-D144.

SCHAUSER, L., ROUSSIS, A., STILLER, J. & STOUGAARD, J. 1999. A plant regulator controlling development of symbiotic root nodules. *Nature,* 402**,** 191-195.

SCHIESSL, K., LILLEY, J. L., LEE, T., TAMVAKIS, I., KOHLEN, W., BAILEY, P. C., THOMAS, A., LUPTAK, J., RAMAKRISHNAN, K. & CARPENTER, M. D. 2019. NODULE INCEPTION recruits the lateral root developmental program for symbiotic nodule organogenesis in *Medicago truncatula*. *Current Biology,* 29**,** 3657-3668. e5.

SCHINDELIN, J., ARGANDA-CARRERAS, I., FRISE, E., KAYNIG, V., LONGAIR, M., PIETZSCH, T., PREIBISCH, S., RUEDEN, C., SAALFELD, S. & SCHMID, B. 2012. Fiji:

an open-source platform for biological-image analysis. *Nature Methods,* 9**,** 676-682.

SCHMUTZ, J., CANNON, S. B., SCHLUETER, J., MA, J., MITROS, T., NELSON, W., HYTEN, D. L., SONG, Q., THELEN, J. J. & CHENG, J. 2010. Genome sequence of the palaeopolyploid soybean. *Nature,* 463**,** 178-183.

SCHMUTZ, J., MCCLEAN, P. E., MAMIDI, S., WU, G. A., CANNON, S. B., GRIMWOOD, J., JENKINS, J., SHU, S., SONG, Q. & CHAVARRO, C. 2014. A reference genome for common bean and genome-wide analysis of dual domestications. *Nature Genetics,* 46**,** 707-713.

SEROVA, T. A., TIKHONOVICH, I. A. & TSYGANOV, V. E. 2017. Analysis of nodule senescence in pea (*Pisum sativum* L.) using laser microdissection, real-time PCR, and ACC immunolocalization. *Journal of Plant Physiology,* 212**,** 29-44.

SEROVA, T. A., TSYGANOVA, A. V. & TSYGANOV, V. E. 2018. Early nodule senescence is activated in symbiotic mutants of pea (*Pisum sativum* L.) forming ineffective nodules blocked at different nodule developmental stages. *Protoplasma,* 255**,** 1443-1459.

SHARMA, V., BHATTACHARYYA, S., KUMAR, R., KUMAR, A., IBAÑEZ, F., WANG, J., GUO, B., SUDINI, H. K., GOPALAKRISHNAN, S. & DASGUPTA, M. 2020. Molecular basis of root nodule symbiosis between *Bradyrhizobium* and 'crack-entry' legume groundnut (*Arachis hypogaea* L.). *Plants,* 9**,** 276.

SHIRZAEI, M., KHOSHMANESH, M., OJHA, C., WERTH, S., KERNER, H., CARLSON, G., SHERPA, S. F., ZHAI, G. & LEE, J.-C. 2021. Persistent impact of spring floods on crop loss in US Midwest. *Weather and Climate Extremes,* 34**,** 100392.

SHRESTHA, A., ZHONG, S., THERRIEN, J., HUEBERT, T., SATO, S., MUN, T., ANDERSEN, S. U., STOUGAARD, J., LEPAGE, A. & NIEBEL, A. 2021. *Lotus japonicus* Nuclear Factor YA1, a nodule emergence stage-specific regulator of auxin signalling. *New Phytologist,* 229**,** 1535-1552.

SINCLAIR, T. R. & NOGUEIRA, M. A. 2018. Selection of host-plant genotype: the next step to increase grain legume $N_2$ fixation activity. *Journal of Experimental Botany,* 69**,** 3523-3530.

SINGH, S., KATZER, K., LAMBERT, J., CERRI, M. & PARNISKE, M. 2014. CYCLOPS, a DNA-binding transcriptional activator, orchestrates symbiotic root nodule development. *Cell Host & Microbe,* 15**,** 139-152.

SMA-AIR, S. & RITCHIE, R. J. 2020. Photosynthesis in a *Vanda* sp orchid with Photosynthetic Roots. *Journal of Plant Physiology,* 251**,** 153187.

SMIGIELSKI, L., LAUBACH, E.-M., PESCH, L., GLOCK, J. M. L., ALBRECHT, F., SLUSARENKO, A., PANSTRUGA, R. & KUHN, H. 2019. Nodulation induces systemic resistance of *Medicago truncatula* and *Pisum sativum* against *Erysiphe pisi* and primes for powdery mildew-triggered salicylic acid accumulation. *Molecular Plant-Microbe Interactions,* 32**,** 1243-1255.

SMIT, P., LIMPENS, E., GEURTS, R., FEDOROVA, E., DOLGIKH, E., GOUGH, C. & BISSELING, T. 2007. *Medicago* LYK3, an entry receptor in rhizobial nodulation factor signaling. *Plant Physiology,* 145**,** 183-191.

SOLANKI, M. K., WANG, F.-Y., LI, C.-N., WANG, Z., LAN, T.-J., SINGH, R. K., SINGH, P., YANG, L.-T. & LI, Y.-R. 2020. Impact of sugarcane–legume intercropping on diazotrophic microbiome. *Sugar Tech,* 22**,** 52-64.

SOLIMAN, E. R. & MEYER, P. 2019. Responsiveness and adaptation to salt stress of the redox-responsive transcription factor 1 (*RRTF1*) gene are controlled by its promoter. *Molecular Biotechnology,* 61**,** 254-260.

STAUDINGER, C., MEHMETI-TERSHANI, V., GIL-QUINTANA, E., GONZALEZ, E. M., HOFHANSL, F., BACHMANN, G. & WIENKOOP, S. 2016. Evidence for a rhizobia-induced drought stress response strategy in *Medicago truncatula*. *Journal of Proteomics,* 136**,** 202-213.

STURMS, R., KAKAR, S., TRENT III, J. & HARGROVE, M. S. 2010. *Trema* and *Parasponia* hemoglobins reveal convergent evolution of oxygen transport in plants. *Biochemistry,* 49**,** 4085-4093.

SULIEMAN, S., ABDELRAHMAN, M. & TRAN, L.-S. P. 2022. Carbon metabolic adjustment in soybean nodules in response to phosphate limitation: A metabolite perspective. *Environmental and Experimental Botany***,** 104810.

TERPOLILLI, J. J., O'HARA, G. W., TIWARI, R. P., DILWORTH, M. J. & HOWIESON, J. G. 2008. The model legume *Medicago truncatula* A17 is poorly matched for $N_2$ fixation with the sequenced microsymbiont *Sinorhizobium meliloti* 1021. *New Phytologist,* 179**,** 62-66.

TIMMERS, A., AURIAC, M.-C. & TRUCHET, G. 1999. Refined analysis of early symbiotic steps of the Rhizobium-*Medicago* interaction in relationship with microtubular cytoskeleton rearrangements. *Development,* 126**,** 3617-3628.

TRINICK, M. 1979. Structure of nitrogen-fixing nodules formed by Rhizobium on roots of *Parasponia andersonii* Planch. *Canadian Journal of Microbiology,* 25**,** 565-578.

TSAVKELOVA, E. A., GLUKHAREVA, I. D., VOLYNCHIKOVA, E. A., EGOROVA, M. A., LEONTIEVA, M. R., MALAKHOVA, D. V., KOLOMEITSEVA, G. L. & NETRUSOV, A. I. 2022. Cyanobacterial Root Associations of Leafless Epiphytic Orchids. *Microorganisms,* 10**,** 1006.

TSYGANOVA, A. V., SELIVERSTOVA, E. V., BREWIN, N. J. & TSYGANOV, V. E. 2019. Comparative analysis of remodelling of the plant–microbe interface in *Pisum sativum* and *Medicago truncatula* symbiotic nodules. *Protoplasma,* 256**,** 983-996.

UNITED NATIONS, D. O. E. A. S. A., POPULATION DIVISION 2022. World Population Prospects 2022: Summary of Results. UN DESA/POP/2022/TR/NO. 3 ed.

VAHABI, K., REICHELT, M., SCHOLZ, S. S., FURCH, A. C., MATSUO, M., JOHNSON, J. M., SHERAMETI, I., GERSHENZON, J. & OELMÜLLER, R. 2018. *Alternaria brassicae* induces systemic jasmonate responses in *Arabidopsis* which travel to neighboring plants via a *Piriformsopora indica* hyphal network and activate abscisic acid responses. *Frontiers in Plant Science,* 9**,** 626.

VAN DE VELDE, W., GUERRA, J. C. P., KEYSER, A. D., DE RYCKE, R., ROMBAUTS, S., MAUNOURY, N., MERGAERT, P., KONDOROSI, E., HOLSTERS, M. & GOORMACHTIG, S. 2006. Aging in legume symbiosis. A molecular view on nodule senescence in *Medicago truncatula*. *Plant Physiology,* 141**,** 711-720.

VAN DE VELDE, W., ZEHIROV, G., SZATMARI, A., DEBRECZENY, M., ISHIHARA, H., KEVEI, Z., FARKAS, A., MIKULASS, K., NAGY, A. & TIRICZ, H. 2010. Plant peptides govern terminal differentiation of bacteria in symbiosis. *Science,* 327**,** 1122-1126.

VAN DEYNZE, A., ZAMORA, P., DELAUX, P.-M., HEITMANN, C., JAYARAMAN, D., RAJASEKAR, S., GRAHAM, D., MAEDA, J., GIBSON, D. & SCHWARTZ, K. D. 2018. Nitrogen fixation in a landrace of maize is supported by a mucilage-associated diazotrophic microbiota. *PLoS Biology,* 16**,** e2006352.

VAN VELZEN, R., HOLMER, R., BU, F., RUTTEN, L., VAN ZEIJL, A., LIU, W., SANTUARI, L., CAO, Q., SHARMA, T. & SHEN, D. 2018. Comparative genomics of the nonlegume *Parasponia* reveals insights into evolution of nitrogen-fixing rhizobium symbioses. *Proceedings of the National Academy of Sciences,* 115**,** E4700-E4709.

VAN ZEIJL, A., WARDHANI, T. A., SEIFI KALHOR, M., RUTTEN, L., BU, F., HARTOG, M., LINDERS, S., FEDOROVA, E. E., BISSELING, T. & KOHLEN, W. 2018. CRISPR/Cas9-mediated mutagenesis of four putative symbiosis genes of the tropical tree *Parasponia andersonii* reveals novel phenotypes. *Frontiers in Plant Science,* 9**,** 284.

VELANDIA, K., REID, J. B. & FOO, E. 2022. Right time, right place: The dynamic role of hormones in rhizobial infection and nodulation of legumes. *Plant Communications***,** 100327.

VERMA, M., SINGH, A., DWIVEDI, D. H. & ARORA, N. K. 2020. Zinc and phosphate solubilizing *Rhizobium radiobacter* (LB2) for enhancing quality and yield of loose leaf lettuce in saline soil. *Environmental Sustainability,* 3**,** 209-218.

VERNIÉ, T., KIM, J., FRANCES, L., DING, Y., SUN, J., GUAN, D., NIEBEL, A., GIFFORD, M. L., DE CARVALHO-NIEBEL, F. & OLDROYD, G. E. 2015. The NIN transcription factor coordinates diverse nodulation programs in different tissues of the *Medicago truncatula* root. *The Plant Cell,* 27**,** 3410-3424.

WALKER, L., LAGUNAS, B. & GIFFORD, M. L. 2020. Determinants of host range specificity in legume-rhizobia symbiosis. *Frontiers in Microbiology,* 11**,** 3028.

WALL, L. G., VALVERDE, C. & HUSS-DANELL, K. 2003. Regulation of nodulation in the absence of $N_2$ is different in actinorhizal plants with different infection pathways. *Journal of Experimental Botany,* 54**,** 1253-1258.

WANG, D., GRIFFITTS, J., STARKER, C., FEDOROVA, E., LIMPENS, E., IVANOV, S., BISSELING, T. & LONG, S. 2010. A nodule-specific protein secretory pathway required for nitrogen-fixing symbiosis. *Science,* 327**,** 1126-1129.

WANG, H. & SCHIPPERS, J. H. 2019. The role and regulation of autophagy and the proteasome during aging and senescence in plants. *Genes,* 10**,** 267.

WANG, M. M., ZHU, Q. G., DENG, C. L., LUO, Z. R., SUN, N. J., GRIERSON, D., YIN, X. R. & CHEN, K. S. 2017. Hypoxia-responsive ERF s involved in postdeastringency softening of persimmon fruit. *Plant Biotechnology Journal,* 15**,** 1409-1419.

WANG, Y., YANG, W., ZUO, Y., ZHU, L., HASTWELL, A. H., CHEN, L., TIAN, Y., SU, C., FERGUSON, B. J. & LI, X. 2019. GmYUC2a mediates auxin biosynthesis during root development and nodulation in soybean. *Journal of Experimental Botany,* 70**,** 3165-3176.

WARDHANI, T. A., ROSWANJAYA, Y. P., DUPIN, S., LI, H., LINDERS, S., HARTOG, M., GEURTS, R. & VAN ZEIJL, A. 2019. Transforming, Genome Editing and Phenotyping the Nitrogen-fixing Tropical Cannabaceae Tree *Parasponia andersonii*. *Journal of Visualized Experiments***,** -.

WESTHOEK, A., CLARK, L. J., CULBERT, M., DALCHAU, N., GRIFFITHS, M., JORRIN, B., KARUNAKARAN, R., LEDERMANN, R., TKACZ, A. & WEBB, I. 2021. Conditional

sanctioning in a legume–Rhizobium mutualism. *Proceedings of the National Academy of Sciences,* 118**,** e2025760118.

WHO, F. I. U. W. 2022. The state of food security and nutrition in the world 2022 (SOFI).

WILMOTH, J. C., WANG, S., TIWARI, S. B., JOSHI, A. D., HAGEN, G., GUILFOYLE, T. J., ALONSO, J. M., ECKER, J. R. & REED, J. W. 2005. NPH4/ARF7 and ARF19 promote leaf expansion and auxin-induced lateral root formation. *The Plant Journal,* 43**,** 118-130.

WU, Q., LI, P. C., ZHANG, H. J., FENG, C. Y., LI, S. S., YIN, D. D., TIAN, J., XU, W. Z. & WANG, L. S. 2018. Relationship between the flavonoid composition and flower colour variation in Victoria. *Plant Biology,* 20**,** 674-681.

WU, Z., CHEN, H., PAN, Y., FENG, H., FANG, D., YANG, J., WANG, Y., YANG, J., SAHU, S. K. & LIU, J. 2022. Genome of *Hippophae rhamnoides* provides insights into a conserved molecular mechanism in actinorhizal and rhizobial symbioses. *New Phytologist*.

XIAO, A., YU, H., FAN, Y., KANG, H., REN, Y., HUANG, X., GAO, X., WANG, C., ZHANG, Z. & ZHU, H. 2020. Transcriptional regulation of NIN expression by IPN2 is required for root nodule symbiosis in *Lotus japonicus*. *New Phytologist,* 227**,** 513-528.

XIAO, T. T., SCHILDERINK, S., MOLING, S., DEINUM, E. E., KONDOROSI, E., FRANSSEN, H., KULIKOVA, O., NIEBEL, A. & BISSELING, T. 2014. Fate map of *Medicago truncatula* root nodules. *Development,* 141**,** 3517-3528.

YANG, M., WANG, L., CHEN, C., GUO, X., LIN, C., HUANG, W. & CHEN, L. 2021. Genome-wide analysis of autophagy-related genes in *Medicago truncatula* highlights their roles in seed development and response to drought stress. *Scientific Reports,* 11**,** 22933.

YANG, S., TANG, F., GAO, M., KRISHNAN, H. B. & ZHU, H. 2010. R gene-controlled host specificity in the legume–rhizobia symbiosis. *Proceedings of the National Academy of Sciences,* 107**,** 18735-18740.

YOKOYAMA, T. 2008. Flavonoid-responsive nodY-lacZ expression in three phylogenetically different *Bradyrhizobium* groups. *Canadian Journal of Microbiology,* 54**,** 401-410.

YOSHIDA, S., ITO, M., NISHIDA, I. & WATANABE, A. 2001. Isolation and RNA gel blot analysis of genes that could serve as potential molecular markers for leaf senescence in *Arabidopsis thaliana*. *Plant and Cell Physiology,* 42**,** 170-178.

YOUNG, N. D., DEBELLÉ, F., OLDROYD, G. E., GEURTS, R., CANNON, S. B., UDVARDI, M. K., BENEDITO, V. A., MAYER, K. F., GOUZY, J. & SCHOOF, H. 2011. The *Medicago* genome provides insight into the evolution of rhizobial symbioses. *Nature,* 480**,** 520-524.

YU, H., WANG, F., SHAO, M., HUANG, L., XIE, Y., XU, Y. & KONG, L. 2021. Effects of rotations with legume on soil functional microbial communities involved in phosphorus transformation. *Frontiers in Microbiology,* 12**,** 661100.

ZARRABIAN, M., MONTIEL, J., SANDAL, N., FERGUSON, S., JIN, H., LIN, Y.-Y., KLINGL, V., MARÍN, M., JAMES, E. K. & PARNISKE, M. 2022. A promiscuity locus confers *Lotus burttii* nodulation with rhizobia from five different genera. *Molecular Plant-Microbe Interactions,* 35**,** 1006-1017.

ZHANG, Y., TAN, S., GAO, Y., KAN, C., WANG, H. L., YANG, Q., XIA, X., ISHIDA, T., SAWA, S. & GUO, H. 2022. CLE42 delays leaf senescence by antagonizing ethylene pathway in *Arabidopsis*. *New Phytologist,* 235**,** 550-562.

ZHONG, C., MANSOUR, S., NAMBIAR-VEETIL, M., BOGUSZ, D. & FRANCHE, C. 2013. *Casuarina glauca*: a model tree for basic research in actinorhizal symbiosis. *Journal of Biosciences,* 38**,** 815-823.

ZHOU, X., CHANDRASEKHARAN, M. B. & HALL, T. C. 2004. High rooting frequency and functional analysis of GUS and GFP expression in transgenic *Medicago truncatula* A17. *New Phytologist,* 162**,** 813-822.

ZOTZ, G. & WINKLER, U. 2013. Aerial roots of epiphytic orchids: the velamen radicum and its role in water and nutrient uptake. *Oecologia,* 171**,** 733-741.